

# ELECTRONIC WARFARE LABORATORY

AD 749 796

ECOM-5386

INFRARED TECHNOLOGY AND ITS APPLICATION FOR  
MEASUREMENT OF AIRCRAFT

BY

EDWARD VALENZUELA

LEONARD H. HOLDEN, JR.

MARCH 1972

DISTRIBUTION OF THIS DOCUMENT IS UNLIMITED

D D C  
RECORDED  
OCT 16 1972  
RECORDED  
C

**BEST  
AVAILABLE COPY**

**MISSILE ELECTRONIC WARFARE TECHNICAL AREA  
WHITE SANDS MISSILE RANGE**

# ECOM

Represented by  
NATIONAL TECHNICAL  
INFORMATION SERVICE

UNITED STATES ARMY ELECTRONICS COMMAND • FORT MONMOUTH, N.J.

ACC SCIC	
NTIS	<input checked="" type="checkbox"/> Yes Section
DOC	<input type="checkbox"/> Yes Section
UWAR	<input type="checkbox"/>
JUSTIFICATION	
BY	
DISSEMINATION/AVAILABILITY	C. 03
Div.	Aviation Section
A	

Disclaimer

The findings in this report are not to be construed as an official Department of the Army position.

## DOCUMENT CONTROL DATA - R &amp; D .

(Security classification of title, body of abstract and indexing annotation must be entered when the overall report is classified)

1. ORIGINATING ACTIVITY (Corporate author) U. S. Army Electronics Command Electronic Warfare Laboratory Fort Monmouth, NJ 07703		2a. REPORT SECURITY CLASSIFICATION UNCLASSIFIED	
		2b. GROUP	
3. REPORT TITLE INFRARED TECHNOLOGY AND ITS APPLICATION FOR MEASUREMENT OF AIRCRAFT			
4. DESCRIPTIVE NOTES (Type of report and inclusive dates)			
5. AUTHOR(S) (First name, middle initial, last name) Leonard H. Holden, Jr. and Edward Valenzuela			
6. REPORT DATE March 1972		7a. TOTAL NO. OF PAGES 186	7b. NO. OF REFS
8a. CONTRACT OR GRANT NO.		8b. ORIGINATOR'S REPORT NUMBER(S)	
b. PROJECT NO. 1-F-1-62208A-148			
c.		9b. OTHER REPORT NO(S) (Any other numbers that may be assigned this report)	
d.			
10. DISTRIBUTION STATEMENT Distribution of this document is unlimited			
11. SUPPLEMENTARY NOTES		12. SPONSORING MILITARY ACTIVITY U.S. Army Electronics Command Missile EW Technical Area White Sands Missile Range, NM 88002	
13. ABSTRACT This study, confined to the measurement of infrared radiation emitted by aircraft, includes a catalog of each type of aircraft in the US Army inventory. Each type is represented because the measurement procedures used may differ for each depending upon size, speed, and intended tactical use. A brief discussion of the physical laws involved in taking such measurements is also included, as is a discussion on the different backgrounds encountered in a measurement program.  The need for adequate instrument calibration is emphasized. Various measurement techniques and their application are discussed. Data reduction and analysis are covered briefly, and several parameters that are routinely determined by analysis are considered.			

14. KEY WORDS	LINK A		LINK B		LINK C	
	ROLE	WT	ROLE	WT	ROLE	WT
Aircraft radiation Infrared Spectral Signatures						

ECOM-5386

INFRARED TECHNOLOGY AND ITS APPLICATION FOR  
MEASUREMENT OF AIRCRAFT

BY

EDWARD VALENZUELA

LEONARD H. HOLDEN, JR.

MARCH 1972

DISTRIBUTION OF THIS DOCUMENT IS UNLIMITED

PROJECT NO. 1-F-1-62208A-148

MISSILE ELECTRONIC WARFARE TECHNICAL AREA  
ELECTRONIC WARFARE LABORATORY, USA ELECTRONICS COMMAND  
WHITE SANDS MISSILE RANGE  
NEW MEXICO

## ABSTRACT

This study, confined to the measurement of infrared radiation emitted by aircraft, includes a catalog of each type of aircraft in the US Army inventory. Each type is represented because the measurement procedures used may differ for each depending upon size, speed, and intended tactical use. A brief discussion of the physical laws involved in taking such measurements is also included, as is a discussion on the different backgrounds encountered in a measurement program.

The need for adequate instrument calibration is emphasized. Various measurement techniques and their application are discussed. Data reduction and analysis are covered briefly, and several parameters that are routinely determined by analysis are considered.

## ACKNOWLEDGMENT

The authors are indebted to many people for discussions held during the writing of this report. Particular thanks are extended to Mr. Thomas Atherton, Mr. Thomas Hoskins, and to Mr. Burton Wheeler who were frequently consulted concerning technical details of the writing.

## FOREWORD

Infrared radiation and its interaction with matter is the most widespread and important heat exchange process encountered. Unlike heat exchange by conductivity and convection, radiative heat exchange occurs in the absence of direct contact and depends to a considerable extent upon the temperature level involved. Radiative heat exchange is accompanied by a conversion of thermal energy into electromagnetic energy.

This study is confined to the measurement of infrared radiation emitted by aircraft, and since a basic understanding of the physical laws involved is required to comprehend the processes by which these measurements are made, a discussion of these laws is included.

Background radiation must always be taken into consideration when taking measurements of any target. In this case Army aircraft are considered as targets; therefore, the different backgrounds that could be encountered in such a measurement program are also discussed.

Infrared measurements performed without adequate instrument calibration are virtually worthless, and accurate instrument calibration requires comprehensive knowledge of instrumentation. For this reason, both of these subjects are discussed in this study. However, since calibration depends upon the type of instrument used to make the measurement or upon a specific instrument--and no two are exactly alike--some of the discussions are generalized. Several measurements techniques that can be used in an infrared measurement program are presented.



This study also covers certain phases of data reduction and analysis. Specific analyses to be performed depend to a great extent upon the objectives of specific measurements. Several parameters routinely determined by analyzing data obtained from infrared measurements are included.

The work described herein was supported by the US Army Eustis Directorate Air Mobility Research and Development Laboratory, Fort Eustis, Virginia.

## CONTENTS

	<u>Page</u>
ABSTRACT	ii
ACKNOWLEDGMENT	iii
FOREWORD	iv
CHAPTER I -- INFRARED RADIATION THEORY	1
Blackbody Radiation	3
Planck's Radiation Law	3
Wien's Displacement Law	6
The Stefan-Boltzmann Law	6
Kirchoff's Law	8
Lambert's Cosine Law	8
Radiometric and Spectral Quantities	9
Spectral Radiometric Quantities	11
Standard Units, Symbols, and Defining Equations	13
CHAPTER II -- BACKGROUNDS and TARGETS	15
Infrared Emission from Aircraft	16
Background Radiation	21
Cloud Radiance	24
Ground Radiance	24
Ocean Radiance	25
CHAPTER III -- CALIBRATION	26
Radiometric Calibration	27
Field Calibration	35
Spectrometer Calibration	37

## CONTENTS

	<u>Page</u>
Resolution	42
Other Parameters	43
Calibration of Sources	45
CHAPTER IV -- MEASUREMENT TECHNIQUES	46
Spectral Measurements	51
Contrast Techniques	53
Total Chop Techniques	54
Tests of Aircraft	54
Attitude Determinations	56
Aspect Geometry	57
Ground-to-Ground	67
Ground-to-Air	68
Air-to-Air	72
Summary	72
CHAPTER V -- INSTRUMENTATION	74
Rapid Scan Instruments	90
Fourier Transform Spectrometers	92

## CONTENTS

	<u>Page</u>
Detectors	98
System Sensitivity	106
Boresight Cameras	109
Imaging Systems	110
Meteorological Instruments	113
Collimator	113
Pedestal Tracking System	115
CHAPTER VI -- DATA REDUCTION AND ANALYSIS	120
Accumulation of Data	120
Spectrometric Data	121
Atmospheric Transmission	125
Data Analysis	135
Acquisition Range	135
Emission Spectroscopy	139
CHAPTER VII -- TYPES OF AIRCRAFT	141
Helicopters	141
UH-1	141
AH-1G	146
OH-6A	150

## CONTENTS

	<u>Page</u>
OH-58A	153
CH-47	157
CH-54A	160
OH-13H	163
OH-23G	165
CH-34A, C	167
UH-19D	169
Fixed Wing Aircraft	171
OV-1	171
U-8	173
U-21	175
O-1A	177
U-1A	179
U-5A	181

### FIGURES

1-1. Blackbody Curves, 100° to 1000°K	7
1-2. Blackbody Cruves, 1000 to 2000°K	7
1-3. Lambertian Source	9
1-4. Geometry of Radiance Definition	10
2-1. Sky Emission Spectra of Average Day, 22.9°C	23
2-2. Sky Emission Spectra of Average Day, 5.6°C	23
3-1. Spectral Irradiance of a Blackbody Source Over a Path of Five Feet (Per Unit Area)	36

## CONTENTS

	<u>Page</u>
3-2. Variation in Path Distance for Varying Angles of Incidence	39
4-1. Relative Spectral Response	48
4-2. Target Spectral Radiant Intensity	48
4-3. Atmospheric Transmission	48
4-4. Target Spectral Irradiance	50
4-5. Instrument Response to Spectral Irradiance	50
4-6. Aircraft in Level Flight Illuminated by Ground Radar	59
4-7. Projection of Above Figure on a Horizontal Plane	59
4-8. Side View of a Sphere with the Radar at Point "A"	61
4-9. Roll, Pitch, and Heading Quantities in Terms of $R$ , $\theta$ , and $\phi$	63
4-10. Portion of the Roll Circle	65
4-11. Portion of the Pitch Circle	65
4-12. New Separations Showing $\theta$ and $\phi$ Determined	66
4-13. Flight Pattern for Fly-by Test	71
5-1. Emission Spectrum of a Xenon Lamp	76
5-2. Infrared Emission from Xenon Lamp	77
5-3. Relation Between Object, Image, and Focal Distances for Mirrors	80
5-4a. Optical Systems	83
5-4b. Optical Systems (Additional)	84
5-5. Deviation of a Ray Through a Prism	86
5-6. Rayleigh Criterion for Resolution	87
5-7. CVF Spectrometer Optical Diagram	91

## CONTENTS

	<u>Page</u>
5-8. Optical Layouts of Modular Interferometers	95
5-9. Path of a Ray in a Michelson Interferometer	96
5-10. Photoconductor Circuit Configuration	103
5-11. Spectral Detectivities of Detectors	105
5-12. Selection of Optimum Bias for Typical Photoconductor Detector	107
5-13. Schematic of Optical Unit	112
5-14. Optical Schematic of Off-axis Collimator	114
6-1. Irradiance Contours Emanating from Target as a Function of Azimuth Angle	122
6-2. Atmospheric Transmission (Calculated) 25% RH	128
6-3. Atmospheric Transmission (Calculated) 75% RH	129
6-4. Infrared Absorption by Atmospheric Dust	134
7-1. Designation of Army Aircraft	142
7-2. YUH-1D and UH-1D/H Helicopter	144
7-3. General Arrangement -- Typical UH-1D	145
7-4. Principal Dimensions -- AH-1G	148
7-5. Engine and Transmission Compartment Cooling AH-1G	149
7-6. OH-6A Helicopter	151
7-7. General Arrangement Diagram -- OH-6A	152
7-8. Three Views of the OH-58A Helicopter	155
7-9. General Arrangement -- OH-58A	156

## CONTENTS

	<u>Page</u>
7-10. Overall Dimensions -- CH-47	158
7-11. Rear and Lower Views of Engine Section -- CH-47	159
7-12. General Arrangement -- Exterior CH-54A	161
7-13. Diagram of Engine Intake -- CH-54A	162
7-14. General Arrangement Diagram -- OH-13H	164
7-15. Diagram Showing Three Views of OH-23F Aircraft and Cooling System	166
7-16. General Arrangement. -- Right-hand Side (Typical) of the CH-34A Helicopter	168
7-17. General Arrangement -- CH-19D Helicopter	170
7-18. Diagram Showing Overall Dimensions -- Mohawk	172
7-19. Four Views of U-8F Aircraft (Seminole)	174
7-20. Three Views of the Ute Aircraft	176
7-21. Four Views of the O-1 Aircraft	178
7-22. Various Views of the U-1A Aircraft (Otter)	180
7-23. Various Views of the Beaver Aircraft	182
<b>TABLES</b>	
I-1 Radiometric Quantities	14
II-1 Molecular Emission Bands (Gaydon)	20
II-2 Major Infrared Absorption Bands of Gases	20
<b>BIBLIOGRAPHY</b>	183



## CHAPTER I

### INFRARED RADIATION THEORY

That portion of the electromagnetic spectrum which lies between the extreme of the visible (0.75 micrometers) and the shortest microwaves (1000 micrometers) is considered to be the infrared region. The types of radiation distributions found in the infrared can be classified as continuous, band, and line spectra. Each type of distribution is the result of different molecular or atomic processes which differ both in mechanics and energetics.

The quantum processes which lead to the emission of infrared radiation are changes in the degree of excitation of the system. The system is de-excited (in emission), that is, it goes to a state of lower energy with the photon released containing the energy lost. Such a transition between two energy states may involve electronic, vibrational and rotational energy levels, or some combination of these. Continuum radiation can result from the processes of ionization and dissociation, that is, changes in the electronic states of a system. This type of diffuse radiation is found in the near-infrared portion of the spectrum rather than in the longer wavelength regions. Discrete radiation takes two forms: band and line spectra. Line spectra are quite sharp and very intense and correspond to changes in the electronic states of atoms or molecules. Band spectra have

a characteristic structure associated with the subsidiary changes in rotational energy simultaneous with a change in vibrational states. The individual rotational lines can only be observed for the lighter molecules ( $\text{CO}_2$ ,  $\text{H}_2\text{O}$ ) at high resolution and low pressures. At higher pressures (and longer pathlengths) or lower resolution, the lines merge into a broad band without structure. In the very far-infrared are found bands of overlapping lines due only to changes in the rotational energy states of light molecules. Heavier molecules have their rotational emission lines in the microwave region.

The simplest and probably the most important type of infrared radiation is the continuum radiation commonly known as thermal, or blackbody, radiation which is emitted by all objects above the temperature of absolute zero. This radiation consists of photons in thermal equilibrium with matter and with one another. A knowledge of the laws characterizing blackbody radiation is essential to the study of infrared emission.

## BLACKBODY RADIATION

It is a matter of common observation that bodies when heated emit radiant energy, the quantity and quality of which depend upon the temperature of that body. Thus, the rate at which an incandescent lamp filament emits radiation increases rapidly with increased temperature of the filament. As the temperature rises, the emitted light becomes whiter. If this light is dispersed by a prism or other dispersing element, a continuous spectrum without line structure is formed. Thus, thermal or blackbody radiation emitted by a solid at some temperature is dependent only on the absolute temperature. The maximum intensity of the emitted radiation shifts to shorter wavelengths as the temperature of the body increases, and the continuous nature of the radiation leads to a closed functional form for the wavelength dependence of the emitted radiation.

These properties of blackbody radiation are treated mathematically by the Stefan-Boltzmann law, the Wien displacement law, and the Planck equation, respectively. The application of these "ideal" radiation laws to real objects requires only the further knowledge of Kirchoff's law along with experimental information concerning the nature of the material and the nature of the surface being studied.

## THE PLANCK RADIATION LAW

The wavelength dependence of blackbody radiation is given by Planck's law which is the basis for almost all radiometric considerations. From Planck's law both the Stefan-Boltzmann and the Wien laws can be derived by an integration and differentiation, respectively.

Historically, Planck established his law by trying to fit experimental data with some functional form which would also yield the appropriate limiting forms of the Rayleigh-Jeans' and Wien's laws. To arrive at such a functional form, Planck had to deviate from classical thermodynamics and introduce new assumptions about the nature of blackbody radiation. These were:

1. An oscillator, or any similar physical system, has a discrete set of possible energy values or levels. Energies intermediate between these discrete values never occur.

2. The emission and absorption of radiation are associated with transitions, or jumps, between discrete levels. The energy, thereby lost or gained by the oscillator, is emitted or absorbed as a quantum of radiant energy of magnitude  $h \nu$ ,  $\nu$  being the frequency of the emitted radiation.

Planck actually derived his radiation formula by considering the interaction between the radiation inside an isothermal enclosure and electric oscillators which he imagined to exist in the walls of the enclosure. It can be shown that there would be  $8 \pi d \lambda / \lambda^4$  modes of oscillation or degrees of freedom per unit volume in the wavelength range  $\lambda$  to  $\lambda + d \lambda$ . If we multiply this number by the average energy per oscillator  $\bar{\epsilon}$ , where

$$\bar{\epsilon} = E/N = h \nu / \exp (h \nu / kT) - 1 \quad (1-1)$$

we obtain

$$w_{\lambda} d \lambda = \frac{8 \pi d \lambda}{\lambda^4} \frac{h \nu}{e^{h \nu / kT} - 1} \quad (1-2)$$

By substitution of  $v = c/\lambda$ ,  $c$  being the speed of light in a vacuum, we obtain Planck's radiation equation for the wavelength dependence of the radiant energy density

$$w_{\lambda} = \frac{8 \pi ch}{\lambda^5 \exp (ch/\lambda kT) - 1} \quad (1-3)$$

This equation can also be written in the more familiar form of radiant energy

$$M_{\lambda} = \frac{c_1}{\lambda^5 \exp (c_2/\lambda T) - 1} \quad (1-4)$$

where  $c_1$  and  $c_2$  are constants with the values

$$\begin{aligned} c_1 &= 2 \pi c^2 h = 3.7415 \times 10^{-12} \text{ watt-cm}^2 \\ &= 3.7415 \times 10^4 \text{ watt-}\mu\text{m-cm}^{-2} \end{aligned} \quad (1-5)$$

$$c_2 = ch/k = 1.4388 \text{ cm-}^{\circ}\text{K}$$

The spectral radiance of a blackbody source is given by the spectral radiant intensity divided by the projected area of the aperture of the blackbody, or in terms of the Planck equation

$$L_{\lambda} = I_{\lambda}/A \cos \theta = M_{\lambda}/\pi \quad (1-6)$$

or

$$L_{\lambda} = \frac{c_1}{\pi \lambda^5 \exp(c_2/\lambda T) - 1}$$

Thus, armed with a knowledge of Planck's law, we can calculate the radiant energy output of a blackbody at any temperature as a function of wavelength. The following graphs (figures 1-1 and 1-2) show the radiant exitance of a blackbody over temperatures and wavelengths which are of interest to workers in infrared. In actual practice, tables of radiation functions are used to determine

radiative parameters rather than using the Planck equation directly. Similarly, the emissivity of an ideal blackbody is one, but for real blackbodies the emissivity will have to be determined, although it is generally very close to one.

#### WIEN'S DISPLACEMENT LAW

The wavelength,  $\lambda_m$ , at which the spectral emittance is a maximum at any temperature can be found by differentiating  $Q_\lambda$  with respect to  $\lambda$  and setting the derivative equal to zero. The result is

$$\lambda_m T = 2897.8 \text{ micrometer-degree K.} \quad (1-7)$$

The wavelength of maximum spectral emittance is, therefore, inversely proportional to the absolute temperature. As the temperature is increased, the maximum shifts toward the shorter wavelengths. This is known as Wien's displacement law.

#### THE STEFAN-BOLTZMANN LAW

The total radiant emittance (over all wavelengths) of a blackbody can be found by integrating the Planck expression over all wavelengths

$$M = \int_0^{\infty} M_\lambda d\lambda = \frac{\pi^4 c_1 T}{15 c_2^4} \quad (1-8)$$

or  $M = \sigma T^4$ , where the Stefan-Boltzmann constant

$$\sigma = \frac{\pi^4 c_1}{15 c_2^4} = 5.6697 \times 10^{-12} \frac{\text{watt}}{\text{cm}^2 - \text{deg}^4 \text{ K}} \quad (1-9)$$

when  $T$  is in degrees Kelvin and  $M$  in watts/cm<sup>2</sup>. The Stefan-Boltzmann law then states that the radiant exitance of a blackbody is proportional to the fourth power of the absolute temperature.

## KIRCHOFF'S LAW

A certain fraction of the radiation incident upon an opaque surface is absorbed and the remainder reflected.

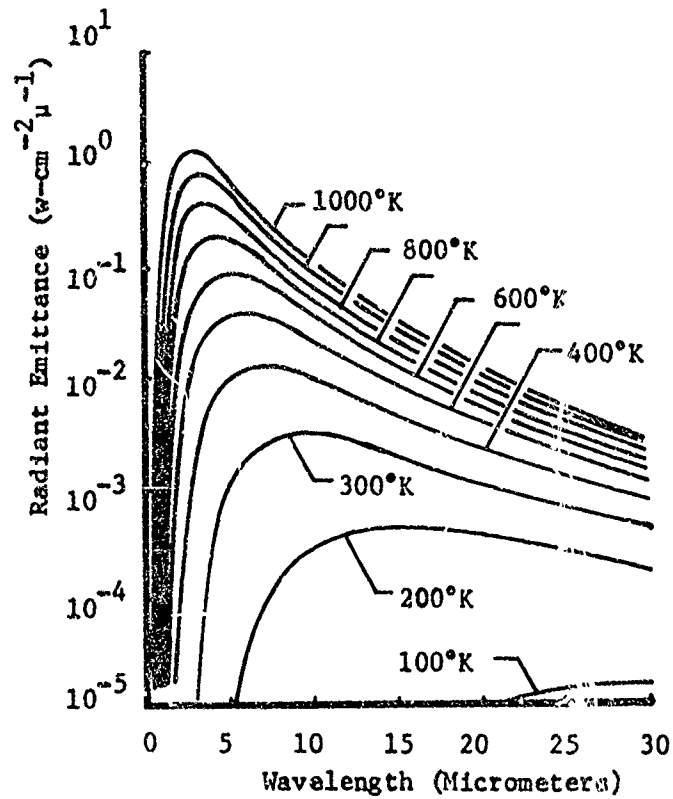


Figure 1-1. Blackbody Curves, 100°K to 1000°K

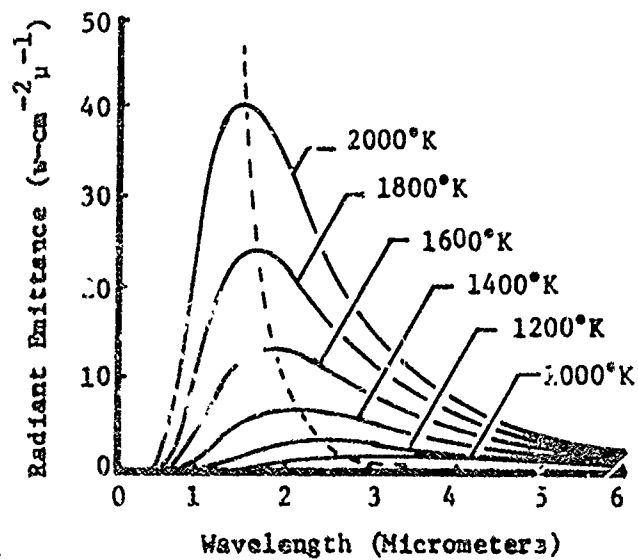


Figure 1-2. Blackbody Curves, 1000°K to 2000°K

## KIRCHOFF'S LAW

The relationship between reflectance and absorptance for an opaque surface is simply

$$\rho + \alpha = 1$$

where

$\rho$  = reflectance

$\alpha$  = absorptance (1-10)

Kirchoff's law states that the ratio of radiant exitance of such a source to that of a blackbody at the same temperature is equal to the absorptance, or

$$\alpha = M/M_{bb} \quad (1-11)$$

This shows that a good absorber is also a good emitter; therefore, the emissivity of an opaque source is defined as  $\epsilon = \alpha$  and for a blackbody, which is a perfect absorber,  $\epsilon = 1 - \rho$ ,  $\rho = 0$ . A greybody is one which does not absorb all incident radiation but reflects some part of that radiation. Thus, if  $M_{bb}$  is the flux per unit area which an ideal blackbody would emit, a greybody will emit an amount  $\epsilon M_{bb}$ . Thus, the laws of blackbody radiation for real bodies must be modified by the inclusion of the emissivity  $\epsilon = \epsilon(T, \lambda)$ . The properties, reflectance, absorptance, emissivity, and transmittance, all vary with wavelength for different materials. This variation is known for most common materials.

## LAMBERT'S COSINE LAW

The radiation per unit solid angle from a plane surface varies with the angle made with the normal to the surface. Thus, more energy is emitted at small angles from the normal to the surface than in any other direction from the plane surface. Lambert's cosine law gives the quantitative expression of this observation, and states that the amount of radiation in a small solid angle (figure 1-3) is proportional to the solid



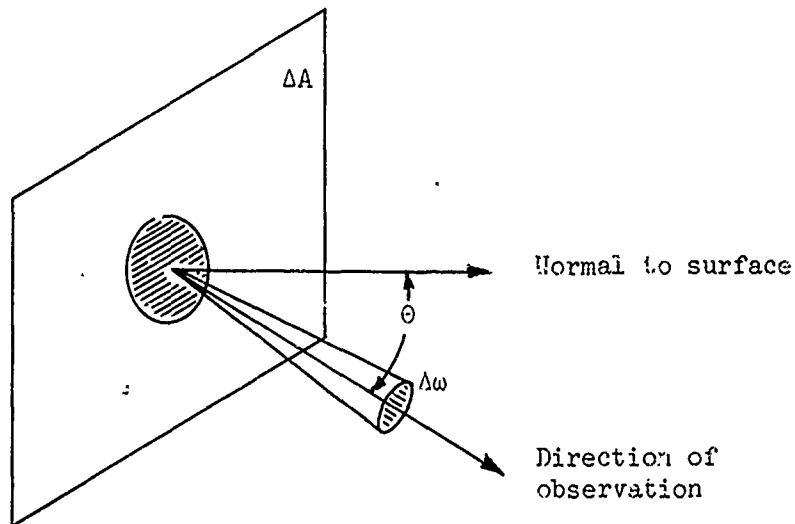


Figure 1-3. Lambertian Source

angle and varies as the cosine of the angle between the direction of observation and the normal to the surface. Thus, the power radiated from a small surface element of area,  $dA$ , in a small solid angle,  $d\omega$ , in a direction making an angle,  $\theta$ , with the normal, is given by

$$dM = \frac{\epsilon \sigma T^4}{\pi} \cos \theta d\omega df \quad (1-12)$$

#### RADIOMETRIC AND SPECTRAL QUANTITIES

Consider a point source, isolated in space and emitting electromagnetic radiation in all directions. There is no directional dependence of the radiation from a point source. The radiant energy,  $Q$ , emitted by the source in all directions, is given in joules. The rate of transfer of this radiant energy, or the radiant flux,  $\phi$ , is just the time rate of change of radiant energy and is given in watts. The radiant density,  $W$ , is the radiant energy per unit volume given in joules per  $\text{cm}^3$ .

If the source is not a point source, but covers a finite area, it is characterized by the amount of radiant flux emitted per unit area of its surface.  $M$ , the radiant exitance, is given in units of  $\text{watts}/\text{cm}^2$ .

In actual practice, a source can only be characterized by measurements made at some distance from the source and over a limited receiving area. In addition to the radiant exitance, two other measures of the properties of a source are the radiant intensity,  $I$ , and the radiance,  $L$ . A sphere has a surface area of  $4\pi r^2$  and contains a solid angle of  $4\pi$  steradians about its center. For a point source, we can define the radiant flux crossing a unit solid angle for any sphere surrounding the source because the radiation is isotropic. This quantity is  $I$ , the radiant intensity, and has units of watts/steradian. According to Lambert's cosine law, radiation emitted from a surface varies with the angle made with the normal to the surface. If the directional dependence of the emitted radiation follows this law, the source is said to be Lambertian. Consider a receiving surface lying in a plane perpendicular to the direction of measurement (figure 1-4). Let  $\theta$  be the angle the direction of observation makes with the normal to the emitting surface, then a unit area of the emitting surface projected onto the receiver is smaller by a factor of  $\cos \theta$ .

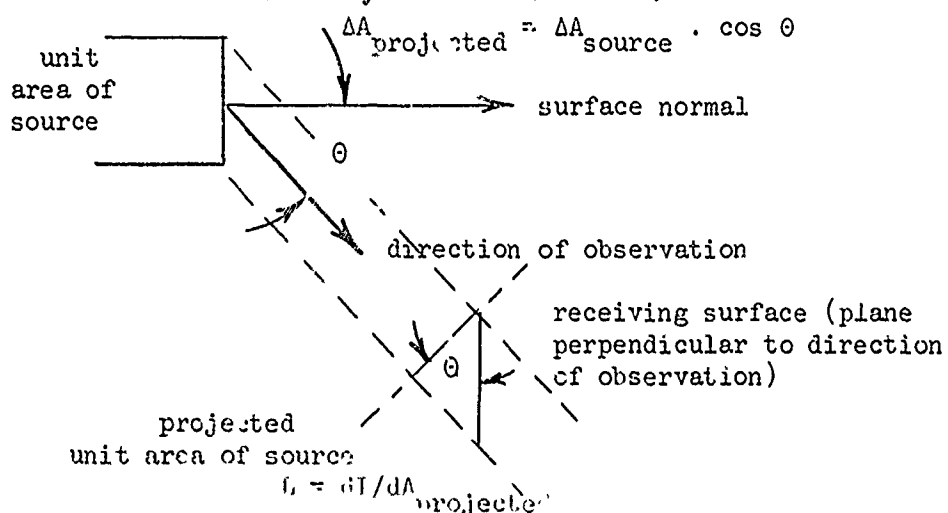


Figure 1-4. Geometry of Radiance Definition

Then the radiance,  $L$ , is the radiant flux emitted into a unit solid angle per unit of projected area of the source. Thus, a determination of radiance from measurements made at a distance from a source requires a knowledge of the orientation of the direction of observation with the normal to the emitting surface, but for a Lambertian source, the radiance is the same in all directions.

The three quantities,  $M$ ,  $I$ , and  $L$ , are used to characterize the source of the radiation. Any measurement of the radiation emitted by a source must be converted into one of these quantities if the results are to be meaningful. For a flat Lambertian surface radiating into a hemisphere ( $2\pi$  steradians) we have the relations

$$L = \frac{M}{\pi} \quad I = \int_{\text{area}} L dA \quad (1-13)$$

A measurement usually gives not the amount of radiation emitted by the source, but the amount of radiation received by a detector. The amount of radiant flux received by a surface, per unit area of the surface, is known as the irradiance  $E$  in units of watts/cm<sup>2</sup>. Note that this quantity has the same units as radiant exitance but refers to the radiation incident upon the receiving surface rather than that being emitted by the source.

#### SPECTRAL RADIOMETRIC QUANTITIES

Whereas the radiometric quantities, radiant exitance, radiant intensity, radiance, and irradiance are numerical values characterizing the radiation emitted by a certain area of a source into a particular solid angle (directional) or received by a distant receiver

over a limited area, the numerical quantities must be accompanied by the wavelength interval over which the radiation was measured. The wavelength dependence of both the emitted and received radiation, from many types of sources other than blackbody, takes a complex form which can only be properly specified by spectrometric rather than radiometric instruments. It becomes beneficial to define quantities which are differential with respect to wavelength.

The spectral radiant flux,  $\phi_\lambda$ , is the radiant flux per unit wavelength interval  $\phi_\lambda = \partial\phi/\partial\lambda$ . Similarly, we can define the spectral radiant exitance,  $M_\lambda$ , spectral radiant intensity,  $I_\lambda$ , spectral radiance,  $L_\lambda$ , and the spectral irradiance,  $E_\lambda$ . Hereafter the subscript  $\lambda$  will be used to denote spectral radiometric quantities. These will all be functional quantities whose value at a particular wavelength can be determined. The values over different wavelength intervals may be determined by a suitable integration. Thus, the radiant flux between  $\lambda_1$  and  $\lambda_2$  is given simply by integrating the spectral radiant flux,

$$\phi = \int_{\lambda_1}^{\lambda_2} \phi_\lambda d\lambda \quad (1-14)$$

Although the functional form of the wavelength dependency may be quite complex, a numerical integration is always possible where no closed expression suffices as an approximation to the measured radiation levels.

Given a properly calibrated spectrometer (Chap. III), the irradiance or spectral irradiance can be measured. Assuming there is no attenuation between the radiating source and receiver, and the distance between

these two points is known, the radiant intensity can be determined by extrapolating to the emitting source. If  $d$  is the distance from source to receiver, then

$$I = d^2 E \quad (1-15)$$

Thus having obtained the spectral irradiance,  $E_\lambda$ , by direct measurement, the spectral radiant intensity of the source can be calculated. If the radiation is attenuated in traversing through a medium with transmission,  $\tau_\lambda$ , the spectral radiant intensity is given as a function of wavelength.

$$I(\lambda) = d^2 E(\lambda) / \tau(\lambda). \quad (1-16)$$

#### STANDARD UNITS, SYMBOLS, AND DEFINING EQUATIONS

The symbols and definitions of the most widely used radiometric quantities are given in Table I-1.

TABLE I-1

RADIOMETRIC QUANTITIES

<u>Quantity</u>	<u>Symbol</u>	<u>Units</u>	<u>Defining Equation</u>	<u>Definition</u>
Radiant Energy	Q	Joules		Energy traveling in the form of electromagnetic waves
Radiant Density	$\omega$	Joules/cm <sup>3</sup>	$\omega = dQ/dV$	Radiant energy per unit volume
Radiant Flux	$\phi$	Watts	$\phi = dQ/dt$	Rate of transfer of radiant energy
Radiant Exitance	M	Watts/cm <sup>2</sup>	$M = d\phi/dA$	Radiant flux density leaving an element of surface
Radiant Intensity	I	Watts/steradian	$I = d\phi/d\omega$	Radiant flux emitted from a source per unit solid angle in the direction considered
Radiance	L	Watts/ster-cm <sup>2</sup>	$L = d^2\phi/d\omega dA \cos\theta$	Radiant flux emitted from a source per unit solid angle per projected unit area
Irradiance	E	Watts/cm <sup>2</sup>	$E = d\phi/dA$	Radiant flux incident upon a surface
Wavelength	$\lambda$	Micrometers		
Temperature	T	degree Kelvin		
Emissivity	$\epsilon$	Numeric	$\epsilon = M/M_{\text{blackbody}}$	The ratio of the radiant emittance of a source to that of a blackbody at the same temperature
Transmittance	$\tau$	Numeric	$\tau = \frac{\phi_{\text{transmitted}}}{\phi_{\text{incident}}}$	Ratio of radiant energy transmitted to that received.

## CHAPTER II

### BACKGROUNDS AND TARGETS

A target is an object which is to be detected and perhaps tracked by means of infrared techniques. The infrared system must be capable of detecting the radiation emitted by the object while discriminating against the other sources of radiation reaching the detector. Since all bodies above the temperature of absolute zero emit infrared radiation, the extraneous (background) radiation will come from the parts of the instrument itself which the detector "sees" and from all objects in the field-of-view of the instrument. Although the ideal procedure will be to observe a hot object against a cold background so that the background radiation will be negligible compared to the target radiation, these optimum conditions will not generally be the case when measuring airborne targets.

Infrared targets include airborne, ground, and seaborne objects. Likewise, the detecting instrument may be situated in any of these media, so the background will differ depending on the conditions of the measurement. For our purposes, a target will consist of an aircraft moving in the earth's atmosphere with the sky as a background. It may be necessary at other times to consider the sea or the earth as a background, but our main concern will be with ground-to-air measurements. A description of the target will require knowledge of the infrared radiation from the

target as a function of wavelength, range, aspect angles, and atmospheric conditions.

Infrared measurements of low temperature sources, which could conceivably be lower than 200°C, are complicated by the effects of differing background radiation. The ground and the ocean emit and reflect variable amounts of infrared radiation depending on the nature of the surface, its temperature, and weather conditions. The continuous sky emission is caused by radiation emitted from the molecules in the atmosphere, and the remainder of the sky background is caused by sunlight scattered by the molecules, dust, aerosol particles and other particulate matter, and condensation products in the atmosphere. The cloud pattern will, of course, greatly affect the scattered radiation from the sun. In these cases, knowledge of the sky and earth radiation incident upon the aircraft and the detector will be necessary.

Depending on the range of the target and the field-of-view of the detecting instrument, a point-by-point scan of the emitted radiation provides more useful information than is provided when the target is entirely in the instrument's field-of-view. Thus, the use of a thermal image system would greatly complement the spectral information obtained by a spectrometer.

#### INFRARED EMISSION FROM AIRCRAFT

In general, a target will emit two types of radiation. The metal body of the target will emit a continuum of radiation related to the blackbody radiation from a source at some temperature. The



temperature will vary at different points along the aircraft. The aircraft will also exhibit a plume of hot gases, which are emitting infrared radiation consisting of complex band structure and perhaps also line and continuous spectra.

Infrared radiation is the result of a variety of quantum processes. There is continuous thermal emission, referred to as black-body radiation, which, for temperatures obtainable in the laboratory, lies in the infrared portion of the electromagnetic spectrum. The thermal emission is due to the electromagnetic radiation constantly being emitted and absorbed by particles in motion. Continuum radiation can also result from the processes of ionization and dissociation in atomic and molecular systems, but this is rare in the infrared. Discrete radiation takes two forms: line and band spectra. Line spectra are usually quite sharp and very intense and correspond to changes in the electronic states of atoms or molecules. Band spectra have a characteristic structure corresponding to a simultaneous change in the rotational and vibrational energies of molecules. The individual rotational lines can be distinguished, under high resolution, for the lighter molecules in such a vibrational band. The hot gases released by aircraft demonstrate all of the above types of emission processes. Although most of the heat is lost by conduction and convection to the surrounding metal parts of the aircraft and the air, a large fraction of the heat released by combustion is radiated in the infrared region.

The principal combustion products responsible for emission are :  
CO<sub>2</sub>, H<sub>2</sub>O, CO, OH, and C<sub>2</sub> in hydrocarbon fuels and N<sub>2</sub>O, NO, CN, NO<sub>2</sub>,  
SO<sub>2</sub>, HCL, and HF in other common fuels. Continuous spectra can be  
emitted by hot carbon particles, and free radicals in the exhaust  
can also provide continuum radiation.

Molecules can receive energy by absorption of radiation, by  
transforming kinetic energy from inelastic collisions with elec-  
trons or atoms, by resonance transfer of vibrational energy  
from other molecules which have absorbed energy, and by being  
produced in highly excited states as the result of chemical reactions.  
At the temperatures commonly found in the exhaust systems of air-  
craft, the molecules are found to be in excited vibrational states,  
which may have come about through any one of the above mechanisms.  
From these excited states, the molecules can decay to lower vib-  
ration-rotational levels accompanied by the release of a photon.  
The energy of this photon lies in the infrared region of the spectrum.

It can be seen that the emission from an aircraft will be very  
complicated and, in general, radiometric determinations of total  
spectral intensity will not be sufficient either to characterize  
the craft or for data analysis. Only spectral data, properly cali-  
brated, will yield detector-independent data which can be used in  
further calculations or for predictions of infrared emission under  
varying conditions. Because of the rapidly changing absorption  
and emission of both the target and the atmosphere, a knowledge of  
the spectral characteristics of both sources is necessary in order

to compensate for varying atmospheric conditions. A calculation of the atmospheric attenuation of the radiation emitted from the target must be carried out and radiometric data thus cannot be used.

The infrared emission at the source differs from the radiation which will be received at the detector due to the effects of atmospheric absorption. Kirchhoff's law gives the relationship between emission and absorption. A gas emits strongly only at wavelengths corresponding to absorption lines. Thus the spectral radiant intensity from the source is attenuated due to atmospheric  $\text{CO}_2$ ,  $\text{H}_2\text{O}$ , and  $\text{N}_2\text{O}$ . At higher altitudes ozone might also influence the absorption. Unless this attenuation can be well characterized, the spectral data will be limited in its usefulness.

The band centers of the vibration-rotation emission bands are shifted from the wavelengths usually given for absorption because the transitions are from highly excited states rather than the lowest-lying states. These shifts, of course, will depend upon the temperature of both the exhaust and the cooler surrounding atmosphere, but approximate wavelength locations can be given (Tables II-1 and II-2).

TABLE II-1

## MOLECULAR EMISSION BANDS (GAYDON)

<u>Molecular Species</u>	<u>Wavelengths of Emission</u>
CO <sub>2</sub>	1.99, 2.8, 4.4, 4.45, 14.9
H <sub>2</sub> O	0.95, 1.45, 2.8, 5.3, 5.5, 6.7
OH	2.8
CO	2.3, 4.6
C <sub>2</sub>	1.01, 1.2
CN	1.09
N <sub>2</sub> O	4.0, 4.75
NO	5.49

TABLE II-2

## MAJOR INFRARED ABSORPTION BANDS OF GASES (HERZBERG)

<u>Molecular Species</u>	<u>Approximate Centers in Microns</u>
H <sub>2</sub> O	1.88, 2.66, 2.74, 3.17, 6.27
CO <sub>2</sub>	1.96, 2.01, 2.06, 2.69, 2.77, 4.26, 4.68, 4.78, 4.82, 5.17, 15.0
CO	1.57, 3.24, 4.66
N <sub>2</sub> O	2.87, 3.90, 4.06, 4.54, 7.78, 8.57, 16.98
NO	2.67, 5.30
NO <sub>2</sub>	4.50, 6.17, 15.4
HCl	3.46
OH	1.99, 2.15, 2.80, 2.94, 3.08, 3.25, 3.43, 3.63, 3.87, 4.14, 4.47
SO <sub>2</sub>	4.0, 4.34, 5.34, 7.35, 8.69
CN	1.01, 1.20

The infrared emissions from aircraft depend on a great many variables. It will be necessary to categorize and standardize all procedures and variables so that data taken in many different laboratories will be meaningful. The universal nature of the spectra will depend totally on calibration of the spectra and detecting system. Procedures for achieving this will be specified later. Relevant information, such as fuel used, type of engine, fuel/oxidizer ratio, power settings, aspect angle, field of view, and atmospheric conditions present, must be specified if other laboratories are to use the data. Aspect angle is particularly crucial since the spectra may change from molecular band spectra at 90 degrees aspect to a continuum at 0 degree aspect. The range of the target from the detector, and density of the air mass will change the envelope of the spectra considerably so meteorological data must be obtained. Infrared measurements of aircraft thus are seen to present many problems of technique to workers in this field.

#### BACKGROUND RADIATION

The sources of infrared radiation can be classified into target and background sources. The target will be the object under study and the background is some distribution of radiant flux external to the object which interferes with and perhaps clutters the data received from the object. Since we would like to be able

to distinguish the target radiation from the background radiation, a knowledge of the variability and extent of background radiation would be helpful. The backgrounds we shall consider will be the radiance from the sky, ground, and ocean.

#### Clear-Sky Radiance

Just as is the case for aircraft, the downward radiation observed when there is a clear sky comes from a variety of sources:

The emission from various molecules in the atmosphere,

The thermal (blackbody) radiation from matter in the air,  
and

The scattering of radiation from the sun.

Just as in absorption, atmospheric emission is primarily due to  $H_2O$ ,  $CO_2$ , and  $O_3$  molecules, with the minor constituents providing very little emission. The spectral radiance of a clear sky due to thermal radiation is the product of the emissivity of the sky and the spectral radiance of a blackbody at that temperature. The effective temperature of the atmosphere is usually in the range of 200 to 300° K, so that the maximum emission occurs near 10 micrometers and has a value of approximately  $10^{-4}$  watt/cm<sup>2</sup>- $\mu$ m. At shorter wavelengths, the scattered sunlight predominates, so that the molecular emission can be neglected below 3  $\mu$ m in the daytime and is very small in this region at night. Beyond 4  $\mu$ m, the scattered sunlight can be neglected because the molecular emission is much larger (Fig-  
ures 2-1 and 2-2).

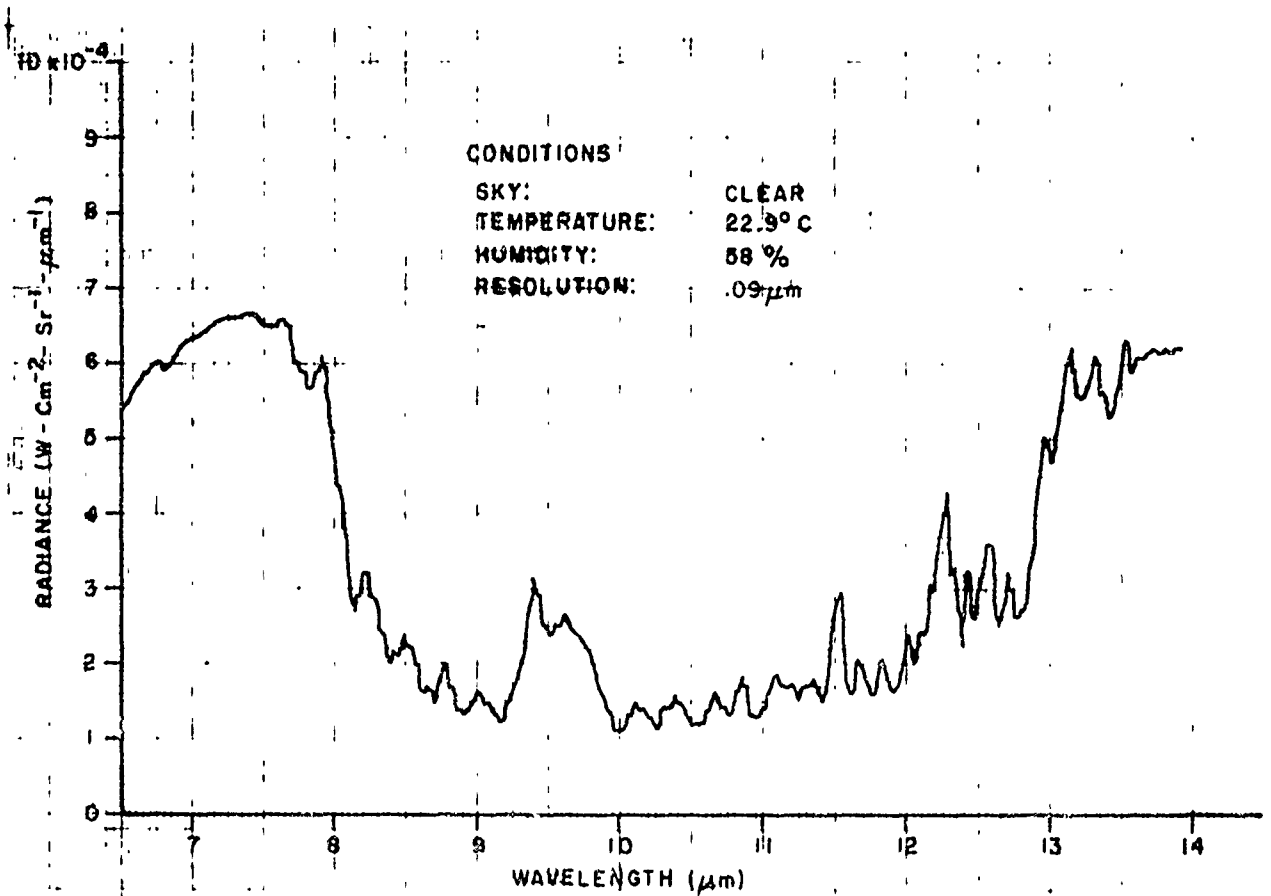


Figure 2-1. Sky Emission Spectra of Average Day, Temp. 22.9°C

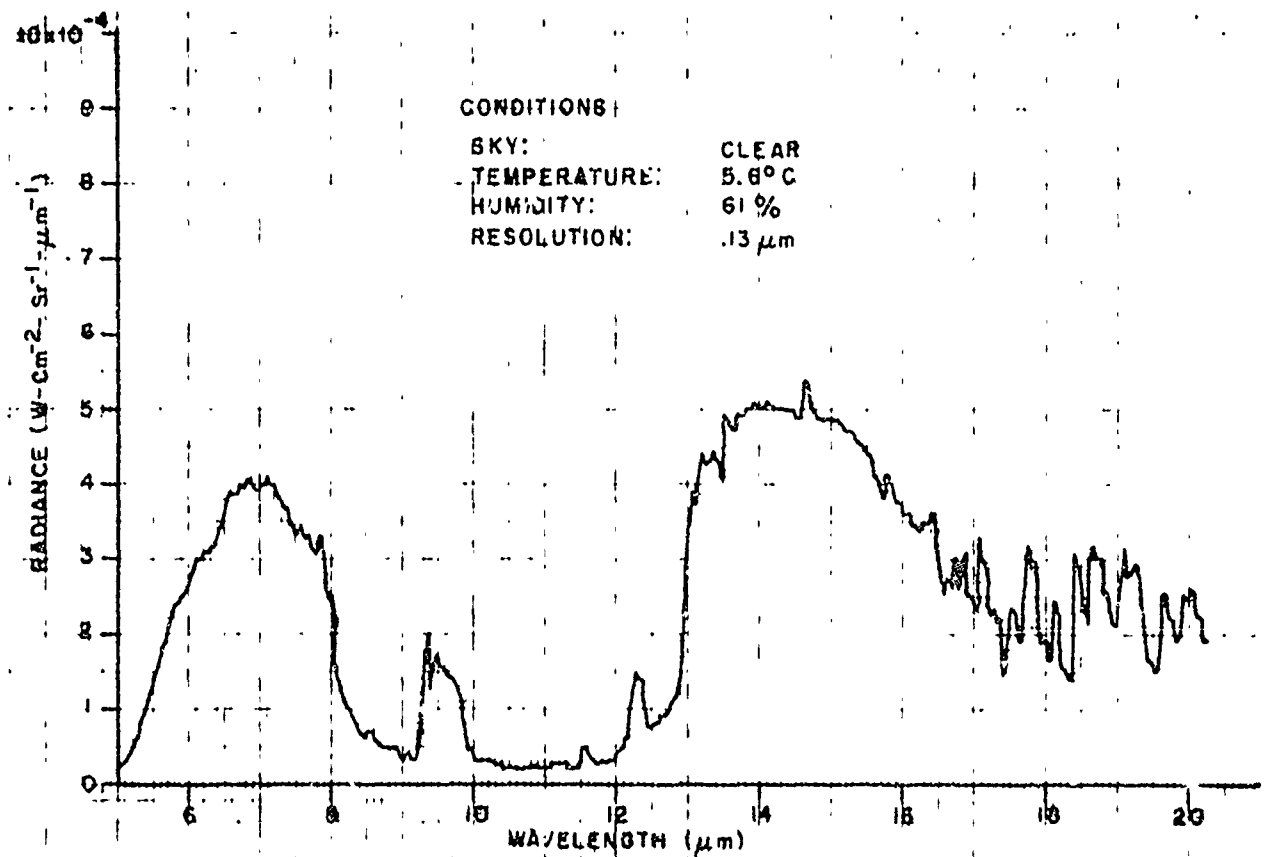


Figure 2-2. Sky Emission Spectra of Average Day, Temp. 5.6°C

Because the radiation from the sky is due to both molecular emission and scattering, the spectral radiance of a clear sky varies with air temperature, slant path or elevation angle, and water vapor content of the atmosphere. In any measurement, a background evaluation should be carried out to determine the magnitude of the extraneous flux reaching the detector from that source.

#### CLOUD RADIANCE

Since clouds are composed of water vapor, they will alter the radiance of the sky by scattering the sunlight incident upon their upper surfaces and by molecular emission from their lower surfaces. Because  $H_2O$  molecules are good absorbers, infrared radiation traversing a cloud layer is rapidly absorbed. But because a good absorber is a good emitter (Kirchhoff's law), a cloud radiates strongly in the normal atmospheric absorption bands. Usually, clouds are a few degrees colder than the ambient temperature on the ground, consequently they will radiate as blackbodies in the normal atmospheric window regions at lower temperatures than the intervening air mass.

#### GROUND RADIANCE

The radiant energy emitted by the ground is determined by the emissivity, reflectivity, and temperature of the ground. The radiation from terrain is the sum of the reflected sky radiation plus the radiation emitted by a blackbody at the surface temperature times the emissivity of the surface. For grassy terrain, approximately 15 percent of the incident radiation is reflected, that the emissivity of the surface is near 0.85. Below  $4 \mu m$  most of



the radiation is from scattered or diffusely reflected sunlight, while above  $4 \mu\text{m}$  the radiation corresponds to blackbody radiation attenuated by atmospheric absorptions. The daily variation of the radiance from various types of terrain follows the temperature change of the emitter. The radiance of the ground falls rapidly near sundown, more slowly throughout the night, and reaches a maximum shortly after noon. The scattered radiation below  $4 \mu\text{m}$  quite often is 10 times larger than the blackbody radiation near  $10 \mu\text{m}$ .

#### OCEAN RADIANCE

A water surface is a good reflector and a poor emitter. Thus, most of the radiation occurs below  $4 \mu\text{m}$  for such a surface. The waves on the ocean surface reflect light in different directions depending on their orientation, so sunlight can be reflected at very low elevation angles as well as the angle of incidence.

## CHAPTER III

### CALIBRATION

The calibration of instrumentation used to measure the characteristics of infrared electromagnetic radiation is complex and probably the most difficult part of a measurement. At the same time, the calibration step is the most important procedure in any measurement. The purpose of a calibration is to make the measurement independent of the measuring instrument. The data which results from the measurement must mean something to someone else in the same field. In order to achieve this aim, standard calibration procedures have been set up.

Our principal aim is to measure and characterize the radiant emission of Army' aircraft (slow-moving, low-flying objects with fairly low exhaust temperatures). The values of radiant intensity should be referred to blackbody calibration sources traceable to the National Bureau of Standards (NBS) so that all interested laboratories can readily interpret each other's results.

The exact details of the calibration of an infrared instrument depend on the type of instrument, the spectral region in which it operates, the type of measurement to be performed, and the operator's familiarity with the instrument. As closely as possible, the calibration technique should follow the actual techniques to be used in the measurement.

Radiometers and spectrometers are the primary instruments used to measure infrared radiation. Because broadband missile seekers are sometimes used in the overall measurement of aircraft, the calibration of broadband radiometers, as well as spectral instrumentation, will be discussed.

#### RADIOMETRIC CALIBRATION

The calibration of broadband radiometers specify the essential characteristics of the particular instrument in use. The characteristics listed should enable another worker in the field to recognize and assess the capabilities of the instrument. This requires a knowledge of the spectral response, sensitivity, resolution, field-of-view, frequency response, and the noise level of the radiometer.

The two primary parameters that are determined by the calibration of a broadband radiometer are the spectral response and the Noise Equivalent Irradiance (NEI).

#### Relative Spectral Response

Thermal detectors, such as thermocouples or bolometers, have a spectral response which is uniform over a very wide wavelength interval. Because photon (selective spectral response) detectors are much more sensitive than thermal detectors, they are preferred for use in detecting low-intensity radiation sources; however, they respond only to finite wavelength intervals. There are many such detectors, and appropriate ones can be found for almost any wavelength range of interest.

Because of the wavelength-selective nature of photon detectors, it is necessary to characterize their response and to include this parameter in the calibration procedure.

The following symbols will be used in the succeeding discussion.

$V(\lambda)$  = the voltage output of the system

$R(\lambda)$  = the response of the system to some amount of radiation

where

$$R(\lambda) = V(\lambda) / E(\lambda) \quad (3-1)$$

$E(\lambda)$  = the irradiance produced by the source at the radiometer aperture

$A_s$  = the aperture area of the calibration source

$A_d$  = the area of the radiometer aperture or area of the collecting optics

$M_\lambda$  = the blackbody spectral radiant exitance

$d$  = the distance from the source to the radiometer aperture

Assume the source of the radiation is an NBS traceable blackbody at temperature  $T$ , then the spectral radiant exitance is given by the Planck equation

$$M_\lambda = \frac{c_1}{\lambda^5 \exp(c_2/\lambda T) - 1} \quad (3-2)$$

In the absence of an attenuating medium between the source and receiver, the irradiance at the radiometer collecting optics is given by

$$E_\lambda = I_\lambda / d^2 \quad (3-3)$$

For a thermal detector, such as a thermocouple or bolometer, the spectral response is relatively flat so that it may be considered constant over suitable wavelength intervals. Then  $R$ , the constant of proportionality between the irradiance produced at the collecting optics and the voltage output of the radiometer, is a true constant over the wavelength interval. The wavelength interval being considered in this case is the effective bandpass of a photon detector used in the radiometer. For the thermal detector then, the output voltage produced by irradiation over the wavelength interval from  $\lambda_1$  to  $\lambda_2$  is

$$V = \int_{\lambda_1}^{\lambda_2} R E(\lambda) d\lambda \quad (3-4)$$

A dispersive monochromator or series of narrow bandpass filters can be used as spectrally selective elements to isolate narrow portions of the spectrum. The wavelength interval selected by either the bandpass filters or the monochromator must be sufficiently small so that the responsivity of the detector is essentially constant over the wavelength interval (the quantum detector in this case). The essentially monochromatic radiation so produced is used as the irradiating source upon the system being calibrated and on a spectrally nonselective thermal detector. Both detectors are positioned so that they are completely and uniformly irradiated by the energy from the source, and the pathlength and traversal of the optics should be made as uniform as possible. The voltage developed by the nonselective detector can be expressed as some function of the following variables

$$v_t(\lambda) = E(\lambda) \cdot (\lambda) R_t(\lambda) \quad (3-5)$$

Thus, the output voltage of the thermal detector depends upon the spectral irradiance at the collecting optics, the spectral transmissivity between source and detector, and the spectral responsivity of the detector. Note that in this case

$$R_t (\lambda) = R \quad (3-6)$$

R is a constant.

Similarly, when irradiated by the same spectrally selective device, the voltage developed by the photon (quantum) detector to be calibrated can be expressed by

$$V_q (\lambda) = E (\lambda) \tau (\lambda) R_q (\lambda) \quad (3-7)$$

where

$$R_q (\lambda) = \text{Response of the selective detector}$$

Now, taking the ratio of the two detector outputs over the spectral bandpass of the photon detector yields

$$\frac{V_q (\lambda)}{V_t (\lambda)} = \frac{E (\lambda) \tau (\lambda) R_q (\lambda)}{E (\lambda) \tau (\lambda) R (\lambda)} \quad (3-8)$$

If the radiation from the source traverses optically identical paths to both detectors so that both are irradiated with the same amount of radiation at the detector, then the voltage ratio can be expressed as

$$\frac{V_q (\lambda)}{V_t (\lambda)} = \frac{R_q (\lambda)}{R} \quad (3-9)$$

where the effects of atmospheric attenuation have been cancelled, and all other identical factors have been dropped,

Considering the relative spectral response of the thermocouple or bolometer to be essentially flat across the spectral bandpass of the quantum detector, the responsivity of the radiometer, relative to the thermal detector, is given by the variation of the two voltages over the particular wavelength interval used. This relative responsivity is then normalized to unity and plotted as a function of wavelength.

$$R_q(\lambda) = \frac{V_q(\lambda)}{V_t(\lambda)} \quad (3-10)$$

#### Absolute Spectral Response

Assuming the system to be linear, i.e., if a change in incident radiation produces a corresponding change in output voltage, once the relative response curve has been experimentally established, the absolute spectral response of the system can be obtained.

For these linear cases, the absolute spectral response is proportional to the relative spectral response, and it suffices to measure the absolute value of the spectral response at some wavelength, usually the peak of the response curve. As a check on linearity, the absolute value of the spectral response should be measured over a variety of wavelengths.

Let the maximum value of the relative spectral response curve be  $R_q(\lambda_m)$ , and the relative response curve be denoted by  $f(\lambda)$ , then

$$R_a(\lambda) = f(\lambda) R_q(\lambda_m) \quad (3-11)$$

where

$R_a(\lambda)$  = absolute response

If the radiometer is exposed to a blackbody standard source of spectral irradiance,  $E_\lambda$ , and the voltage output of the radiometer is recorded as  $V_t$ , this can be expressed as

$$V_t = \int_{\lambda_1}^{\lambda_2} V_q(\lambda) d\lambda \quad (3-12)$$

where  $\lambda_1$  and  $\lambda_2$  are the spectral bandpass limits of the detector but the voltage of the detector at any one wavelength is

$$V_q(\lambda) = E(\lambda) R_a(\lambda) \quad (3-13)$$

so that

$$V_t = \int_{\lambda_1}^{\lambda_2} E(\lambda) R_a(\lambda) d\lambda \quad (3-14)$$

In terms of the relative response curve, the output produced by the radiometer is

$$V_t = \int_{\lambda_1}^{\lambda_2} f(\lambda) R_q(\lambda_m) E(\lambda) d\lambda \quad (3-15)$$

but  $R_q(\lambda_m)$  is a constant, and the value of  $E(\lambda)$  can be calculated either from Planck's radiation law or obtained from standard blackbody tables.

Then, since  $V_t$  is determined experimentally, and the integral can be evaluated either numerically or graphically, the value of  $R_q(\lambda_m)$  can be determined. The value of  $R_q(\lambda_m)$  should be checked by varying the temperature of the blackbody source.



By defining the maximum value of the relative spectral response curve in absolute terms and multiplying all other points on this curve by the maximum value, an absolute spectral response curve can be constructed for the radiometer.

#### Irradiance Responsivity

The ratio between radiometer output and incident radiation input is called the radiometer responsivity. There are three major types of radiometric responsivity: power, irradiance, and radiance. Since the scale used for calibration and measurement is established in terms of the radiometric quantity of interest as measured at the collecting optics of the instrument, the irradiance responsivity as measured in volt-cm<sup>2</sup>/watt was chosen.

The wavelength interval in which the radiometer is sensitive is not determined strictly by the detector response, for the spectral characteristics of the optical components (filters, mirrors, gratings, and prisms) limit the bandpass of the instrument. Two approaches can be taken to obtain the spectral responsivity of the radiometer: one is to compute the overall spectral responsivity from data for the spectral characteristics of all of the components involved; the other, to make direct measurements of the relative responsivity of the complete radiometer taken as a unit (as a function of wavelength). A calibration should reproduce as closely as possible the conditions to be used in making measurements. For this reason, a spectral responsivity calibration of the entire instrument is to be preferred.

In order to determine the absolute spectral responsivity of a radiometer, an experimental determination of the relative spectral response of the instrument must first be accomplished. Then a sensitivity measurement is carried out by measuring the voltage of the system when the detector is irradiated by a source of known spectral irradiance, an NBS traceable blackbody.

#### Noise Equivalent Irradiance

The NEI is merely a different form of specifying the noise-equivalent power. NEI is the minimum intensity of radiant energy falling on the surface of the detector which will give rise to a signal voltage equal to the noise voltage of the instrument.

To determine the NEI, the instrument is aligned in the collimated beam of radiation produced by a collimating optics equipped with a blackbody source and a set of apertures to vary the radiant intensity. The collimator exit aperture should be large enough to permit the entire entrance aperture of the radiometer to be filled by the collimated beam, and the system should be purged with dry nitrogen to eliminate atmospheric absorption.

The irradiance produced by a collimated blackbody source may be calculated from the Planck equation and the constants of the collimator.

$$E = \frac{\epsilon_m^n A_s}{\pi f^2} \int_0^{\infty} E_\lambda d\lambda \quad (3-16)$$

where

$A_s$  = the source aperture area

$\epsilon_m^n$  = the reflectance of the collimator mirrors

$n$  = the number of mirror surfaces

$f$  = the focal length of the collimator

The results of such a calculation are shown in figure 3-1.

In determining the NEI, the quantity of primary interest is the irradiance within the spectral bandpass of the instrument. This equation is expressed as

$$E_{\text{eff}} = \frac{\epsilon_m^n A_s}{\pi f^2} \int_{\lambda_1}^{\lambda_2} f(\lambda) E_\lambda d\lambda \quad (3-17)$$

The voltage output of the radiometer is measured for several entrance aperture areas and blackbody temperatures. A best-fit straight line plot of output voltage versus effective irradiance is constructed. The equation of this line will have the form

$$V = R E_{\text{eff}} + C \quad (3-18)$$

where

$R$  and  $C$  are constants

The NEI is then determined by measuring the noise voltage and solving this equation for  $E_{\text{eff}}$ . This value of NEI and the relative response is used for data analysis particularly in the calculation of lock-on ranges of various missile seekers.

#### FIELD CALIBRATION

The preferred method for field calibration is to use a standard blackbody source positioned some distance away from the instrument or at the entrance aperture of a collimator (housed in a moveable van), and to take measurements of this source between successive target

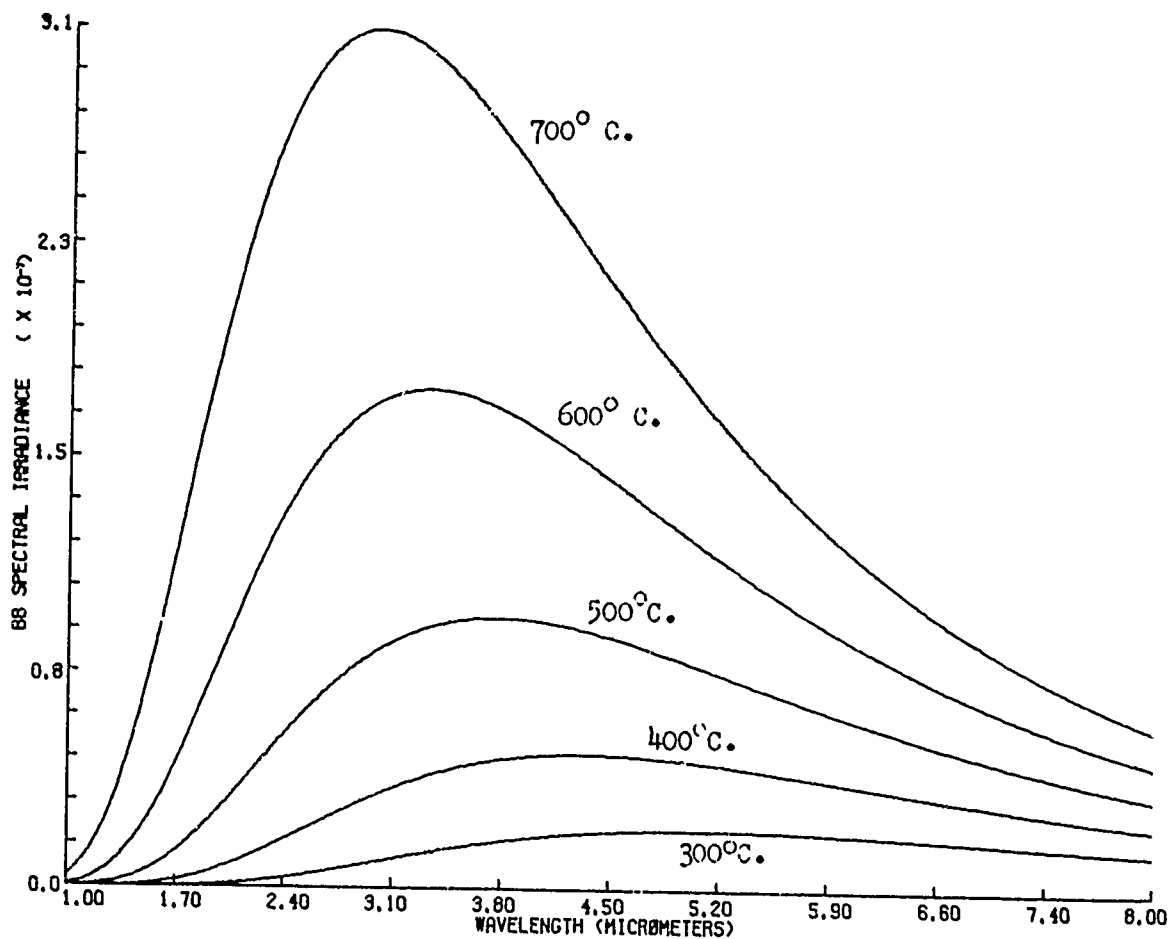
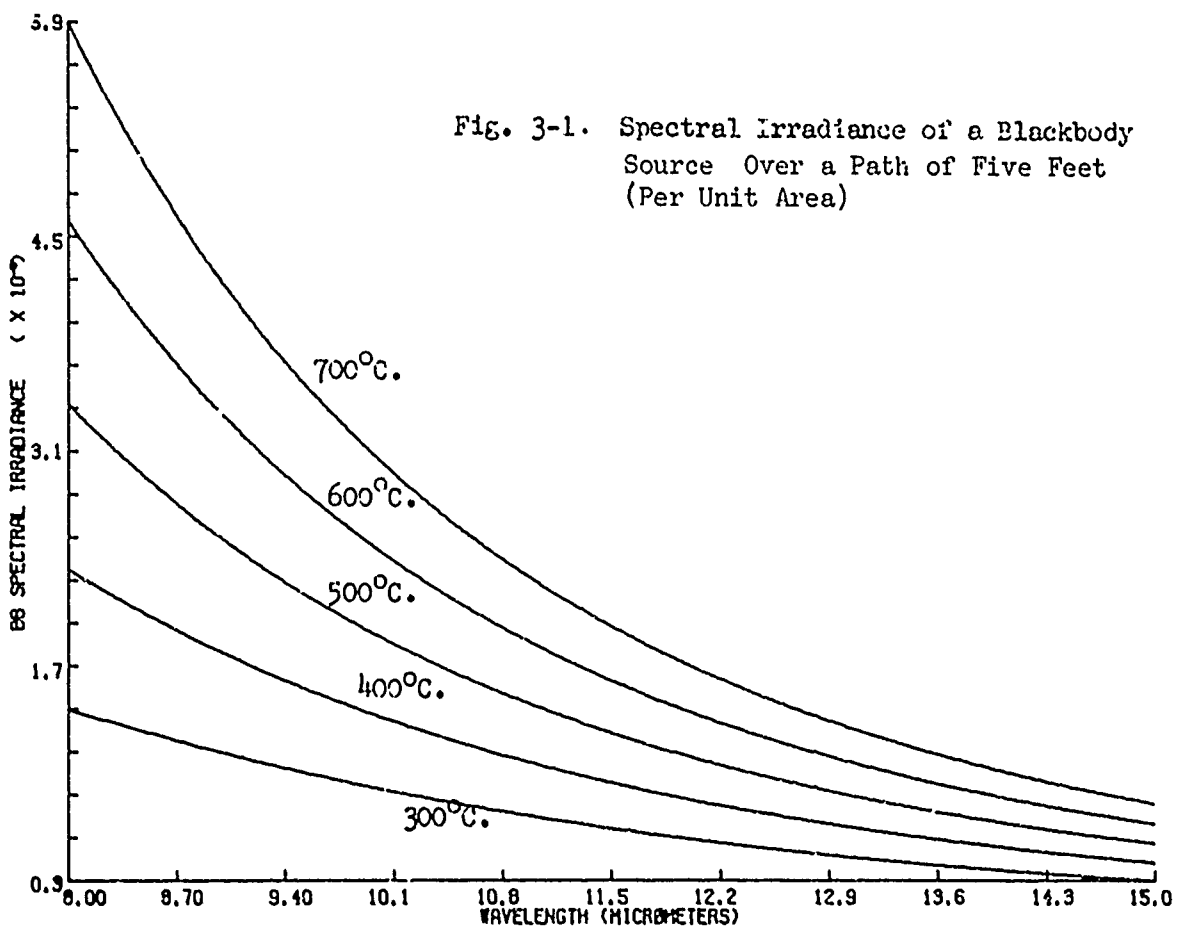


Fig. 3-1. Spectral Irradiance of a Blackbody Source Over a Path of Five Feet (Per Unit Area)



measurements. Note that some provision for atmospheric attenuation must be provided if the optical path between source and receiver is not purged. The use of a collimator makes this feasible, but the instrument must be removed from its pedestal.

#### SPECTROMETER CALIBRATION

Two primary parameters of a spectrometer must be determined by calibration: spectral dispersion, the wavelength dependence of some mechanical variation within the instrument, and absolute spectral response as a function of wavelength. A third parameter, the spectral resolution, must also be known either by experimental means or by calculation.

A spectrometer selects a narrow portion of the radiation incident upon it and selectively focuses this narrow band of energy upon the detector. The selective character of the transmitted radiation may be the result of the rotation of a prism, a grating, a mirror, or a circular variable filter. In all of these cases, the different wavelengths of light are dispersed, or spread out, and only a small portion of this radiation reaches the detector. As the active element is continuously rotated, the entire wavelength interval of interest sweeps across the detector. Thus, a spectrometer may be considered to be a series of radiometers of very narrow bandpass, equal in this case to the resolution of the instrument. Knowing the spectral dispersion of the instrument provides an association of wavelength with some measured mechanical readout of the rotation of the active element within the spectrometer.

The technique for determining the spectral dispersion is the same for all wavelengths, but the materials used vary. If the dispersion is linear, only two points on a plot of wavelength vs rotation need be determined, but in the usual case, the nonlinearity of the dispersion must be measured. The spectrum is taken of a sample of material (either absorbing or emitting), which has a number of sharp spectral lines throughout the region of interest. The wavelengths or frequencies of these lines are then plotted on the dispersion curve. Polystyrene absorption film can be used for instruments operating between 3 and 15 micrometers. In dispersion calibration for instruments operating down to about one micrometer,  $H_2O$  vapor and  $CO_2$  atmospheric absorption lines can be identified. For instruments operating in the near-infrared, there are many gas discharge tubes that may be used. The dispersion curve must contain enough points to clearly define the spectral dispersion of the instrument.

Occasionally, narrowband interference filters are used to isolate a narrow spectral region, and the peak of the transmission curve is assigned some wavelength. The use of these filters for wavelength dispersion calibrations is recommended for approximate measurements only. If they are used at all, the shift in the peak of the transmission curve must be considered. All filters are designed for normal incidence; as the angle of incidence increases, the peak wavelength of the filter is reduced. This shift in wavelength can be seen by considering the following diagram (figure 3-2).

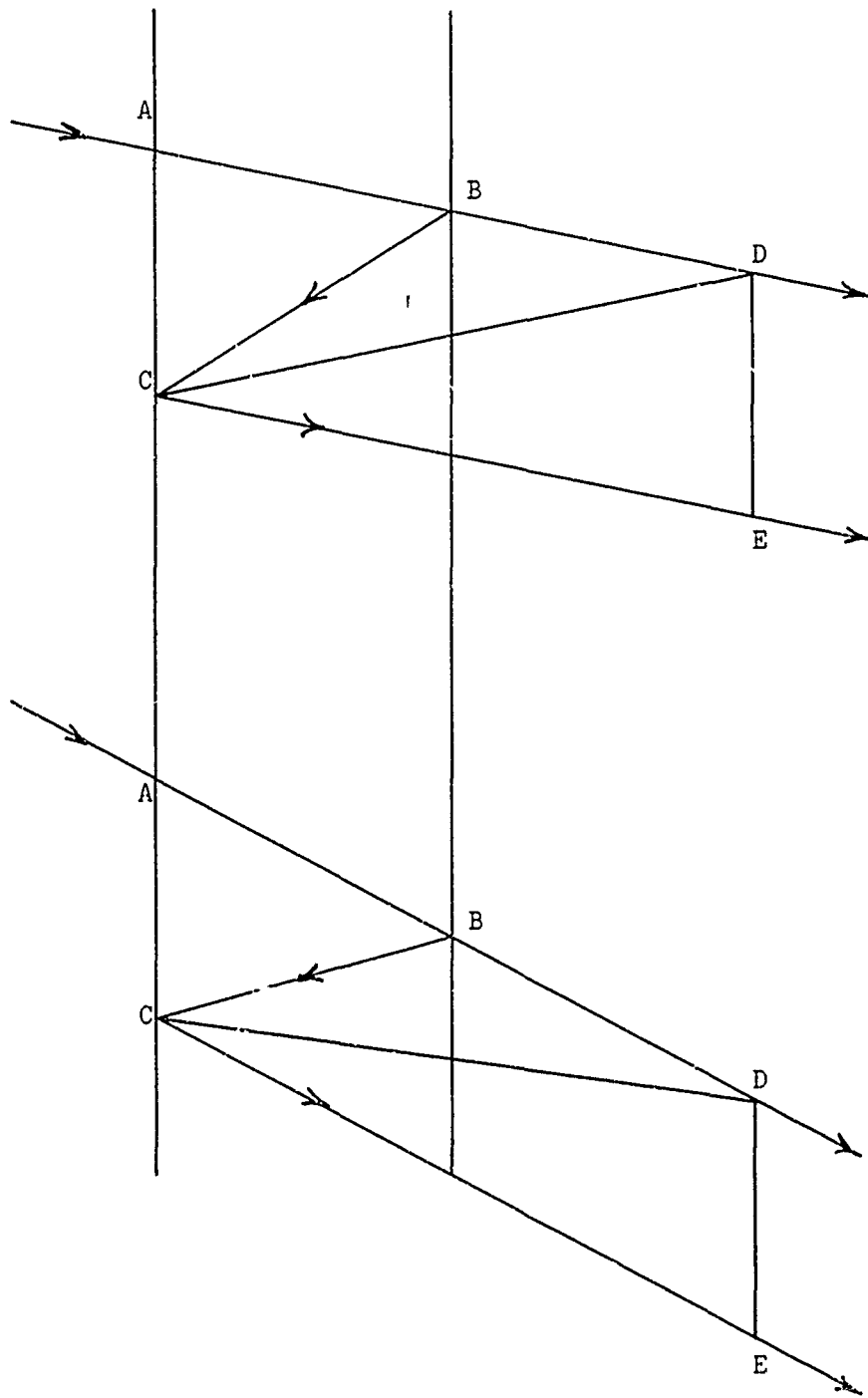


Figure 3-2. Variation in Path Distance for Varying Angles of Incidence

The incident beam enters at point A and is partially reflected at points B and C. Neglecting refractive index changes, the two beams travel the same distance to points C and D (BD = DC); the path difference is CE. The above two examples show that this path difference (CE) becomes shorter at greater incidence angles; therefore, the peak wavelength of a filter will decrease.

The equation for predicting this shift in wavelength is

$$\frac{\lambda_a}{\lambda_n} = \frac{\sqrt{n^2 \sin^2 a}}{n} \quad (3-19)$$

where

a = angle of incidence

$\lambda_a$  = peak wavelength at angle A

$\lambda_n$  = peak wavelength of normal incidence

n = effective index of refraction of the filter

For small angles, the shape of the bandpass does not change appreciably except for a small decrease in overall transmission. At larger angles, the center of the peak is flattened until two peaks appear. This is due to the differing effective index of refraction for the two planes of polarization. The "p" component (parallel) exhibits less shift than the "s" component (perpendicular).



The transmission of a narrowband filter also will shift according to the spectral distribution of the incident radiation. For the above reasons the filter transmission characteristics should be measured under the same conditions used when determining the spectral dispersion of a spectrometer.

The resolution, or sharpness, of these filters generally is not good enough to unambiguously characterize the transmission peak to sufficient accuracy for calibration purposes. For all of the above reasons, use of narrowband interference filters for wavelength calibration is discouraged.

#### Absolute Spectral Response

The absolute spectral response is determined in much the same manner as that of a radiometer, but because a spectrometer acts like a narrowband radiometer, the absolute spectral response can be determined directly. No relative response curve is necessary. A standard black-body source is used to irradiate the optics of the instrument. The Planck equation is integrated over a wavelength equal to the resolution of the instrument to determine irradiance values. Thus, in principle, a spectrometer is easier to calibrate than a radiometer, although the mathematics and data reduction become more complex.

A standard blackbody source should be used as the calibration standard. Several commercial blackbody sources are available for this purpose, all of which require frequent calibration checks. These sources normally operate at temperatures up to 1000° C. The higher temperature sources are needed when calibrating visible and UV spectrometers. Tungsten ribbon lamps that operate at greater than 2700° C are available and are generally used in the visible and UV regions of the spectrum. Although the lamps approximate blackbodies, they require frequent calibration. Any source of continuous radiation could be used to calibrate spectrometers provided the spectral emission is absolutely known. However, usually it is not practical to use a source other than a blackbody or standard lamp.

#### RESOLUTION

The resolution, or resolving power, of an instrument is its ability to distinguish between two adjacent spectral lines. The ability of an instrument to separate two closely spaced spectral lines rather than blending them into one broad line is limited. The resolving power can be expressed as the ratio of the wavelength observed to the smallest difference

between two wavelengths which can just be resolved or distinguished as individual lines. The ratio  $\frac{\lambda}{\Delta\lambda}$  is then the resolving power. Its reciprocal is sometimes used in terms of percentages to distinguish the highest obtainable resolution. Actual working resolution is a function of the slit width, adjustment of the optics, time constant of the instrument and detector time constant, and speed of scan. Resolution should be measured experimentally by trying to resolve two closely spaced lines such as in the atmospheric absorption of water vapor.

#### OTHER PARAMETERS

Additional parameters that apply to both radiometers and spectrometers must be known. The response as a function of target position within the field-of-view, and the frequency or modulation response. These two parameters, while being relatively simple to determine, are extremely difficult to apply in data reduction. The response as a function of field-of-view is determined by use of a collimated point source and an indexing table to provide instrument output as a function of aspect angle. Then a contour plot of the field-of-view response can be constructed. To apply this information to data reduction and analysis, an accurate boresight camera must be used. When accurate

collimation of the optical axis of the camera and instrument has been achieved, the position of the target with respect to the optical axis can be determined. The instrument designer strives to produce an instrument that has a uniform response across the field-of-view. However, perfect alignment of the instrument must be maintained, and frequent checks of the field-of-view response are necessary. The problem of field-of-view response of a spectrometer is even more complex because the target position in the field-of-view may cause dispersion to shift slightly.

The frequency, or modulation, response in most cases is not difficult to take into account. Usually determining the time constant of the instrument is sufficient. However, when the target is an aircraft, it is possible that at certain aspects the radiation emitted by the target or background will pass through the rotor blades or props and be modulated at relatively high frequencies, which is a problem that must be considered. For the case of broadband radiometers, the response as a function of frequency is usually considered to be independent of the wavelength of incident energy. However, this is not strictly true, and the frequency response must be considered when spectral measurements are performed.

## CALIBRATION OF SOURCES

Since the target measurement is based upon the calibration of the instruments, it is very important that standard sources known to be accurate are used for calibration. Several laboratories throughout the United States calibrate these sources: the Army at Redstone Arsenal, Huntsville, Alabama; the Air Force at Newark Air Force Station, Newark, Ohio; the Navy at Point Mugu, California; the Army at White Sands Missile Range, New Mexico; and Eppley Laboratories, Inc., Newport, Rhode Island. The National Bureau of Standards at Gaithersburg, Maryland, maintains national primary standards which are sent to laboratories around the country both for calibration of the standard and certification of the laboratory. Laboratories which have been certified by NBS are capable of calibrating blackbody standards to within one percent of each other and of NBS. All blackbody sources used for calibration purposes must be NBS traceable to insure accurate data.

## CHAPTER IV

### MEASUREMENT TECHNIQUES

The type of test or measurement depends upon the objectives of the program undertaken. Since it would be impossible to discuss in detail all objectives that might be required, this chapter presents a general discussion of infrared measurement techniques before going into the specific problem of obtaining the infrared signature of slow-moving aircraft. The type of data which can be obtained in air-to-air, ground-to-ground, and ground-to-air measurements should be chosen to fulfill the mission requirements.

Several techniques can be utilized to measure infrared radiation. These techniques can be generally categorized into radiometric (broadband) and spectral (narrowband) measurements.

The voltage produced by radiation incident upon a detector can be expressed for either a broadband radiometer or a narrowband spectrometer

by the equation:

$$V = \frac{1}{d^2} \int_{\lambda}^{\lambda + \Delta\lambda} R(\lambda) \tau(\lambda) I(\lambda) d\lambda \quad (4-1)$$

where:  $d$  = Distance from detector to target

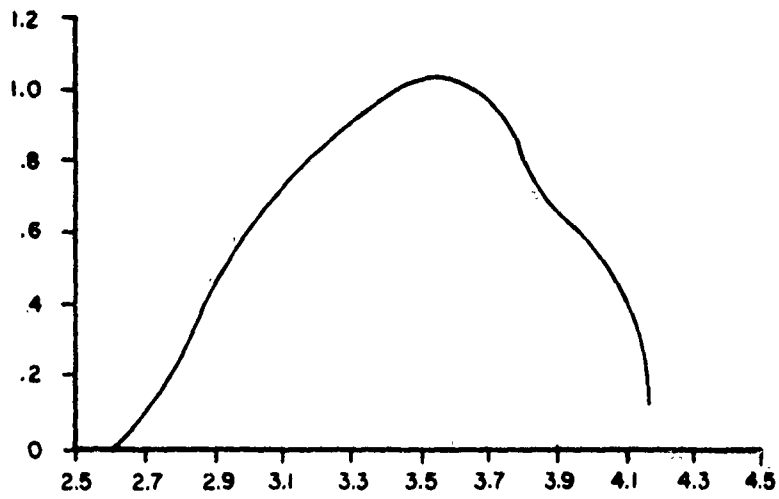
$R(\lambda)$  = Responsivity of the instrument as a function of wavelength

$I(\lambda)$  = Spectral radiant intensity of the target

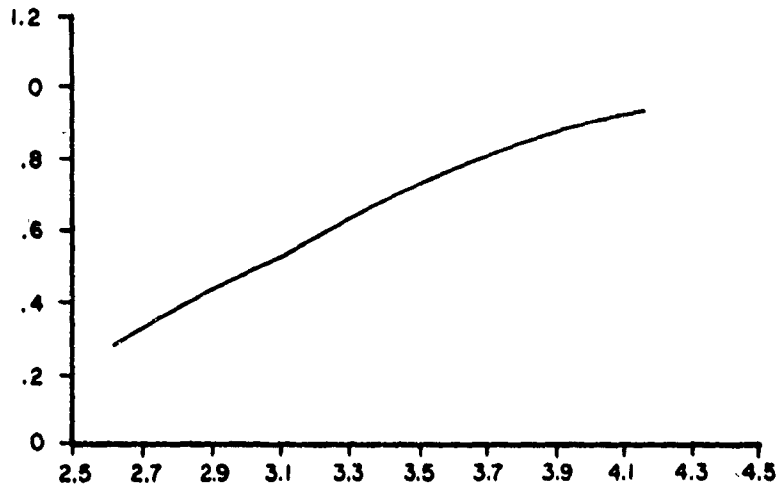
$\tau(\lambda)$  = Atmospheric transmission as a function of wavelength

For the case of a broadband radiometer, the limits of the integration,  $\lambda$  to  $\lambda + \Delta\lambda$ , span the bandpass of the instrument. One number, the total value of the integral, is the resultant of the radiometric measurement. Knowing the responsivity of the detector, the distance from the target, and the voltage output does not determine the radiant intensity of the target unless the attenuation by the atmosphere is also known. Because the absorption of radiation by the atmosphere is a rapidly changing function of wavelength, pathlength, absorber concentration, pressure, and temperature, its effect is not easily determined. One cannot utilize the atmospheric transmission function or the responsivity of the detecting instrument unless the spectral distribution of the target is known. Thus, since the spectral distribution is the needed parameter, radiometric measurements yield only the relative energy levels of a target as detected by the particular instrument. The data cannot be compared with or applied to other instruments with different responses or for different atmospheric conditions.

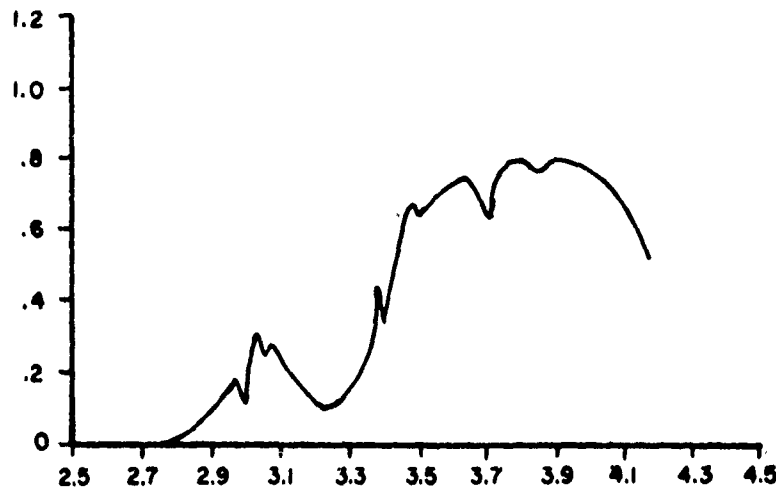
The fact that the total value under the integral sign of equation 4-1 is the only numerical result of a radiometric measurement can be more easily understood by considering a radiometer with a spectral response as shown in figure 4-1, measuring a source with a spectral distribution as shown in figure 4-2, and viewing the source through an atmosphere with a transmission as shown in figure 4-3.



**Figure 4-1. Relative Spectral Response.**



**Figure 4-2. Target Spectral Radiant Intensity.**



**Figure 4-3. Atmospheric Transmission.**



The irradiance incident upon the radiometer and producing the output voltage will have a spectral distribution which is the point-by-point product of the curves of figures 4-2 and 4-3. This product is shown in figure 4-4. Each wavelength of the incident irradiance will cause a response in the instrument according to the response curve and produce a voltage output represented by the point-by-point product of figures 4-1 and 4-4. This product is shown in figure 4-5 and the area under this curve corresponds to the integral which is representative of the voltage output.

The integral of the curve of figure 4-5 expressed mathematically is then:

$$V = \int_{\lambda}^{\lambda + \Delta\lambda} R(\lambda) \tau(\lambda) E(\lambda) d\lambda \quad (4-2)$$

which is the same as equation 4-1 without the factor  $1/d^2$  converting radiant intensity to irradiance.

Thus, it can be easily seen that the voltage will change when the atmospheric transmission (figure 4-3) or the spectral distribution (figure 4-2) of the target radiation changes. The total value of the target radiant intensity can remain constant with a change in its spectral distribution. Thus, two different aircraft employing two different types of fuel could conceivably produce the same total radiant intensity even through their emissions are at different wavelengths lying within the bandpass of the radiometer.

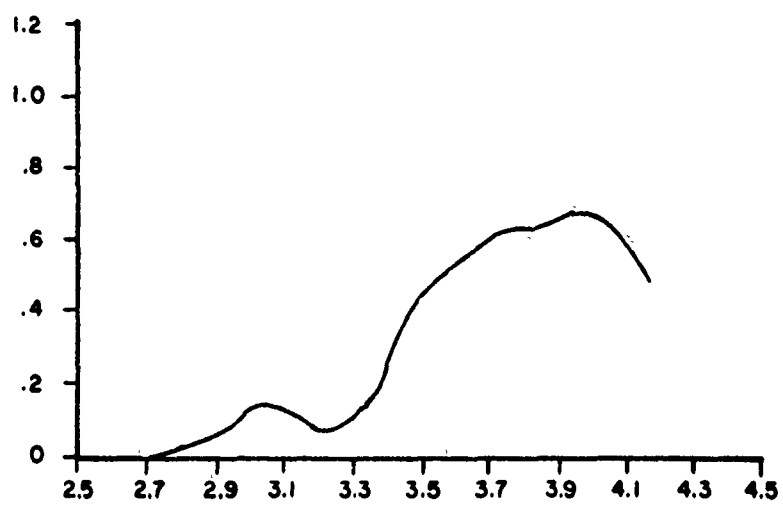


Figure 4-4. Target Spectral Irradiance

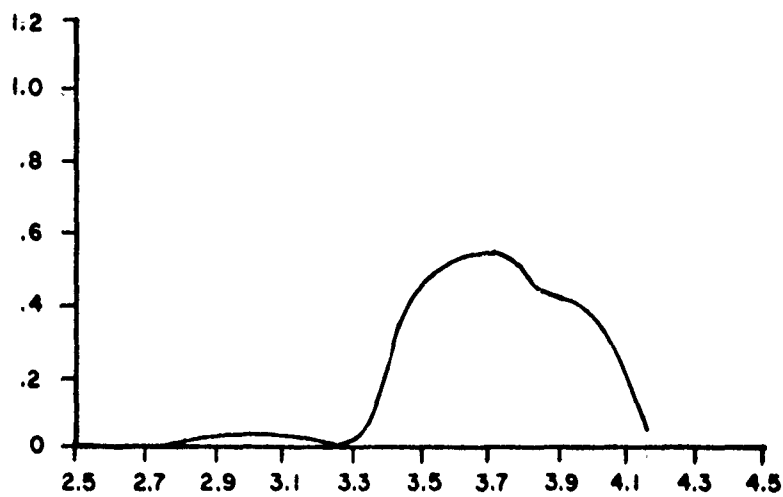


Figure 4-5. Instrument Response To Spectral Irradiance

To obtain meaningful radiation characteristics of an aircraft, it is necessary to describe the spectral radiant intensity of the target. This data then shows the regions in which lie the aircraft's vulnerability to infrared detection. The main difference in the voltage output expression (equation 4-1) for a spectrometer is that the wavelength interval,  $\Delta\lambda$ , is sufficiently narrow so that the response of the instrument is constant; therefore, the atmospheric transmission data can be utilized. Therefore, with the instrument response and the atmospheric transmissivity known, the value of radiant intensity for the wavelength interval,  $\Delta\lambda$ , can be determined. The narrower the spectral resolution, corresponding to  $\Delta\lambda$ , the more accurately the spectral characteristics of the target can be determined.

Most spectrometers for field use are designed to scan a relatively wide spectral region so quickly that the radiant exitance of the target does not change. The result is absolute spectral radiant intensity as a function of time, aspect angle, or other parameter of interest. Spectral data of this type is suitable for further analysis as it contains a great deal of information. A spectrometer (or spectro-radiometer) suitable for this type of measurement should be capable of a resolution below one percent of the instantaneous wavelength. In essence, a spectrometer provides instantaneous radiometric data as a function of wavelength.

#### SPECTRAL MEASUREMENTS

To obtain the absolute spectral radiant intensity of a target, the background radiation and the internal reference radiation of the instrument must be considered. When measuring a target, the output of a typical spectrometer will represent an energy level given by

$$\Delta E_t(\lambda) = \omega_t L_t(\lambda) + \omega_R L_b(\lambda) - \omega_t L_b(\lambda) - \omega_R L_R(\lambda) \quad (4-3)$$

where

- $L_t$  = Spectral radiance of the target
- $L_b$  = Spectral radiance of the background
- $L_R$  = Spectral radiance of the reference source
- $\omega_R$  = Solid angle field-of-view of the instrument
- $\omega_t$  = Solid angle subtended by the target

Equation 4-3 shows that the irradiance represented by the instrument output is the sum of that of the target and background, minus the background obscured by the target, minus the irradiance of the reference source.

A background measurement can be performed to determine the value of the term  $\omega_R L_b(\lambda)$ . In the background measurement the spectral irradiance observed by the instrument can be expressed as

$$\Delta E_b(\lambda) = \omega_R L_b(\lambda) - \omega_R L_R(\lambda) \quad (4-4)$$

Therefore, by measuring the background and target separately and subtracting the background

$$\Delta E(\lambda) = \Delta E_t(\lambda) - \Delta E_b(\lambda) = \omega_t L_t(\lambda) - \omega_t L_b(\lambda) \quad (4-5)$$

But  $\omega_t L_t(\lambda)$  is the spectral irradiance of the target only, and this is the result we wish to determine. Thus, by adding to  $\Delta E(\lambda)$ , the amount of background energy obscured by the target,  $\omega_t L_b(\lambda)$ , we arrive at our result.

$$\omega_t L_t(\lambda) = \Delta E(\lambda) + \omega_t L_b(\lambda) \quad (4-6)$$

In order to find  $\omega_{\dagger}L(\lambda)$ , it is necessary to know the target distance and area of its projected surface since

$$\omega_{\dagger} = A_{\dagger}/d^2 \quad (4-7)$$

Therefore, an absolute measurement can be performed only:

1. When the target can be considered a point source, i.e.,  $\omega_{\dagger}$  is very small compared with  $\omega_R$
2. When the area and distance of the target are known, or,
3. When the background radiation is negligible

Any measurement must utilize one of these three methods for dealing with the background radiation.

#### CONTRAST TECHNIQUES

Since some missile seekers might operate by the contrast method, an understanding of this technique is necessary. The irradiance detected by a contrast seeker is the summation of the irradiance caused by the target contrast, background contrast, and the reference.

For a measurement of the contrast between target and background, the instrument output represents an energy level given by

$$\Delta E_c = [L_b (1/2 \omega_R - \omega_{\dagger}) + L_{\dagger}\omega_{\dagger}] - (L_b 1/2 \omega_R) \quad (4-8)$$

where

$L_b$  = radiance of the background

$\omega_R$  = Total field-of-view of the seeker

$\omega_{\dagger}$  = Angle subtended by the target at the seeker

$L_{\dagger}$  = Radiance of the target

the purpose of designing missiles or for devising methods of suppressing the the infrared radiation emitted by the aircraft. Therefore, it is important to know in which regions of the infrared spectrum the principal emission occurs. For hydrocarbon fuels, such as JP-4, the principal emission occurs in the carbon dioxide and water vapor bands tabulated earlier. Thus, for seekers or detectors operating in the atmospheric transmission windows, this molecular emission may be undetectable, but the gaseous continuum thermal radiation will be detectable. Consequently, the aircraft may or may not be vulnerable to missiles.

A spectral map of the unattenuated spectral radiant intensity of the source over the infrared region of interest is required. The spectral interval may be split up into 1.5-3.0, 3.1-5.1, and 8.0-14.0  $\mu\text{m}$  measurement regions but an attempt should be made to cover the widest total spectrum.

#### Aspect Angle

In addition to the spectral distribution of the radiation emitted by an aircraft, the spatial distribution must also be known. Then, too, the vulnerability of the aircraft to a missile approaching from the nose-on aspect (i.e., above the aircraft, below the aircraft, or directly behind the aircraft) must be known. This knowledge may lead to better evasive tactical maneuvers or the use of shields or contoured exhaust systems to shape the direction of emission. In order to control the flow of infrared radiation from the aircraft, its characteristics must be known.

Spatial knowledge must extend to range, since a knowledge of the radiation levels at various distances from the source is necessary to determine proper launch boundaries. Proper knowledge of the spatial distribution of infrared radiation would show a sphere surrounding the aircraft, with the radiation levels specified for each point within the sphere in terms of range, azimuth, and elevation angles. To acquire this information, various test procedures must be undertaken. These procedures follow.

#### ATTITUDE DETERMINATIONS

Infrared measurements of the radiation emitted from aircraft as a function of aspect angle require precise information about the position and attitude of the aircraft relative to the measuring instrument. Four parameters of the airframe (heading, roll, pitch, and yaw) and three parameters of the instrumentation pedestal (range, azimuth, and elevation) will serve to completely define the aspect of the airframe relative to the measuring instrument.

#### Aircraft Instrumentation

There are two major subsystems in the aircraft instrumentation system, an attitude monitor and a recording or telemetry subsystem. The attitude monitor determines the roll, pitch, yaw, and heading of the aircraft. If the data is recorded in the aircraft, the system would time-multiplex the analog signals, convert them to digital pulses, and record them on tape. Digital time information is transmitted to the aircraft via the communication link for time correlation purposes. If the data is telemetered, the

analog signals would be multiplexed, converted to digital signals, and transmitted to the ground station.

Sampling rates of a few times a second should be adequate to describe the aircraft as a function of time.

Attitude monitoring of the aircraft can be taken from a vertical reference or a stable platform. Most operational vertical references suffer from acceleration errors. Stable platforms, although considerably more expensive, provide accurate attitude information regardless of vehicle maneuvers. Heading information can be derived from a stable platform or from a gyro-stabilized compass system. Earth's rate effects and other geophysical phenomena can be compensated for either by the measuring device or by data corrections based on the aircraft's flight path.

#### Ground Instrumentation

If the data from the aircraft is telemetered to a ground receiving station, provision for recording and timing this information must be provided along with instrumentation for receiving pedestal information. A tracking radar provides the aircraft coordinates and, if the master instrumentation pedestal is slaved to it, also provides the pedestal azimuth and elevation angles.

#### ASPECT GEOMETRY

By common usage, the position of a point in space with respect to an aircraft is defined in terms of  $R$ ,  $\theta$ , and  $\phi$  where

$R$  = slant range

$\theta$  = elevation angle

$\phi$  = angle projected on the horizontal plane through the aircraft measured from the nose.



The information returned from the radar shall consist of the following:

AZ = radar azimuth angle measured from north

ALT = altitude of the aircraft with respect to the radar

R = slant range

$\theta$  = elevation angle

The elevation angle is related to the slant range and the altitude of the aircraft through the usual relation

$$\theta = \text{arc sine } \text{ALT}/R \quad (4-11)$$

so that only three of these parameters are independent.

The information returned from the aircraft shall consist of the following or some parametric version of these:

H = heading angle of the aircraft measured from north

ROL = roll angle of the aircraft

PIT = pitch angle of the aircraft

YAW = yaw angle of the aircraft (measured deviation from heading)

In terms of the above parameters,  $\phi$  is given by the following:

$$\phi = 180^\circ - (H - \text{AZ}) \quad (4-12)$$

Figure 4-6 shows an aircraft in level flight being illuminated by a radar; figure 4-7 shows this situation projected onto a horizontal plane, and serves to define  $\phi$ , heading angle, and radar azimuth angle.

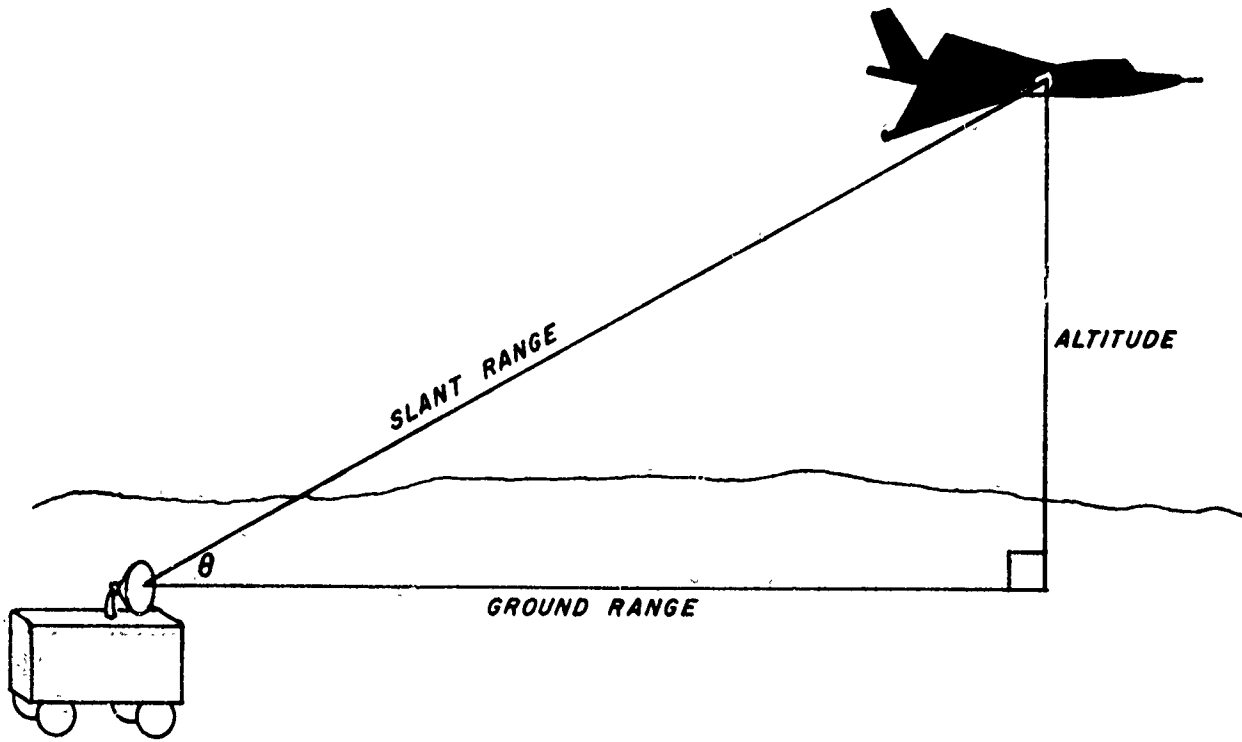


Figure 4-6. Aircraft in Level Flight Illuminated by Ground Radar.

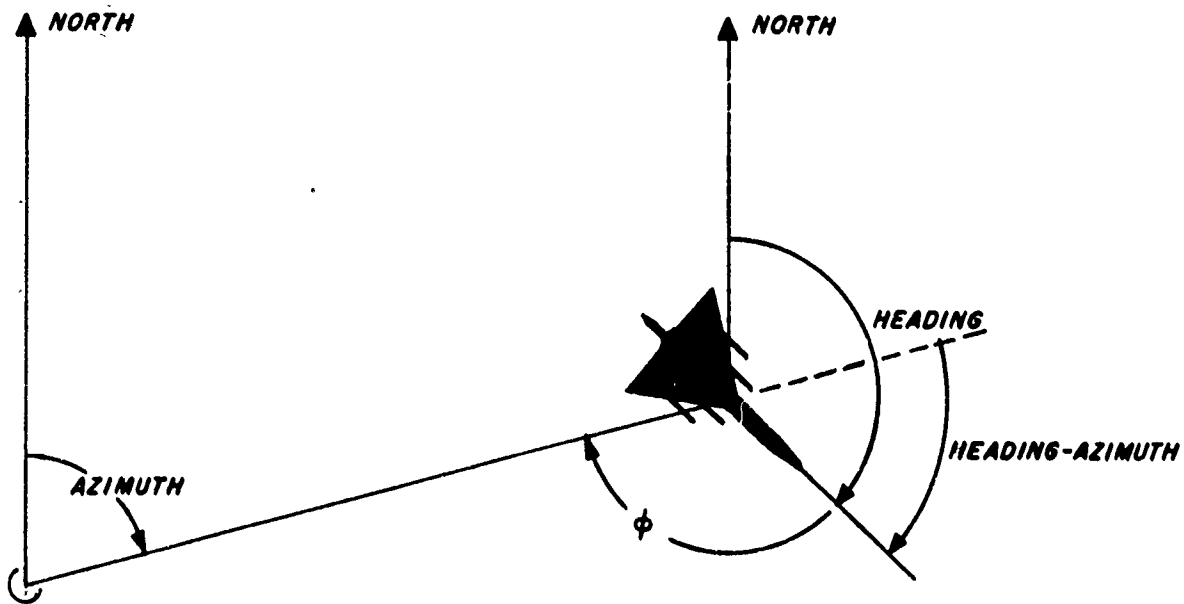


Figure 4-7. Projection of Above Figure on a Horizontal Plane.

The easiest way to visualize the changes in the aspect angles  $\theta$  and  $\phi$  is to imagine the aircraft at the center of a sphere with a radius equal to the slant range,  $R$ . Then changes in roll, pitch, or yaw effectively cause the position of the radar on the surface of the sphere to change correspondingly (figure 4-8). The analysis of these changes to yield the new aspect angles  $\theta''$  and  $\phi''$ , made by Mr. E. G. Meyer and Mr. C. L. Mohre of Radiation Incorporated, Melbourne, Florida, follows:

Visualization of the changes in  $\theta$  and  $\phi$  brought about by pitch and roll angles can be aided by considering the aircraft to be located at the center of a sphere and the radar on the surface of the sphere. Thus, the radius of the sphere is equal to the slant range,  $R$ . Figure 4-8 shows a side view of the sphere with the radar at point A. Changes in aircraft attitude can be considered as changes in the position of the radar with the aircraft remaining stationary. Thus, changes in aircraft heading can be represented as movement of the radar on the heading circle BC. Roll of the aircraft can be represented as movement of the radar on the roll circle DE. Pitch of the aircraft can be represented as movement along the pitch circle which passes through point A. A combination of roll and pitch, as an example, would be represented by movement from A along the roll circle to F, followed by movement along the new pitch circle to point G. The order of the movement is immaterial; the result could have been obtained by proceeding along the pitch circle to point H and then along the new roll circle to point G.

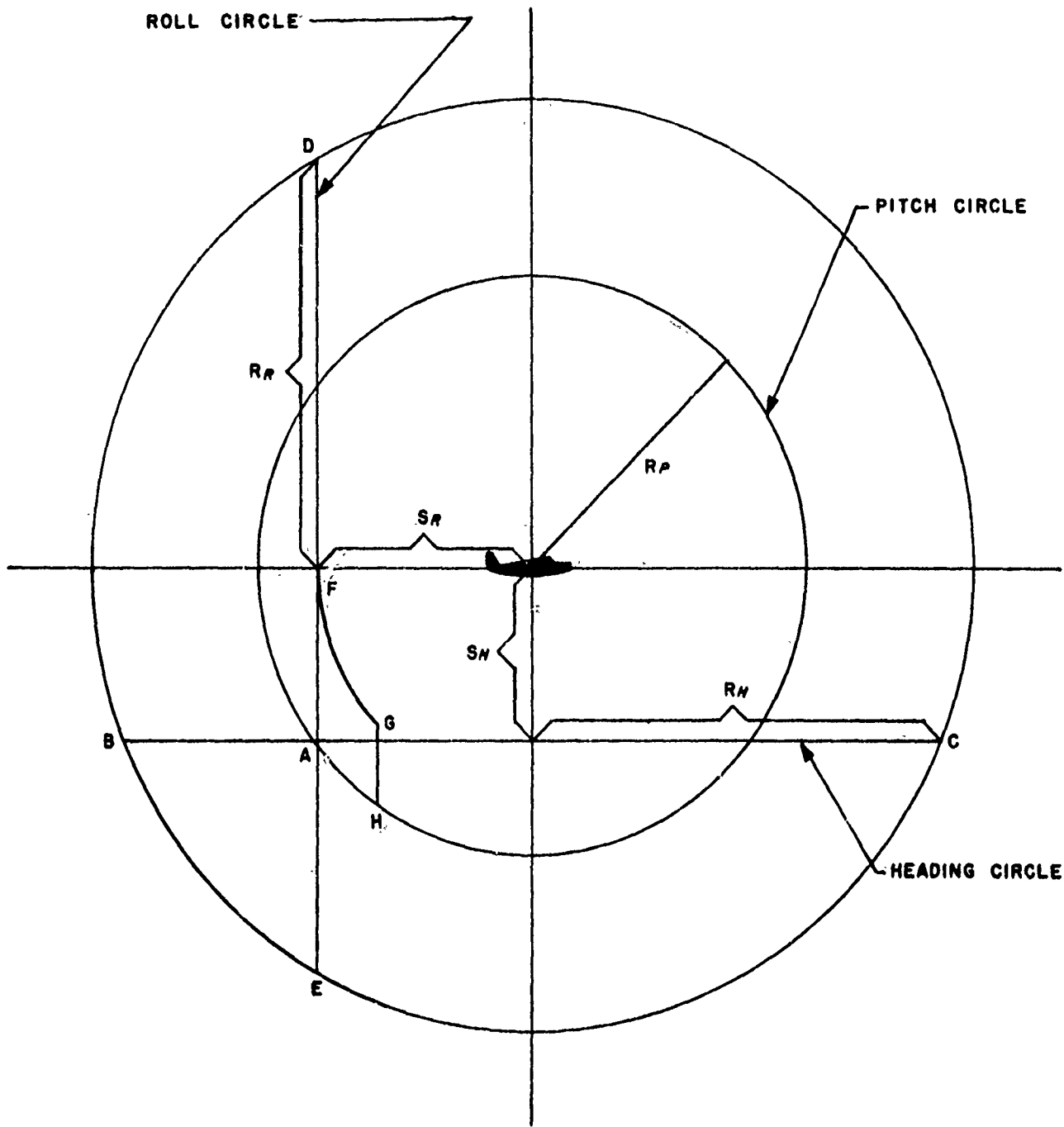


Figure 4-8. Side View of a Sphere with the Radar at Point "A".

With the addition of roll, pitch, and heading circles to the sphere additional quantities may be defined as follows:

- $R_R$  = radius of the roll circle
- $R_P$  = radius of the pitch circle
- $R_H$  = radius of the heading circle = ground range
- $S_R$  = separation of roll circle, or the distance from the center of the roll circle to the origin of the sphere
- $S_H$  = separation of the heading circle = altitude
- $S_P$  = separation of the pitch circle

These may be defined in terms of  $R$ ,  $\theta$ , and  $\phi$  with the aid of figure 4-9.

Thus,  $S_H = ALT = R \sin \theta$  (3)

$R_H = R \cos \theta$  (4)

$S_P = R_H \cos (\phi - 90) = R \cos \theta \cos (\phi - 90)$  (5)

$S_R = R_H \sin (\phi - 90) = R \cos \theta \sin (\phi - 90)$   
 $= R \cos \theta \cos \phi$  (6)

$R_R^2 = S_P^2 + S_H^2 = (R \cos \theta \sin \phi)^2 + (R \sin \theta)^2$   
 $= R^2 [\cos^2 \theta \sin^2 \phi + \sin^2 \theta]$   
 $= R^2 [1 - \cos^2 \theta \cos^2 \phi]$  (7)

$R_P^2 = S_H^2 + S_R^2 = (R \sin \theta)^2 + (R \cos \theta \cos \phi)^2$   
 $= R^2 [\sin^2 \theta + \cos^2 \theta \cos^2 \phi]$   
 $= R^2 [1 - \cos^2 \theta \sin^2 \phi]$  (8)

Since  $\theta$  and  $\phi$  were defined in terms of  $H$ ,  $AZ$ ,  $ALT$ , and  $R$ , all of the quantities are now defined in these terms.

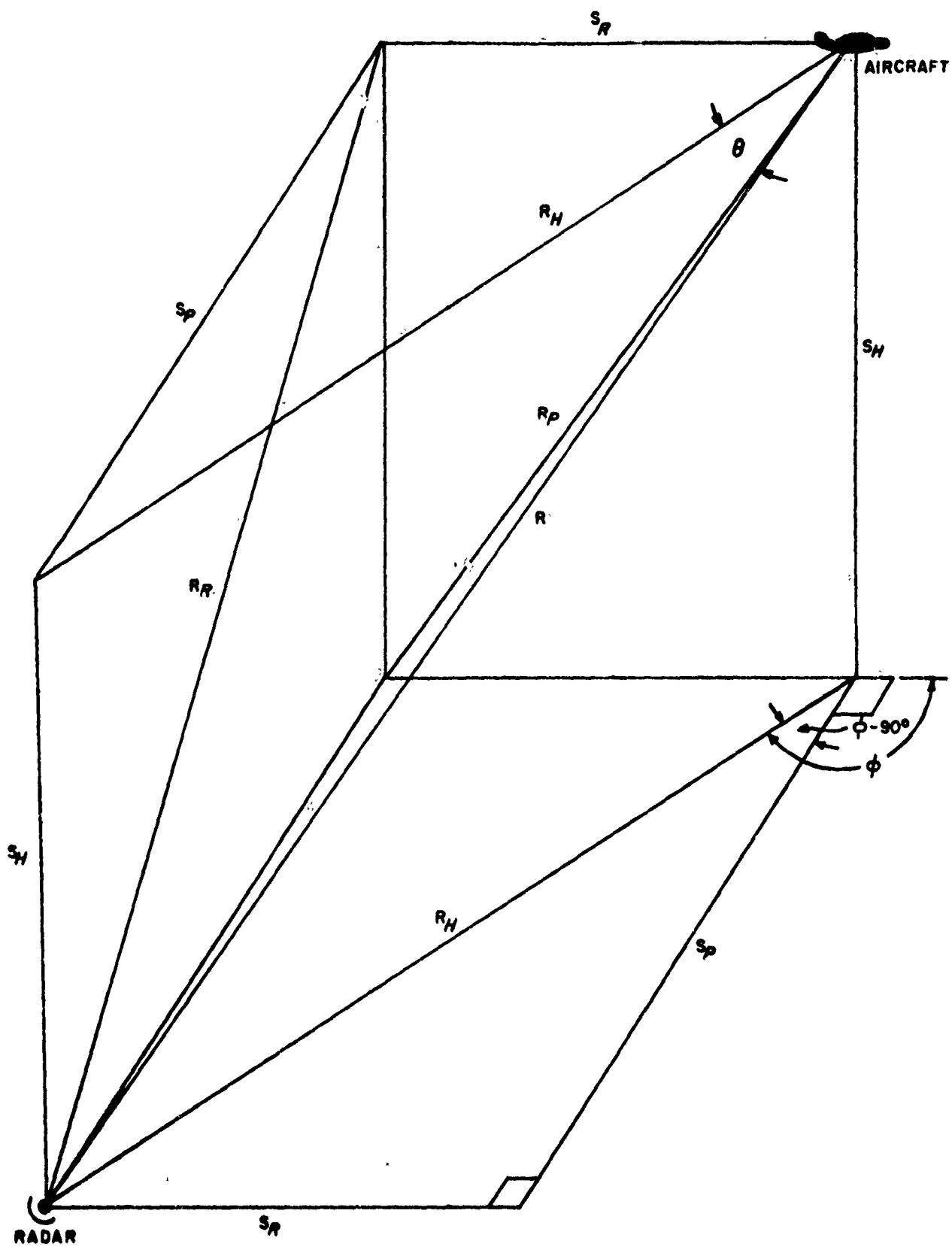


Figure 4-9. Roll, Pitch, and Heading Quantities in Terms of  $R$ ,  $\theta$ , and  $\phi$ .

Now consider the introduction of a roll angle. Figure 4-10 shows a portion of the roll circle with a roll angle,  $\alpha$ , introduced. The roll angle moves the relative position of the radar to new heading and pitch circles with new heading and pitch separations,  $S_{H'}$  and  $S_{P'}$ , and a new pitch circle radius  $R_{P'}$ .

$$S_{H'} = R_R \sin [\alpha + \sin^{-1} S_H/R_R] \quad (9)$$

$$S_{P'} = R_R \cos [\alpha + \sin^{-1} S_H/R_R] \quad (10)$$

$$(R_{P'})^2 = (S_{H'})^2 + S_R^2 \quad (11)$$

Now if a pitch angle,  $\beta$ , is introduced as shown in figure 4-11, the pitch angle moves the relative position of the radar to new heading and roll circles. This results in new heading and roll separations,  $S_{H''}$  and  $S_{R'}$ .

$$S_{H''} = R_{P'} \sin [\beta + \sin^{-1} S_{H'}/R_{P'}] \quad (12)$$

$$S_{R'} = R_{P'} \cos [\beta + \sin^{-1} S_{H'}/R_{P'}] \quad (13)$$

Figure 4-9 may now be redrawn in terms of the new circles and separation (figure 4-12) and resulting  $\theta''$  and  $\phi''$  may be determined.

$$\sin \theta'' = S_{H''}/R \text{ or } \theta'' = \sin^{-1} S_{H''}/R \quad (14)$$

$$\cos (\phi'' - 90) = \sin \phi'' = \frac{S_{P'}}{\sqrt{(S_{R'})^2 + (S_{P'})^2}}$$

or

$$\phi'' = \sin^{-1} \frac{S_{P'}}{\sqrt{(S_{R'})^2 + (S_{P'})^2}} \quad (15)$$

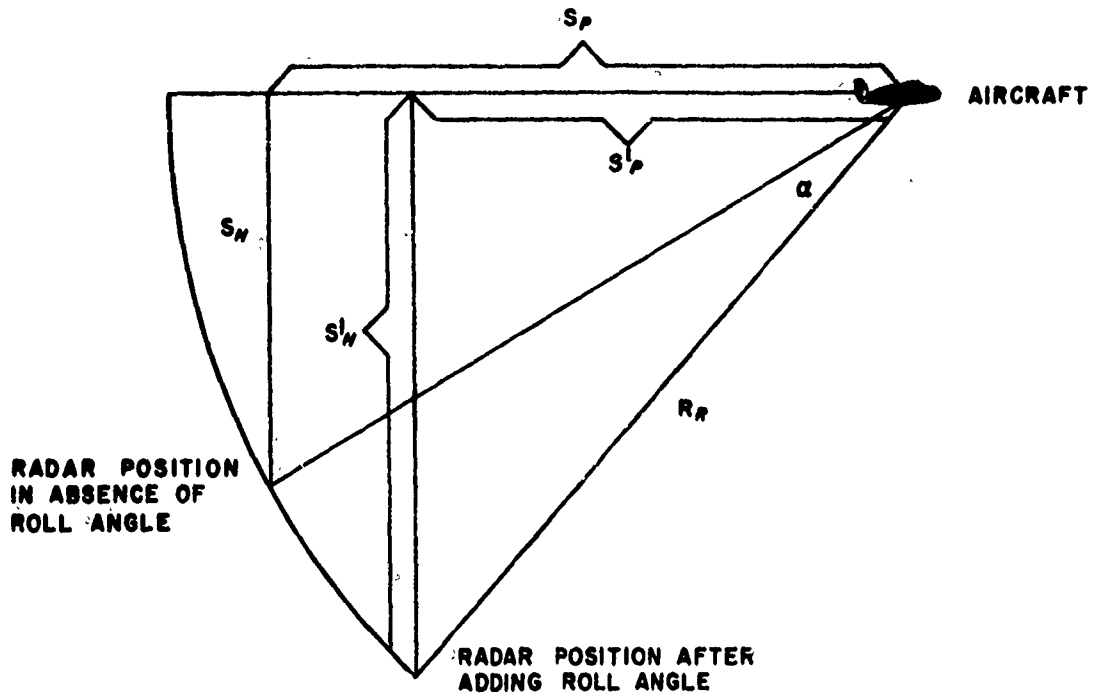


Figure 4-10. Portion of the Roll Circle.

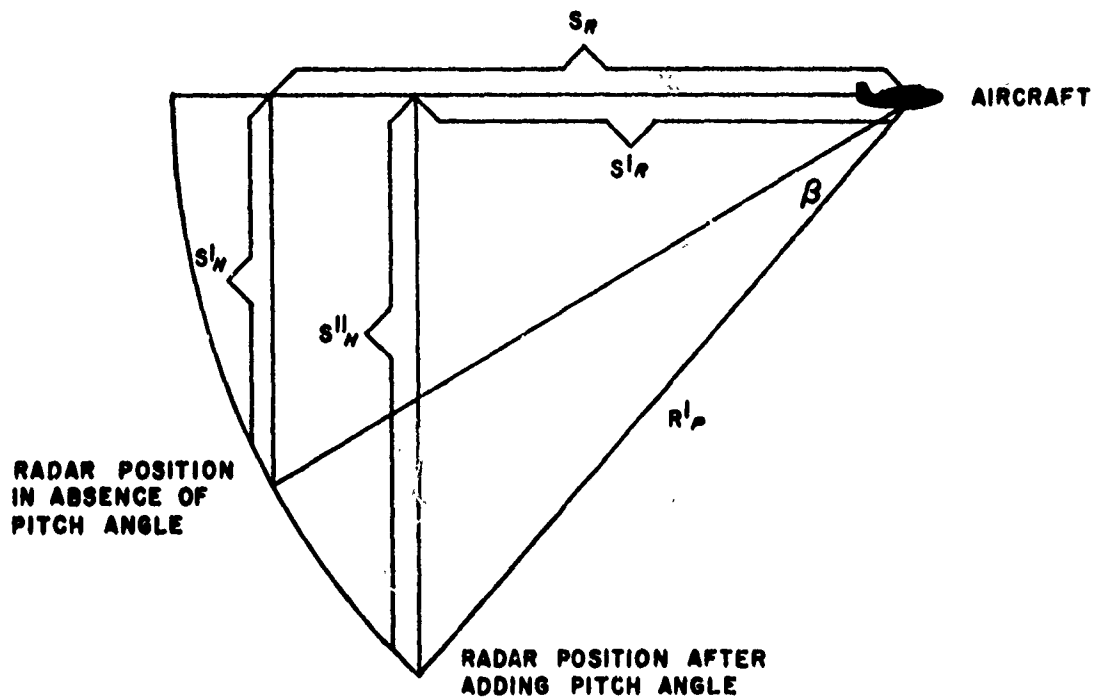


Figure 4-11. Portion of the Pitch Circle.



The resulting angles of the radar with respect to the aircraft may be obtained in terms of the basic parameters of R, AZ, ALT, H,  $\alpha$ , and  $\beta$ .

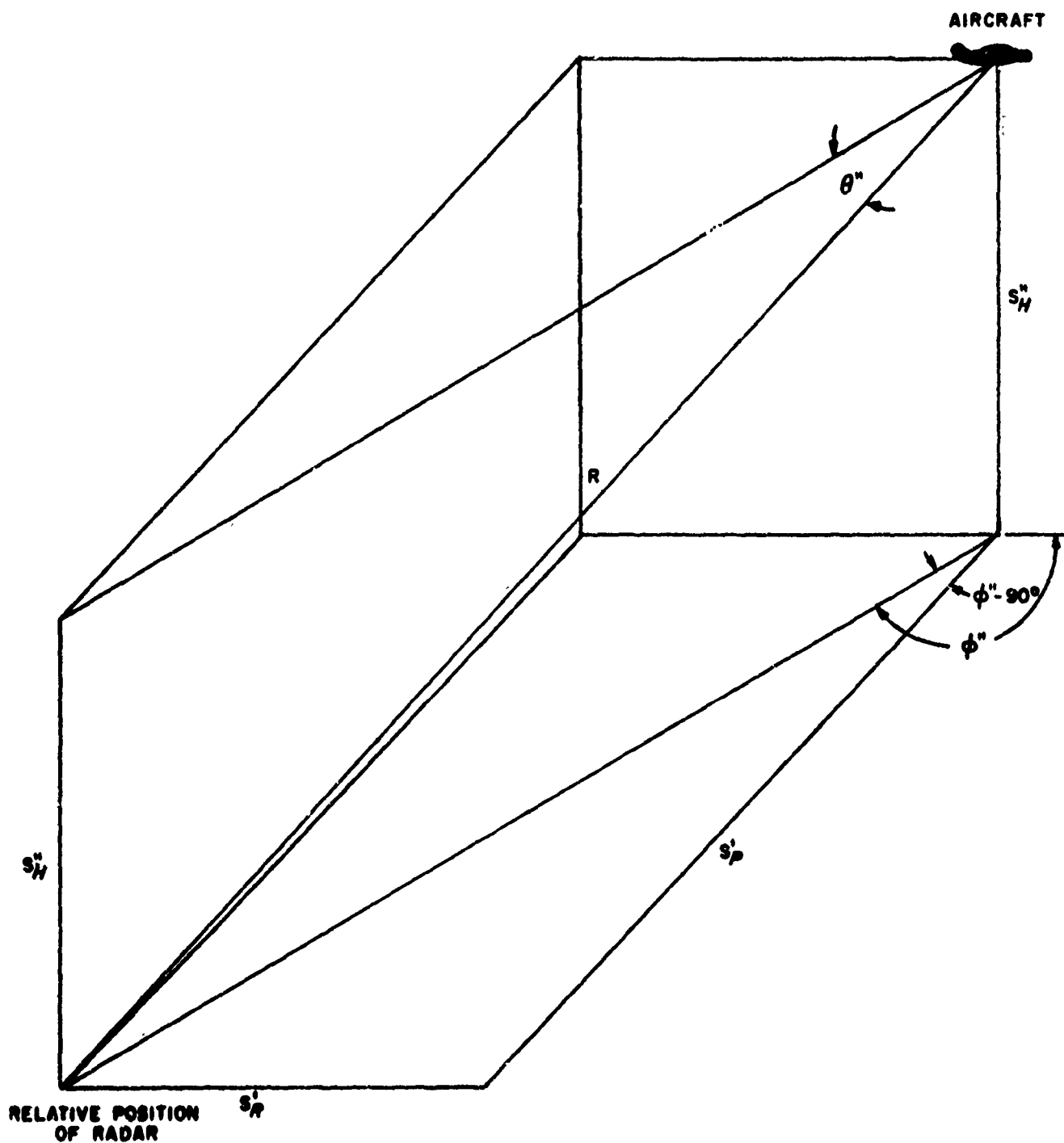


Figure 4-12. New Separations Showing  $\theta''$  and  $\phi''$  Determined.

## GROUND-TO-GROUND

A ground-to-ground test will provide a map of the infrared radiation within a circle about the aircraft. For helicopter measurements a grid should be laid out on the landing pad with a centering mark over which the exhaust pipe should always be placed. Then, if the instrument is in a stationary position, the helicopter can rotate in a circle to define the different aspect angles with respect to the measuring instrument. A spectrometer, boresight camera, and an optical tracking scope are required. The three instruments are mounted on a pedestal and bore-sighted at the point on the landing pad where the exhaust pipe is expected to be. The range can be determined beforehand, but aspect angles must be determined each time the helicopter lands. This can best be done by triangulation using a surveyor's transit or theodolite. Spotters will be necessary to insure that the helicopter is in a correct position before each measurement. Atmospheric data must also be taken.

For other aircraft which are not easily rotated, it may be necessary for the spectrometer itself to be rotated about the pad. This will involve considerable set-up time, so fewer measurements would be taken. In these cases, measurements taken every 15 degrees should suffice. Measurements should not be spaced farther than 30 degrees.

Once an atmospheric attenuation program has been set up, it is merely a matter of geometry and computer time to determine values of radiant intensity at other ranges. A background run should be taken and calibration

procedures carried out. If feasible, it would be quite beneficial to substitute a calibrated blackbody at the target point to determine both absolute radiation levels and atmospheric attenuation experimentally rather than calculating irradiance levels and transmissivity.

#### GROUND-TO-AIR

This will be the most widely used procedure and will necessitate a fly-by of the aircraft making repeated passes across the instruments' scanning region. For this reason flight patterns and instrumentation will be discussed before describing the actual test.

The problem of determining range is easily solved by using range radar, but the problem of determining aspect angle is much more difficult. Two methods of relying on boresight film images for later analysis of aspect angle have been developed by the Naval Weapons Center at China Lake and by the Missile Electronic Warfare Technical Area at White Sands Missile Range. These methods are published elsewhere, but neither is sufficiently accurate to warrant its use. The heading compass within the aircraft is not sufficiently accurate to use to determine aspect angles. The use of an attitude sensor, to be carried onboard the aircraft, in conjunction with a telemetry system will provide real-time data on heading, pitch, and roll. This data can be recorded at the same time as spectral scans are being made. The data and the pedestal data can then be reduced to determine the two aspect angles: azimuth and elevation.

As the experiment becomes more difficult to perform, the equipment used becomes more complex and sophisticated. In proceeding to ground-to-air measurements, a plethora of problems associated with keeping the aircraft stable during the measuring period enters the picture. Fewer errors result during hovering than during fly-by; in either case, the errors involved must be carefully examined.

Instrumentation required then consists of a spectrometer, boresight camera, optical tracking scope, or other means of tracking the aircraft, a range radar, and an attitude sensing device for the aircraft and associated electronic and recording equipment. There may be other instruments involved in specific tests. These will be dealt with in a later chapter.

#### Hover Tests

Since the purpose of a hover test is to determine the amount of radiation emanating from the aircraft at the actual power levels to be used in the field, the general test description is on the same order as for the ground-to-ground tests. The aircraft should be hovering over a point some distance from the test instrument, perhaps as much as ten meters above the ground, depending upon the instrument's field of view. The aircraft should move radially about the target point, hovering at 15-degree increments. If possible, an absolute means for determining range and aspect angles should be used. Range radar may be used for the range determinations, but aspect angle determinations require more ingenuity. A variety of hovering altitudes should be chosen, as 10, 50, and 100 meters.

### Fly-By Tests

A fly-by should incorporate the actual ranges from infrared instruments which might be expected to be encountered in the field, which includes the normal operating altitudes of the aircraft and normally expected ranges. The flight pattern should incorporate the possibility of viewing the aircraft from as many aspect angles as possible.

Altitude - A normal test would use numerous fly-bys, each sequence run at a different altitude, say 100, 500, and 1000 meters above the test site.

Range - Off-sets varying from 0.5 to 10.0 km, depending on the brightness of the source and visibility, should be conducted, probably in steps of 1 km.

Flight-Patterns - A grid pattern should be established on the ground showing the expected flight patterns, headings, and trajectories of the aircraft. This should incorporate flying over the test site at the various aspect angles. A grid pattern is shown in figure 4-13.

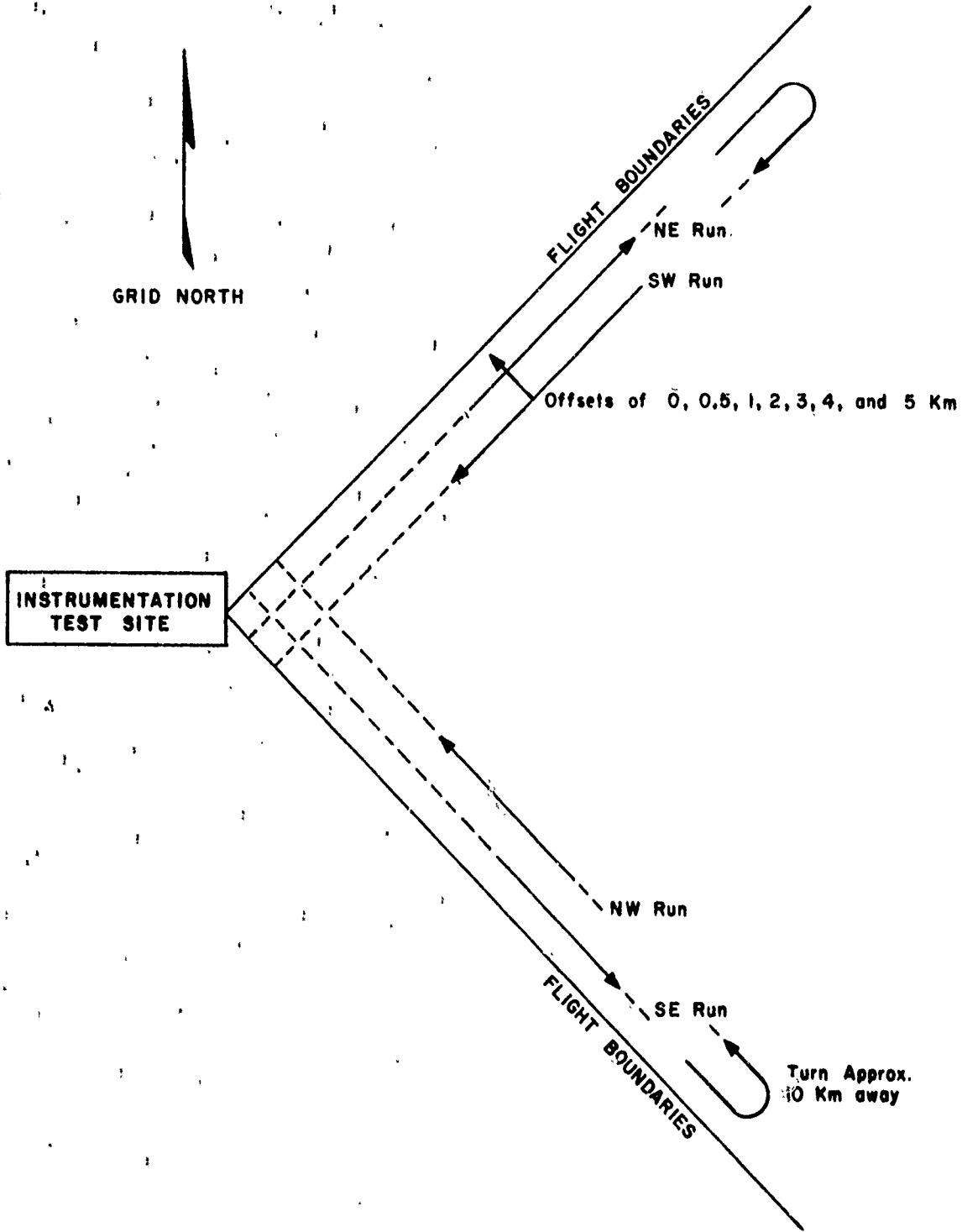


Figure 4-13. Flight Pattern for Fly-by Test.

Depending upon the projected use of the aircraft, tests run at different times of the day or night may prove a source of valuable information. If sufficient correlation exists between data gathered from hovering and fly-by experiments, extensive fly-by tests may prove to be unnecessary. Since there is much better control of the pertinent variables in a hover test, a hover test is preferable if it alone can provide the desired information.

#### AIR-TO-AIR

From the above discussion it can be seen that air-to-air measurements are rampant with complexities not found in other measuring modes. The biggest difficulty is associated with moving all, or most, of the measuring apparatus into an airborne vehicle. Once instrumentation problems are solved, measurement techniques are straight-forward and follow the preceding procedures.

#### SUMMARY

The type of test to be conducted depends upon the objectives of the specific program. The data required determines whether ground-to-ground, ground-to-air, or air-to-air measurements are to be performed. The discussions in this chapter point out, however, that spectral measurements are mandatory to meaningfully describe the radiation characteristics of the target. Once the target spectral characteristics are known, the data can be applied to other areas.

The objectives of the specific program also influence the aspect angles at which data is to be obtained; for instance, ground-to-air measurements are best for obtaining data of the lower hemisphere of an aircraft. The specific aspect angles that will sufficiently describe the lower hemisphere depend upon the type of aircraft. The test decided upon should be as simple as possible, consistent with the gathering of all pertinent information. The test should be thoroughly analyzed to obtain good, meaningful data and to avoid extraneous data.



**CHAPTER V**  
**INSTRUMENTATION**

The instruments required for a test depend upon the level of sophistication of the test. The plan here is to sketch the methods which might be used to determine the parameters necessary for a measurement and then describe a variety of instruments and related accessories which fulfill these functions. The parameters which must be measured are those mentioned in Chapter IV. Instruments to measure these parameters include:

**Trackers and Pedestals**

**Attitude Sensors**

**Missile Seekers**

**Meteorological Devices**

**Range Radar**

**Optical Instruments**

**Boresight Cameras**

**Imaging Systems**

**Spectrometers**

**Interferometers**

Instruments used to measure the amount of infrared radiation incident upon some surface consist of radiometers, spectrometers, and interferometers. The literature on radiometers is quite extensive, consequently their design and function will not be dealt with in this chapter.

A spectrometer would normally consist of four main sections: a source of infrared radiation; optics for collecting and focusing this radiation; a monochromator for dispersing and selecting a particular band of wavelengths; and a detection mechanism for detecting the infrared radiation and producing a record. The source of infrared radiation, external to the measuring or detecting apparatus, will be known as the target.

#### Sources

Sources which may be used in calibration will include NBS traceable blackbodies and lamps such as mercury xenon, tungsten, and, perhaps, as a means of secondary calibration, controlled globar sources. The infrared emission spectrum of a typical xenon lamp whose emission lines can be used for wavelength calibration is shown in figures 5-1 and 5-2.

The globar is a rod of bonded silicon carbide which can be operated at temperatures up to 1500°C. It is important as a high-temperature standard because blackbodies of a cavity-type are difficult to fabricate beyond 1000°C. If the globar, which emits like a graybody, is to be used as a reference source, there must be some means of accurately monitoring and controlling its temperature. The emissivity of globars has been measured in the 0.5 to 15  $\mu\text{m}$  region; the emissivity is about 80 percent in this region. Although the Nernst glower is widely used for relative measurements, it is not recommended as a standard source because of the unstable nature of its emission.

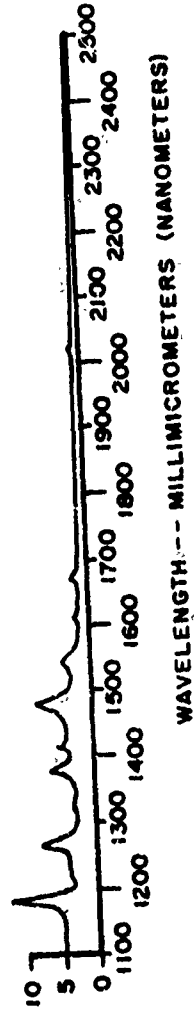
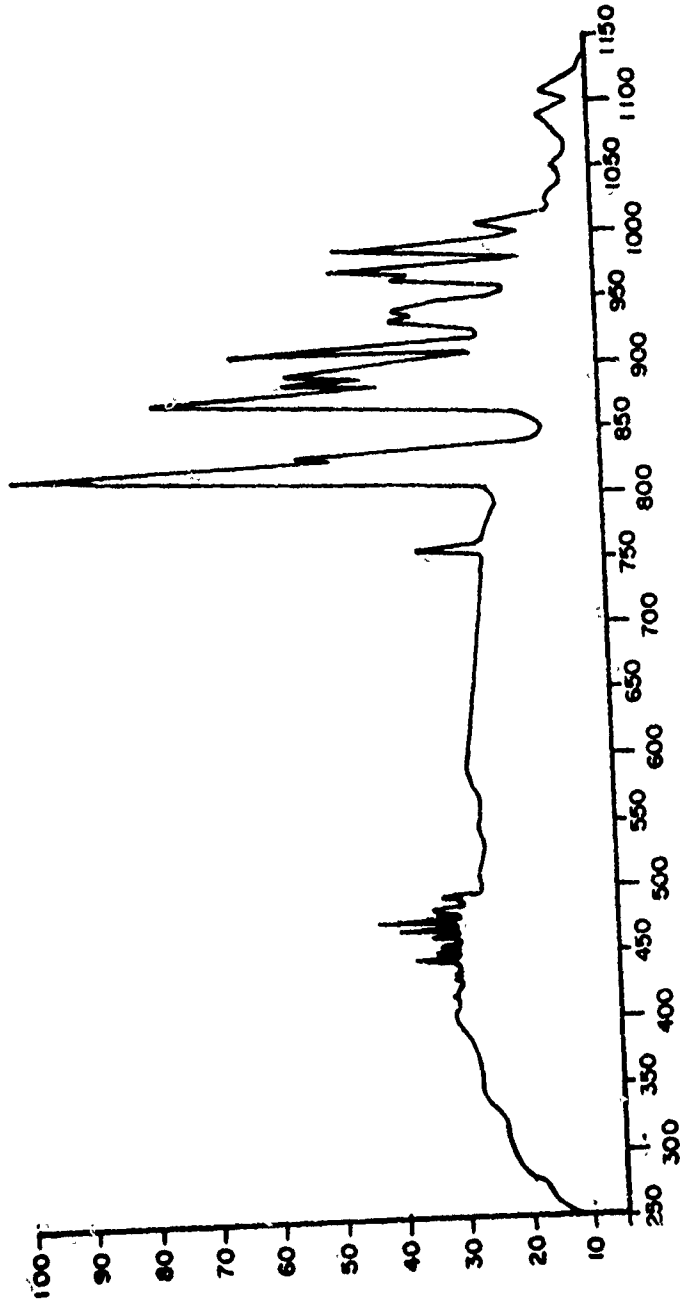


Figure 5-1. Emission Spectrum of a Xenon Lamp

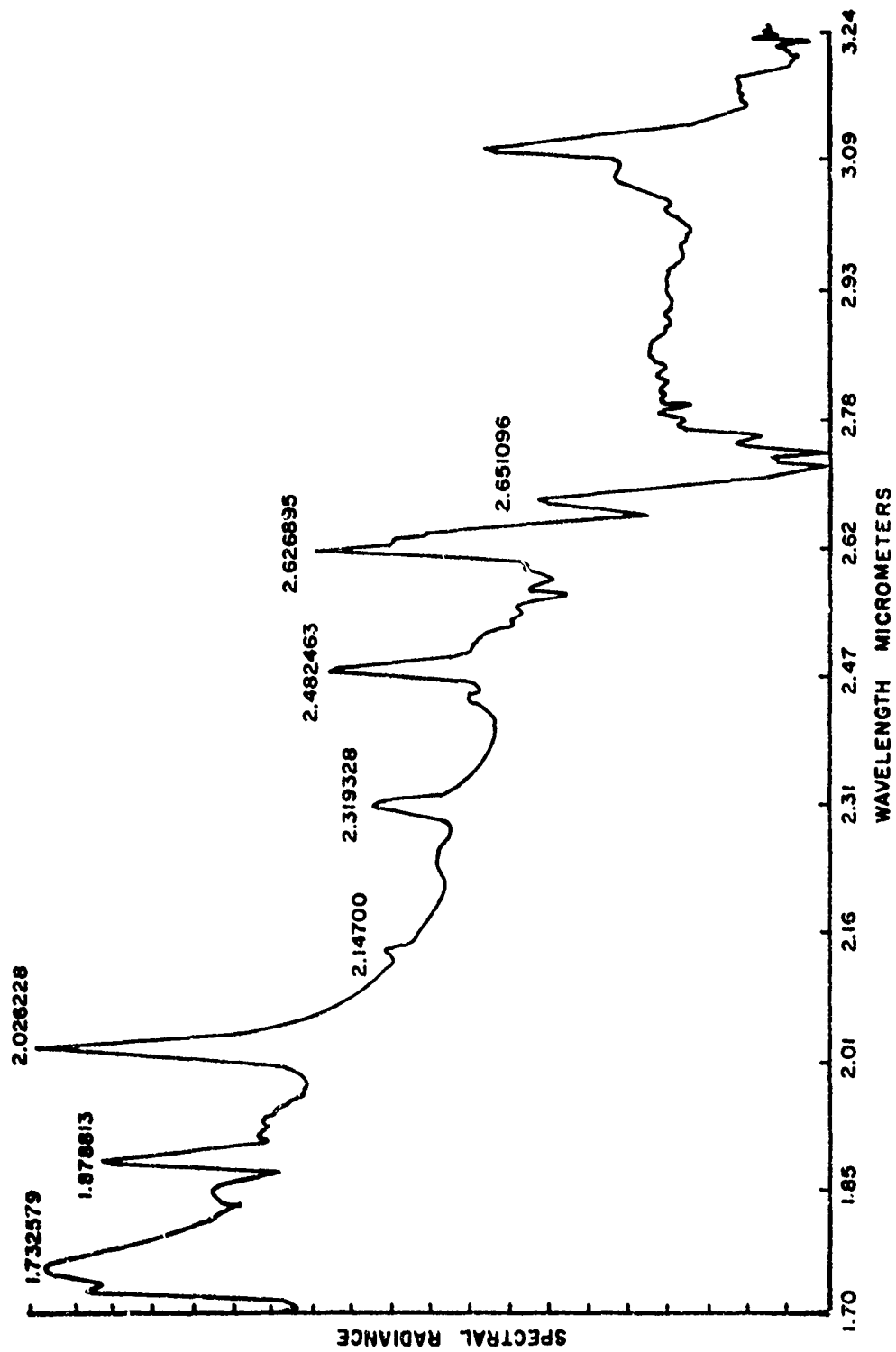


Figure 5-2. Infrared Emission from Xenon Lamp. (Emission Lines given in Micrometers)

Cavity-type blackbody sources are used extensively as standard reference sources, both externally and internally, within spectrometers and radiometers. Cavity-type sources are made from steel, copper, aluminum, and ceramic materials usually blackened by oxidation or by carbon black. The different shapes of cavities used are conical, cylindrical, and double-reversed conical. A heating coil of nichrome wire surrounds the cavity which, in turn, is embedded in a thermally insulated enclosure. A transparent window in the front of the cavity prevents convection currents from altering the temperature. The cavity temperature is monitored by a thermistor, or thermocouple, embedded within the cavity, and a separate controller is generally used to maintain a constant temperature. Some blackbody sources have an aperture plate in front of the cavity to vary the effective area of the source. A chopper blade is sometimes incorporated to modulate the radiation. A properly designed cavity-type source will very closely approach an ideal blackbody source in temperature ranges from ambient to 1000°C. Special blackbodies are available that operate to a temperature of 3000°C.

A laser, such as the CO<sub>2</sub> laser, may also be used as a source of infrared radiation provided it operates in the required region. High power lasers may be quite beneficial when making calibrations over long distances. The problem with lasers is that they provide a check of the calibration at only one wavelength, whereas a blackbody provides a calibration over all wavelengths in the infrared.

## Optics

All infrared systems incorporate an optical section for collecting the incident radiation and focusing it upon the detector. The optics provide a means for varying the amount of radiation collected by the instrument and determining a field-of-view.

FIELD-OF-VIEW. The true field-of-view of an optical system is the area of the target that can be imaged on the detector. The field-of-view is generally expressed as angular field-of-view, either a linear or solid angle. The angular field-of-view is the angle formed by the two extreme principal rays which can be imaged on the detector.

The field-of-view of the instrument is determined not only by the relative size of the collecting optics, but also by any limits placed on the light rays before they strike the detector. Field stops, aperture stops, size of the detector, and exit and entrance slits all may affect the field-of-view. The true field-of-view of the instrument can be determined by imaging a target at the edge of the field and then traversing the instrument until the target is at the opposite edge of the field. The angular displacement of the instrument (or the target) is then the angular horizontal field-of-view expressed in milliradians. The field-of-view of an instrument is sometimes given in terms of a solid angle. For small angles, the solid angle is the area divided by the distance squared, and the value (in steradians) is twice the linear field-of-view for a symmetrical field-of-view.

The field-of-view of an optical system is proportional to the size of the detector and inversely proportional to the image distance, given by the usual mirror equation

$$\frac{1}{f} = \frac{1}{s} + \frac{1}{s'}, \quad (5-1)$$

where

$f$  = focal length

$s$  = target distance

$s'$  = image distance

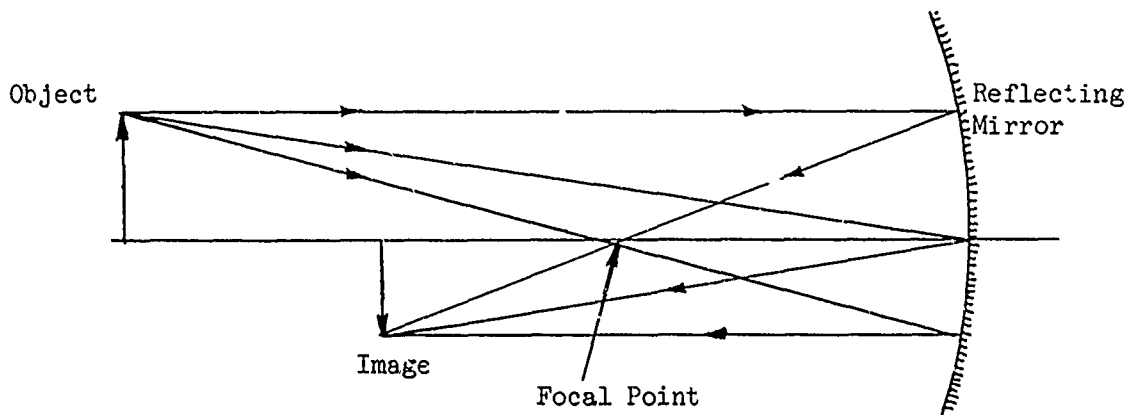


Figure 5-3. Relation Between Object, Image, and Focal Distances for Mirrors.

The mirror equation may also be written in the Newtonian form

$$f^2 = x x' \quad (5-2)$$

where  $x$  and  $x'$  are again object and image distances, but measured from the focal rather than the principal point. Thus  $s = f + x$ , and  $s' = f + x'$ . The field-of-view is increased when the focal length is decreased. A compromise is usually made between focal length and field-of-view in the design of optical systems.

SPEED. The speed of an optical system is the collecting power of a system and indicates the image brightness. The speed is proportional to the area of the objective lens and inversely proportional to the square of the focal length.

F/NUMBER. The ratio of the equivalent focal length to the diameter of the collecting optics, the f/number, is used to describe the amount of radiant flux collected by the optical system.

$$f/\text{no} = f/D_o \quad (5-3)$$

The effective or equivalent focal length of a multi-element lens system is the focal length of a single element system which would image the incident rays at the same point as the actual optics. The smaller the f/number, the larger the lens diameter, or aperture stop, for a given focal length and the greater the light-gathering power, or speed, of the lens.

STOPS. A stop is an optical component that limits the radiation passing through a system. Stops are classified as either aperture stops or field stops, depending upon their location in the optical system. Aperture stops are located in the objective, or collecting, section and limit the amount of energy that can be collected; field stops are located near the image plane and limit the field-of-view.

The field-of-view should be large enough to completely "see" the infrared emission from the target. For example, in the case of an aircraft with twin engines, the field-of-view of the instrument should be large enough to include both exhausts while the aircraft remains within



reasonable distances from the detector but small enough to provide good sensitivity and eliminate unnecessary background noise. A variable field-of-view utilizing selected field stops provides a reasonable solution.

OPTICAL SYSTEMS. For our purposes the largest light-gathering power for the system which can be achieved within a minimum space is required. The lens itself should be the limiting aperture stop, but will require a provision for the inclusion of selected field stops, since many different targets will be measured over different ranges. Thus, a variable field-of-view should be included within the optics of the system. For a given focal length, the smallest f/number and thus the largest speed of a system can be obtained by using a folded pathlength. The Cassegrainian system achieves this with the minimum amount of aberration and blur.

Different combinations of optical components, both refractive and reflective, are shown in figure 5-4. The selection of a combination depends on the particular requirements of the system. The use of reflective optics is preferred; however, the nature of the system may dictate the use of refractive components, but the user should be aware that although such components can be obtained easily, they are more costly than reflective components. Imaging systems require freedom from aberrations; therefore, a Schmidt-Cassegrain or Maksutov system probably would be used. Size and weight are considerations in field and airborne equipment. The field-of-view required is important in most systems; in some, it must be variable. The position of the detector or source is quite often critical.

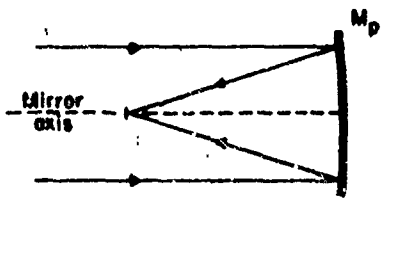
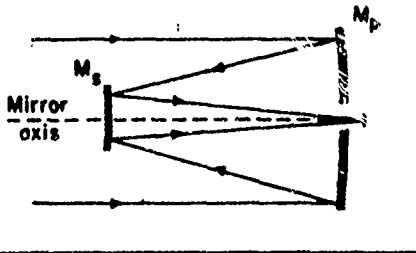
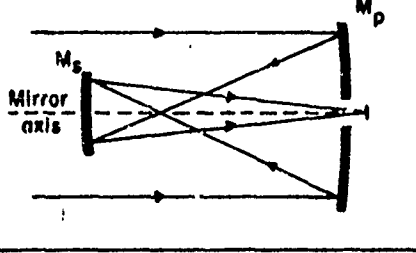
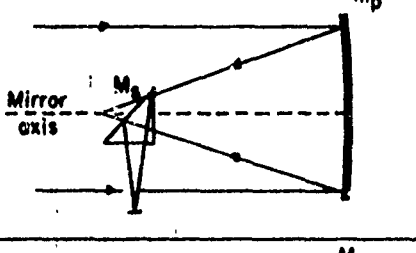
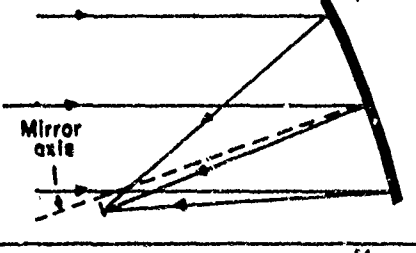
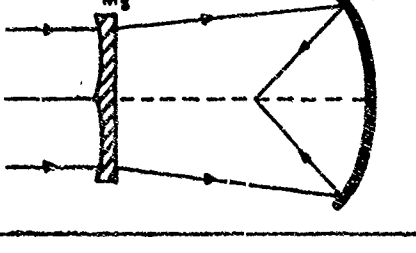
TYPE	RAY DIAGRAM	OPTICAL ELEMENTS	PERTINENT DESIGN CHARACTERISTICS
PARABOLOID		Reflective  $M_p$ = Paraboloidal mirror	<ol style="list-style-type: none"> <li>1. Free from spherical aberration.</li> <li>2. Suffers from off-axis coma.</li> <li>3. Available in small and large diameters and f/numbers.</li> <li>4. Low IR loss (Reflective).</li> <li>5. Detector must be located in front of optics.</li> </ol>
CASSEGRAIN		Reflective  $M_p$ = Paraboloidal mirror $M_s$ = Hyperboloidal mirror	<ol style="list-style-type: none"> <li>1. Free from spherical aberration.</li> <li>2. Shorter than Gregorian.</li> <li>3. Permits location of detector behind optical system.</li> <li>4. Quite extensively used.</li> </ol>
GREGORIAN		Reflective  $M_p$ = Paraboloidal mirror $M_s$ = Ellipsoidal mirror	<ol style="list-style-type: none"> <li>1. Free from spherical aberration.</li> <li>2. Longer than Cassegrain.</li> <li>3. Permits location of detector behind optical system.</li> <li>4. Gregorian less common than Cassegrain.</li> </ol>
NEWTONIAN		Reflective  $M_p$ = Paraboloidal mirror $M_s$ = Reflecting prism or plane mirror	<ol style="list-style-type: none"> <li>1. Suffers from off-axis coma.</li> <li>2. Central obstruction by prism or mirror.</li> </ol>
HERSCHELIAN		Reflective  $M_p$ = Paraboloidal mirror inclined axis	<ol style="list-style-type: none"> <li>1. Not widely used now.</li> <li>2. No central obstruction by auxiliary lens.</li> <li>3. Simple construction.</li> <li>4. Suffers from some coma.</li> </ol>
SCHMIDT		Reflective - refractive  $M_p$ = Spherical mirror $M_s$ = Refractive corrector plate	<ol style="list-style-type: none"> <li>1. Produces a curved field.</li> <li>2. Free of spherical aberration and coma.</li> <li>3. Central obstruction by its own field surface.</li> <li>4. Can obtain low f/number.</li> <li>5. Sharper focus over larger area than paraboloid.</li> <li>6. May be built as solid unit.</li> </ol>

Figure 5-4a. Optical Systems.

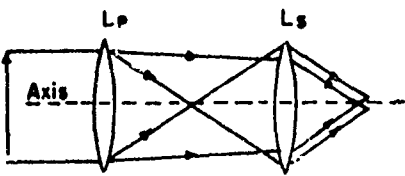
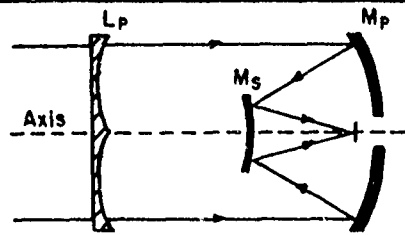
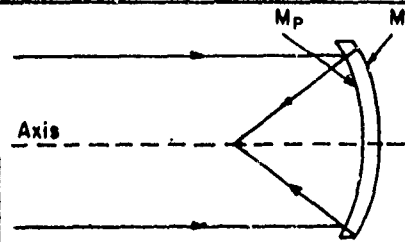
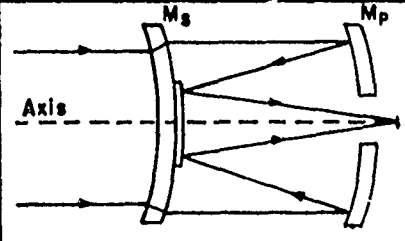
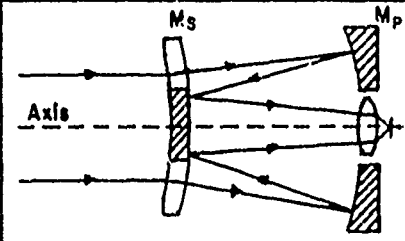
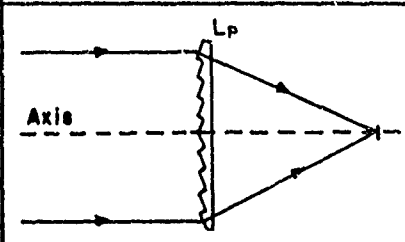
TYPE	RAY DIAGRAM	OPTICAL ELEMENTS	PERTINENT DESIGN CHARACTERISTICS
KEPLERIAN		<p>Refractive</p> <p><math>L_s</math> = Biconvex lens</p> <p><math>L_p</math> = Biconvex lens</p>	<ol style="list-style-type: none"> <li>1. Radiation gathering power less than reflection systems.</li> <li>2. Spectral response limited by lens material.</li> <li>3 Not widely used now.</li> </ol>
SCHMIDT-CASSEGRAIN OR BAKER		<p>Reflective -</p> <p><math>M_p</math> = Aspheric mirror</p> <p><math>M_s</math> = Aspheric mirror</p> <p><math>L_p</math> = Refractive corrector plate</p>	<ol style="list-style-type: none"> <li>1. Produces flat field.</li> <li>2. Very short in length.</li> <li>3. Covers large field.</li> <li>4. Corrector plate has larger curvature than Schmidt.</li> </ol>
MANGIN MIRROR		<p>Refractive - reflective</p> <p><math>M_p</math> = Spherical refractor</p> <p><math>M_s</math> = Spherical reflector</p>	<ol style="list-style-type: none"> <li>1. Suitable for IR source systems</li> <li>2. Free of spherical aberration coma.</li> <li>3. Most suitable for small apertures.</li> <li>4. Covers small angular field.</li> <li>5. Uses spherical surfaces.</li> </ol>
MAKSUTON		<p>Refractive - reflective</p> <p><math>M_p</math> = Meniscus reflector</p> <p><math>M_s</math> = Meniscus refractor - reflector</p>	<ol style="list-style-type: none"> <li>1 Free of spherical aberration, coma, and chromation.</li> <li>2. Very compact.</li> <li>3. Large relative aperture.</li> <li>4. May also use combination of spherical and aspheric elements.</li> </ol>
GABOR		<p>Refractive - reflective</p> <p><math>M_p</math> = Spherical reflector</p> <p><math>M_s</math> = Spherical refractor - plane reflector</p>	<ol style="list-style-type: none"> <li>1. High aperture system.</li> <li>2. Has mean correction of spherical aberration and coma.</li> <li>3. Suitable for IR source systems.</li> </ol>
FRESNEL LENS		<p>Refractive</p> <p><math>L_p</math> = Special fresnel lens</p>	<ol style="list-style-type: none"> <li>1. Free of spherical aberration.</li> <li>2. Inherently lighter weight.</li> <li>3. Small axial space.</li> <li>4. Small thickness reduces infrared absorption.</li> <li>5. Difficult to produce with present infrared transmitting materials.</li> </ol>

Figure 5-4b. Optical Systems (Additional).

Reflective components have the advantage that they can be combined to make an overall shorter system and provide some degree of correction for aberrations. Reflective systems are more temperature sensitive and more difficult to mount and align than refractive systems. Refractive systems have the advantage that there is no obscuration of the field-of-view. The main disadvantage of refractive systems is the loss of energy through absorption in the components and reflections at optical surfaces. In the infrared, the cost and delicacy of refractive optics makes them prohibitive, and reflective optics are to be preferred.

To obtain a large signal-to-noise ratio of a photo-conductive detector and increase the optical range, a large aperture and a short focal length must be used. However, the quality of the image is reduced as the aperture size is increased and the focal length decreased. Many systems employ a small angular instantaneous field-of-view and a low  $f$ /number and, by some means of scanning, traverse this small field over a wider angle.

### Monochromator

The monochromator contains an active element which disperses, or breaks up, the beam of radiation into a continuous band of radiation, which is then either scanned across an aperture or the detector. The active element used can be a prism, a grating, or a Circular Variable Filter (CVF).

PRISMS. A prism is a transparent optical component with two highly polished surfaces inclined towards each other. The deviation produced by a prism on an incident ray (figure -- ) will vary with the

angle of incidence and the wavelength of the radiation. By rotating the prism, the dispersed rays can be directed toward the detector or exit aperture. Common prism materials are NaCl, KBr, CsBr, LiF, and quartz.

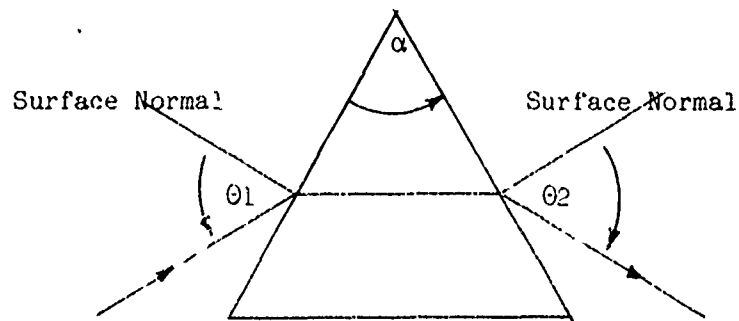


Figure 5-5. Deviation of a Ray Through a Prism.

If a prism is to be used in a spectrometric application, it is necessary to determine its resolution and resolving power--two specifications determine how accurately two very close spectral lines can be measured. The Rayleigh criterion for resolution, as shown in figure 5-6, is the standard adopted. The problem of determining the resolution is to determine the change in deviation angle for a small change in wavelength, i.e., the dispersion. The resolving power equals the effective thickness of the prism times the dispersion of the prism material.

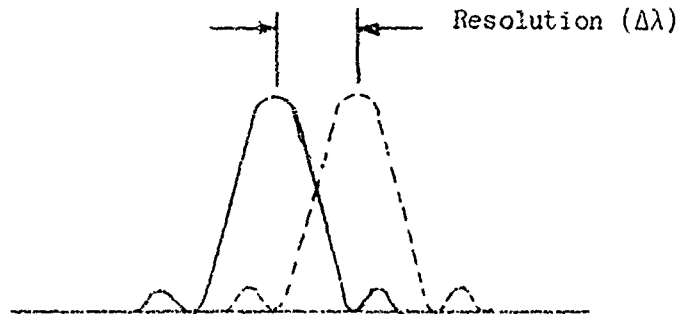


Figure 5-6. Rayleigh Criterion for Resolution.

GRATINGS. A grating consists of a large number of small equally-sized, equally-spaced slits, with each slit causing a diffraction pattern. The waves from the individual slits interfere, and a combined interference diffraction pattern is formed. The grating equation which gives the location of the maximum of each diffraction is

$$d(\sin \theta + \sin \theta') = n\lambda \quad (5-4)$$

where

- $d$  = slit separation
- $\theta$  = angle of incidence
- $\theta'$  = angle of diffraction
- $n$  = the order of the spectrum

The dispersion of a grating is proportional to the order (the value of  $n$ ) of the spectrum. High orders provide greater spectral dispersion, although at a lower intensity.

Gratings present a problem of overlapping of orders. It can be seen from the grating equation that all spectral lines with the same value of  $n$  are diffracted to the same point in the image plane. The  $2\mu\text{m}$  radiation from the first order will overlap the  $1\mu\text{m}$  second-order radiation, and similarly remaining orders will contribute. Thus, only one order must be allowed to reach the detector, which is achieved by filtering the radiation before it reaches the detector, thus eliminating the lower wavelengths from the spectrum. The intensity of a particular order can be enhanced by "blazing" the grating, cutting the grooves at an angle, so that the grating reflects light to a particular order. The angular dispersion of a grating is given by

$$\frac{d\theta'}{d\lambda} = (n/d \cos \theta') \quad (5-5)$$

and the resolving power, which is used to normalize wavelength effects, is given as

$$\frac{\lambda}{d\lambda} = nN \quad (5-6)$$

The resolving power is just equal to the number of lines ( $N$ ) in the grating times the order so that gratings with many lines used in a high order have high resolving power.

CIRCULAR VARIABLE FILTERS. The recent advances in the technology of thin films led to the production of interference filters for the infrared region. These are produced by the deposition of very thin films of a dielectric material on a transmitting substrate, such as germanium, silicon, Irtran, and salt crystals. By a suitable choice of substrate and deposition material, varying the thickness of the dielectric layer allows a filter for any portion of the infrared to be constructed.

The circular variable filter is merely a thin-film interference filter whose thickness varies linearly about a circular substrate. If the thickness at the beginning of the filter is  $t$ , then it is varied linearly until it reaches  $2t$  at some other point of the circular segment. The CVF's can be obtained in either 90-, 180-, or 360-degree segments. Since the rate of change of film thickness with angle of rotation is constant, the wavelength transmitted is a linear function of this angle. The transmittance of a CVF varies with wavelength, but is usually in the range from 30 to 60 percent. The resolution of the filter can be varied, but the usual resolution achieved is in the range of 1 to 4 percent of the spectral region covered by the CVF. The range of wavelengths covered by commercial CVF's is from 1.3 to 15  $\mu\text{m}$ , but they have been constructed for the entire infrared region from 0.4 to 25  $\mu\text{m}$ . Each sector, or segment, covers only a 2:1 wavelength ratio corresponding to the same variation in film thickness. Thus, if the minimum wavelength transmitted is 2  $\mu\text{m}$ , the maximum would be 4  $\mu\text{m}$ . Combinations of either 90- or 180-degree segments are possible to extend the range of one CVF wheel.

The use of the circular variable filter, rather than prisms or gratings, means that the active medium is not an integral component of the optical path. Therefore, the spectrometer design can be greatly simplified resulting in a mobile, compact system. A CVF spectrometer, designed by G.C. Pinnetel, has been used on long-range space missions to obtain ir spectra of planets. The problem of alignment is not serious. Thus, the CVF lends itself readily to field and airborne use. One drawback to the use of the CVF is the low resolution achieved, but



as technology increases, perhaps this will improve somewhat. The spectral characteristics of any interference filter vary with changes in filter temperature, so the design of systems to be used in the field should provide a method for temperature control. The angle of incidence, and the width of the beam as it is incident upon the CVF, also affect the performance and resolution of the CVF.

The design of a circular variable filter wedge spectrometer requires the CVF to be placed at a focal point of the optics for best resolution. Similarly, the field stop and the detector will also be placed at focal points. This necessitates a system design involving either relay lenses or transfer mirrors (figure 5-7).

SUMMARY OF DISPERSIVE ELEMENTS. Three elements, each using different dispersion techniques, have been investigated: prisms, gratings, and CVF's. Of these, prisms are too fragile and expensive for field use. Gratings achieve the best resolution and are not affected by changes in humidity, but since they form part of the optical path, they must be in constant alignment and thus present problems in field and airborne use. (These difficulties may be overcome by rigid mechanical mountings, but this area must be further developed.) The circular variable filter may be the best compromise considering ease of maintenance, mobility, and its ability to withstand field use, if low resolution can be tolerated.

#### RAPID SCAN INSTRUMENTS

The measurement of transient targets requires that the time over which the measurement is performed be shorter than the time of large fluctuations in the source intensity. For spectrometers, this means that a spectral scan must be completed while the radiant exitance of

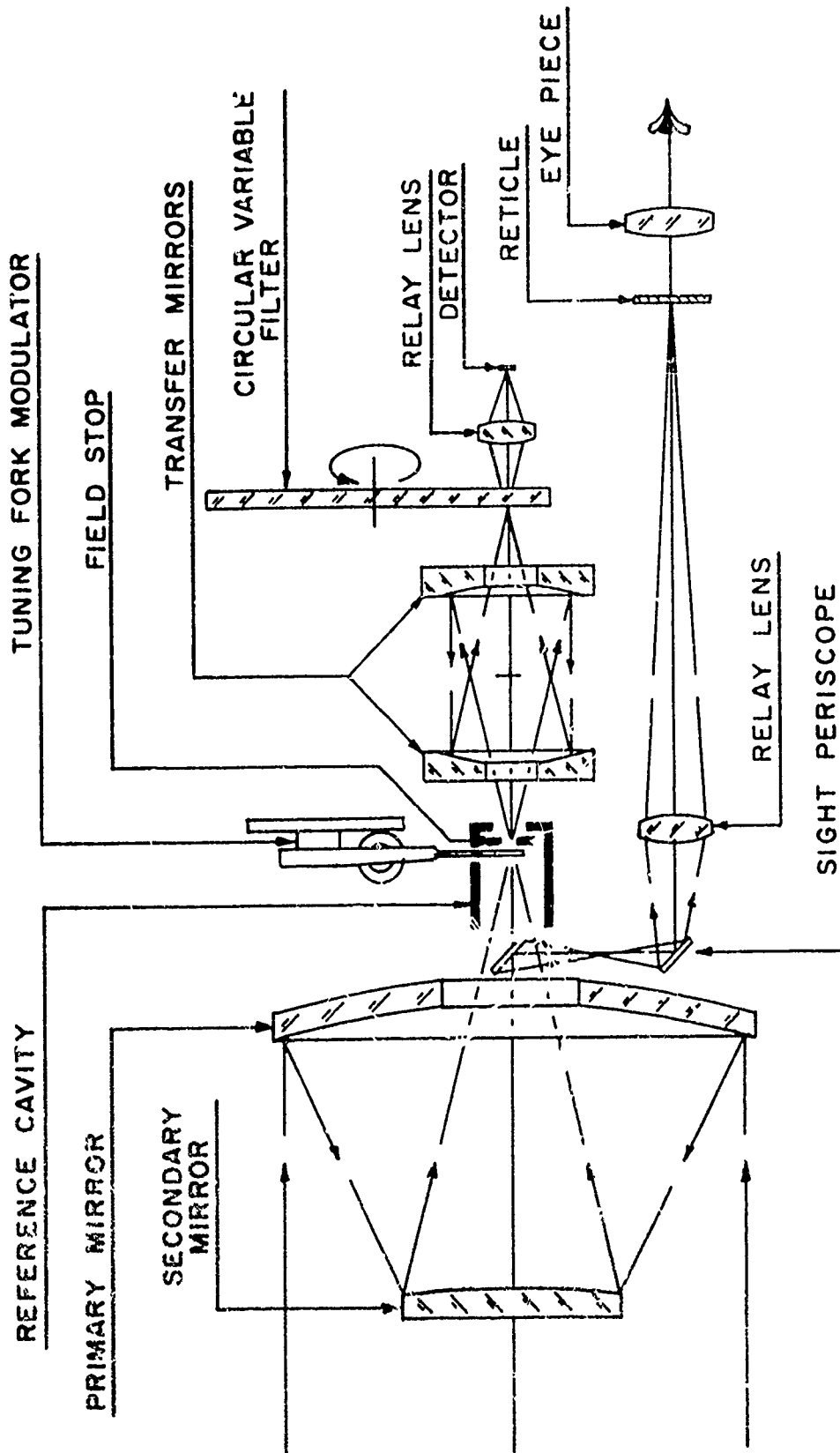


Figure 5 - 7. CVF Spectrometer Optical Diagram.

the target is constant, which requires complete scans in the order of milliseconds.

#### FOURIER TRANSFORM SPECTROMETERS

In addition to radiometers and dispersive spectrometers as detecting instruments for infrared, recently an analogue from the optical portion of the spectrum, the interferometer, has been added. In the dispersion spectrometer, polychromatic radiation is dispersed within the monochromator. Each individual resolution element of the radiation is then measured for intensity, and the result is a spectrum, or plot, of intensity versus frequency. The Fourier transform spectrometer, on the other hand, uses the moving mirror of an interferometer to produce an optical transform of the incoming infrared signal. The radiation at high infrared frequencies is heterodyned to produce low audio frequency signals. The output of the interferometer is an interferogram which contains the spectral information in a multiplex form.

The incoming signal and the interferogram are complementary and constitute a Fourier pair, i.e., by performing a suitable Fourier transformation, the spectrum can be extracted from the interferogram.

The Fourier transform spectrometer offers distinct advantages over the dispersion spectrometer. In the dispersion spectrometer, since each individual resolution element must be measured separately, the time spent on one measurement is a small fraction of the total time required

to scan the spectrum. If there are  $M$  resolution elements and the time required to scan the entire spectrum is  $T$ , the intensity of each element is measured for only a fraction  $T/M$ . The strength, or intensity, of the element is directly proportional to the length of time the detector observes it, whereas noise, being random, is proportional to the square root of the observation time. The S/N ratio of the dispersion spectrometer, theoretically, is then proportional to  $(T/M)^{1/2}$ . The Fourier transform spectrometer, on the other hand, simultaneously measures all of the radiation components incident upon the detector so that all components of the radiation are observed throughout the operating cycle of the instrument. Since the detector of the interferometer sees all resolution elements throughout the entire scan time, the S/N ratio for the interferometer is proportional to  $T^{1/2}$ . The interferometer thus has a higher S/N ratio by a factor of  $M^{1/2}$ . This improvement, called " Fellgett's Advantage," can be quite large under conditions of high resolution. This advantage in S/N ratio can be used to trade resolution for rapid response. A spectrum can be measured with a Fourier transform spectrometer in the same time as with a conventional spectrometer, but at a higher S/N ratio, or conversely, with the same S/N ratio but in a much shorter scan time.

The second advantage of the interferometer is that in the dispersion spectrometer the radiation beam entering the monochromator must be defined by narrow slits, limiting the amount of radiation entering the instrument and reaching the detector. These entrance slits, not required within the interferometer, greatly increase the light gathering capability of the interferometer spectrometer.

Disadvantages of the interferometric method are susceptibility of the instrument to vibration and consequent interference with the signal. The mounting platform must be quite rigid. This does not present problems in the laboratory, but is difficult to obtain in practice in the field. Secondly, because the spectrum is not produced at the same time that it is scanned, it is difficult to set up for an experiment. The amount of data involved and the handling are increased immensely. Performing the Fourier transform routinely requires the use of a digital computer. However, these problems are not insurmountable, and commercial interferometers now use a laser frequency standard as a reference to overcome vibrational interference.

#### Michelson Interferometer.

Just as there are many optical layouts for the conventional spectrometers, there are various arrangements of components of an interferometer. The basic components of an interferometer, mirrors, lenses, and beamsplitters, can be arranged into a Michelson, a Fabry-Perot, a triangular, or a Mach-Zehnder-type interferometer. An optical schematic of each type is shown in figure 5-8. Because the Michelson interferometer is one of the most widely used and simplest to understand, its operation is described below.

Referring to the optical diagram of the Michelson interferometer, (figure 5-9) there are two mirrors:  $M_1$  and  $M_2$ . Mirror  $M_1$  is movable, and a linear actuator is responsible for the movement; mirror  $M_2$  is fixed. An incoming beam of radiation,  $a$ , enters the interferometer cube and strikes the beam-splitter plate,  $S$ . On its inner surface,

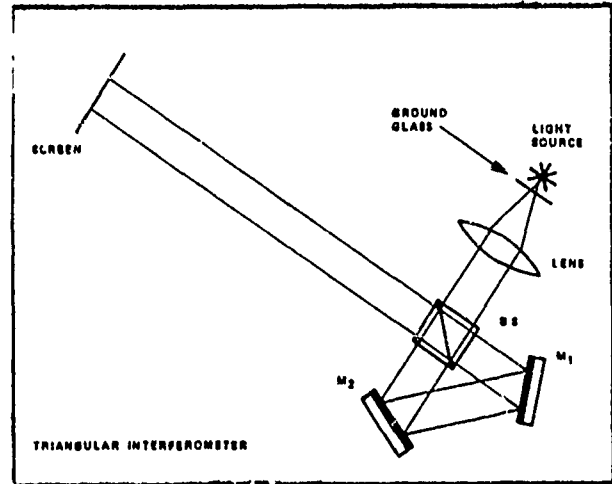
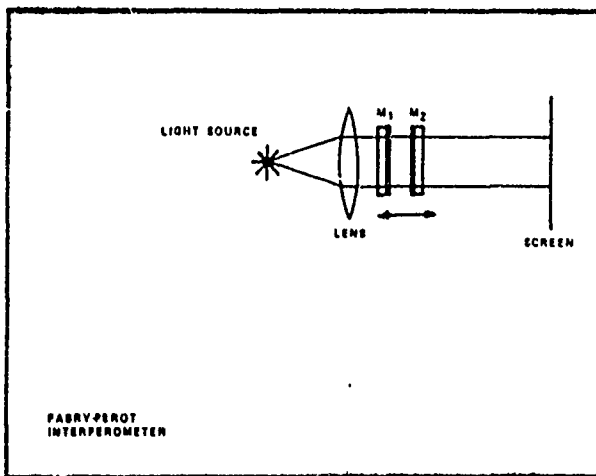
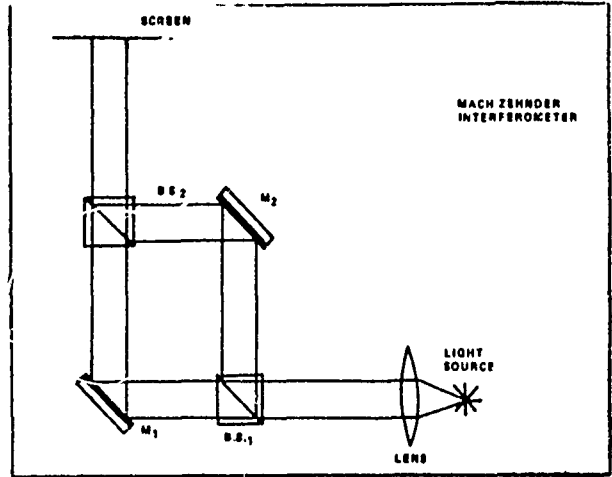
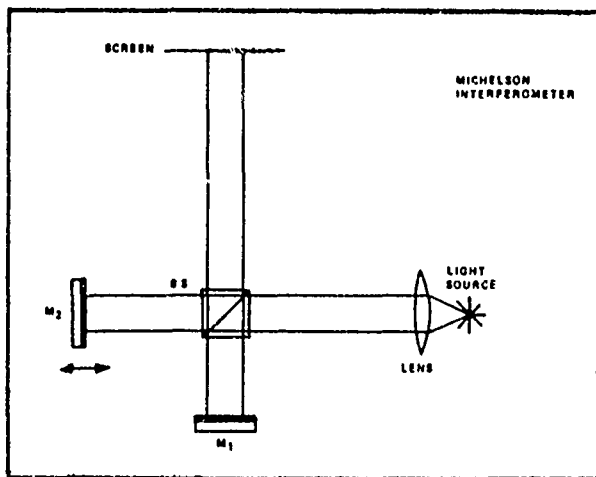


Figure 5-8. Optical Layouts of Modular Interferometers

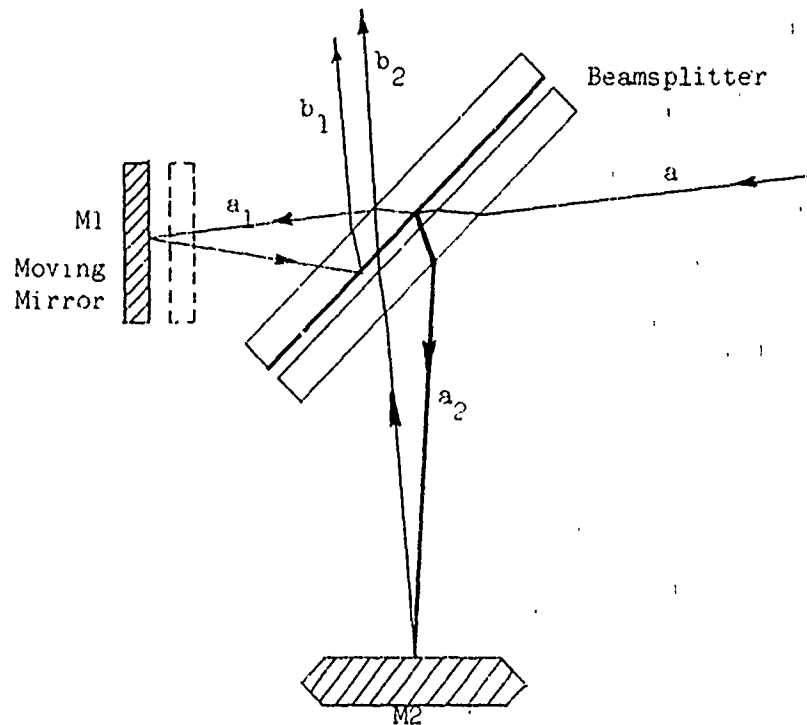


Figure 5-9. Path of a Ray in a Michelson Interferometer.

the beamsplitter plate carries a semireflecting coat; a compensator plate of the same thickness as the beam splitter is located on the opposite side of the reflecting coat. The incoming ray divides into two rays,  $a_1$  and  $a_2$ , at the semireflecting coat. Each ray is reflected by one of the mirrors and returned through the compensator to the semireflecting coat. At the beamsplitter, rays  $a_1$  and  $a_2$  are reflected and

transmitted respectively, and the exiting parallel rays,  $b_1$  and  $b_2$ , interfere either constructively or destructively, depending upon their relative phases. As long as these rays remain parallel, the wave fronts remain parallel and will interfere. The final beam exits out of the optical cube and is directed towards the detector.

The phase of ray  $a_1$ , with respect to that of ray  $a_2$ , can be changed simply by moving mirror  $M_1$ . If mirror  $M_1$  moves a distance  $x$ , ray  $a_1$  travels a distance greater by  $2x$ , and the intensity of the resulting exiting radiation is given by

$$I = I_0 H [1 + \cos \{2\pi\nu (2x)\}] \quad (5-7)$$

where

$I$  = the intensity of  $b_1$

$I_0$  = intensity of  $a$

$H$  = the modulation efficiency (always less than 0.5).

If the mirror excursion is proportional to time, the instantaneous displacement of the mirror is given by

$$x(t) = kt, \quad (5-8)$$

where

$k$  is a constant denoting the constant velocity of mirror travel, then the intensity transmitted by the interferometer is

$$I = I_0 H [1 + \cos 2\pi\nu(2Kt)] \quad (5-9)$$

The transmission is thus periodic in time with a frequency,  $f_\nu$ , which depends upon the wave number (inverse to wavelength) of the entering radiation:

$$f_\nu = 2\nu K \quad (5-10)$$



This relationship shows that the output frequencies of the interferometer are related in an isomorphic manner to the wave numbers of the incoming radiation.

## DETECTORS

The final, and probably the most important, part of the infrared measuring apparatus is the detector. There are many physical phenomena which can be used to measure the quantity of infrared radiation incident upon a specific receiving area. These phenomena serve to divide the types of infrared detectors into two classifications: thermal, in which the radiation of any wavelength is absorbed by a suitable blackened target whose temperature rises slightly, and quantum, in which the radiation of a well-defined wavelength (electronic transition) is absorbed by the material forming the targets. The sensitive element (detector) of the infrared system is the heart of an infrared system, and, to a great extent, determines the instrument's resolution and discrimination capability.

### Detector Characteristics

The quantum, or photon, detector exhibits an output which depends upon the energy of the photons incident on its surface. The absorption of photon energy by a suitably constructed semiconductor material generates a charge carrier within the material, causing an instantaneous change in resistance. This change in an electrical property of the material can then easily be measured. Photon detectors can further be classified according to mode of operation:

1. Photoemissive
2. Photovoltaic

3. Photoconductive
4. Photoelectromagnetic
5. Photoluminescent

Thermal detectors have an output that is directly proportional to the amount of incident radiation striking the detector. Because they respond to the density of photons, they are nonselective and respond equally well to all wavelengths, in contrast to the quantum detectors which respond to the energy of the photon. Some types of thermal detectors, classified according to mode of operation are:

1. Thermopiles
2. Thermocouples
3. Bolometers

#### Performance

Detectors of the same type can be evaluated only under conditions specific for each detector. The operating conditions for the evaluation must be specified.

$T_D$ -OPERATING TEMPERATURE. The actual operating temperature of a semiconductor detector must be known, since the detector's sensitivity varies with temperature. The resistance of the sensitive element depends upon the temperature coefficient of the detector material.

$T_S$ -TEMPERATURE OF SOURCE. The temperature of a blackbody source must be known in order to specify its spectral properties due to the selective nature of spectral response.

$A_d$ -AREA OF THE DETECTOR. The sensitivity of a detector is inversely proportional to the sensitive area of the detector. A knowledge of this area is necessary to evaluate the detector.

$f_c$ -CHOPPING FREQUENCY. If the radiation observed is modulated, it is important to know the frequency distribution of the modulation and the bandpass employed, as some detector characteristics change as a function of the modulation frequency. For example, the sensitivity of some detectors is enhanced at higher chopping frequencies.

$\nu_f$ -NOISE BANDWIDTH. The bandwidth of operation for the noise figure determination.

NEP-NOISE EQUIVALENT POWER. NEP is the minimum intensity of radiant power falling on the surface of a detector that will give rise to a signal voltage equal to the noise voltage of the detector. The noise voltage ( $V_n$ ) of any detector is directly proportional to its temperature multiplied by the square root of the noise bandwidth times the area of the detector ( $A_d$ ).

$$V_n = T (\Delta f)^{1/2} (A_d)^{1/2} \quad (5-11)$$

The NEP of a detector with a signal-to-noise voltage of 1:1 (that is with  $V_s$ , the rms signal voltage, equal to  $V_n$ , the rms noise voltage) is given by

$$\text{NEP}(1:1) = E \cdot A_d \cdot V_n / V_s (\nu_f)^{1/2} \quad (5-12)$$

where  $E$  is the irradiance in  $\text{watts/cm}^2$ . The smaller the NEP, expressed in  $\text{watts/cm}^2$ , the higher the sensitivity of the detector.

$D_\lambda^*$ -SPECTRAL DETECTIVITY. Detectivity is a measure of detector sensitivity.

$D_\lambda^*$  is an area-independent parameter given by

$$D_\lambda^* = A_d^{1/2} / \text{NEP} \quad (5-13)$$

$\tau$  - TIME CONSTANT. The speed of response of a detector is referred to as the time constant of that detector. It is the time required for

a signal to decay from maximum amplitude to 1/e of its peak. The frequency response and the time constant are related by

$$\tau = 1/2\pi f \quad (5-14)$$

where

$\tau$  = the time constant in seconds.

$f$  = the modulating frequency in hertz at the point where the response is down to one-half its maximum output (3 db point).

Other parameters of interest concerning detectors are the responsivity,  $R_s$ , of the detector and the spectral response,  $R_\lambda$ . The responsivity is the response per unit radiation input, which relates the magnitude of the response to the quantity of incident radiation. The responsivity quite often is dependent upon the bias load resistance chosen for the detector; the spectral response is merely a variation of  $D_\lambda^*$  vs wavelength.

DETECTOR FIELD-OF-VIEW. Detector field-of-view also must be specified for comparison of similar detectors because  $D_\lambda^*$  increases as the field-of-view is narrowed.

The above parameters are specified whenever detectors are compared. A typical sensitivity specification for a detector might then be

$$D_\lambda^* (3.0, 1000, 1, 30) = 1 \times 10^{11}$$

where

3.0 = wavelength at which  $D_\lambda^*$  was measured (micrometers)

1000 = chopping frequency (Hz)

1 = electronic bandwidth (noise bandwidth) (Hz)

30 = field-of-view of detector (degrees)

Occasionally detector sensitivity is averaged over the detector spectral range of sensitivity rather than being specified at a particular wavelength. This averaged quantity is referred to as blackbody D\*. Thus, the irradiating source for the sensitivity measurement would be a blackbody operating at some specific temperature. The temperature of operation is specified rather than the wavelength of measurement.

#### Operation

The two principal modes of operation for quantum detectors are photovoltaic (PV) and photoconductive (PC). The photovoltaic detectors offer the highest obtainable sensitivity in a particular spectral region, but because it is easier to manufacture photoconductive detectors, their use is more widespread.

PHOTOVOLTAIC DETECTORS. Photovoltaic detectors are constructed from semiconductor materials in the form of PN junctions. When infrared radiation of a suitable frequency is incident upon the junction, photons are absorbed by the material and an emf is generated. The small voltage developed is produced by the intrinsic excitation of hole-electron pairs from the valence to the conduction band. The consequent separation of these pairs across the junction due to the internal space charge (opposing the internal voltage drop) results in the development of the photovoltage.

PHOTOCONDUCTIVE DETECTORS. The photoconductive mode of operation depends upon a marked increase in electrical conductivity which is exhibited as a change in resistance due to the generation of hole-electron current carriers. The production of current carriers can be either intrinsic, as in the case of photovoltaic detectors, or extrinsic, in

which case electrons are excited from or to impurity levels which lie within the forbidden band of the semiconductor. These impurity levels are controlled by the amount and character of doping material added to the semiconductor. Thus, it is relatively easy to produce new detectors for different regions simply by changing the dopant. The use of this type of detector requires a bias supply as shown in figure 5-10. The bias should be selected to obtain the highest possible responsivity consonant with maximum thermal power dissipation of the detector.

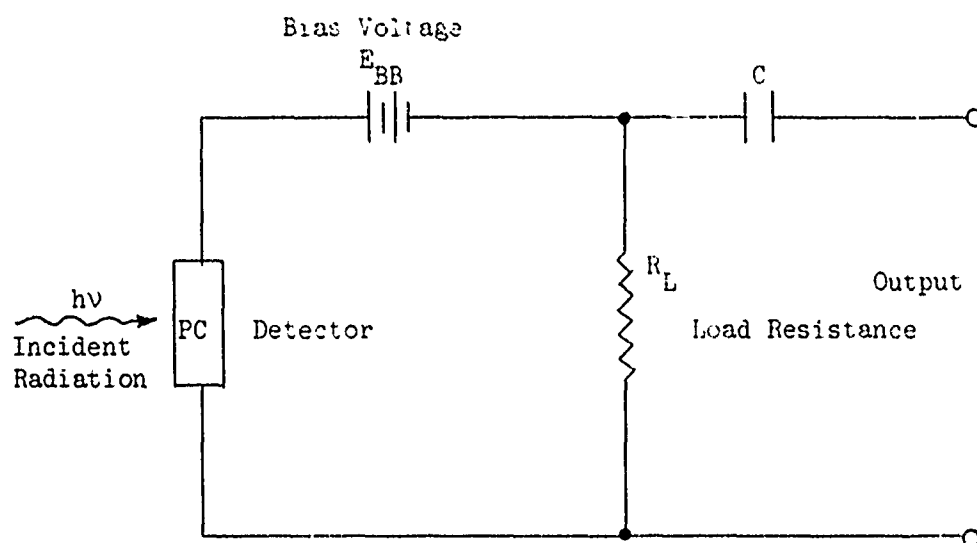


Figure 5-10. Photoconductor Circuit Configuration.

The most sensitive detector for a particular spectral region is not always the most suitable. For example, in the 8-14  $\mu\text{m}$  region, mercury-doped germanium [Ge(Hg)] has the highest detectivity, but this is not obtained until the detector reaches 30°K using liquid hydrogen as a coolant. The use of liquid hydrogen as a coolant leaves much to be desired, since the potential hazards are quite great. Similarly, the use of liquid helium as a coolant presents operational difficulties in field use. Thus, for field use, a mixed detector of the mercury-cadmium-telluride (HgCdTe) type probably should be used. The type of detector to be used depends upon the type of experiment to be performed. If sensitivity is the most important criteria, then perhaps the doped germanium detectors should be used with liquid helium as the coolant.

Today the most commonly used detectors are indium arsenide (InAs) and lead sulfide (PbS) in the 1-3  $\mu\text{m}$  region, indium antimonide (InSb) and lead selenide (PbSe) in the 3-5  $\mu\text{m}$  region, and HgCdTe and Ge:Hg in the 8-14  $\mu\text{m}$  region (figure 5-11). All of these, except the Ge:Hg, employ liquid nitrogen as a coolant, which is cheap, readily available, and easily handled. However, recently a new compound, lead-tin-telluride (PbSnTe) was developed as detectors in the 8-14  $\mu\text{m}$  region. The PbSnTe detector also uses liquid nitrogen as a coolant.

#### Bias Conditions

Infrared detectors which operate in the photoconductive mode require a set bias condition in order to operate properly. The optimum bias condition is that which results in the largest output signal-to-noise ratio for a constant input signal. In order to determine the proper bias, a

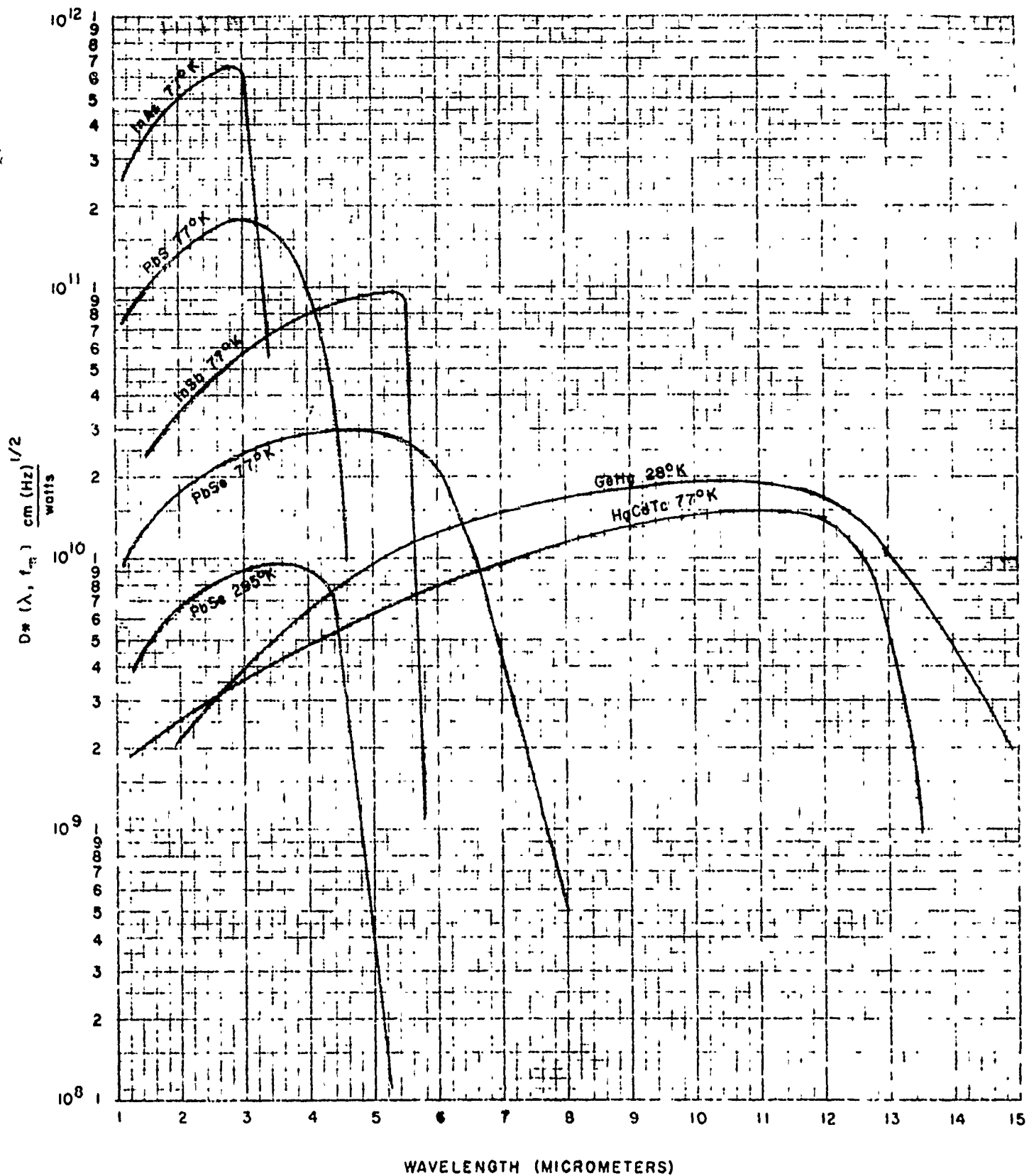


Figure 5-11. Spectral Detectivities of Detectors.



measurement of the noise voltage,  $V_n$ , as a function of bias current must be carried out with values of the signal voltage,  $V_s$ . These two curves are then plotted as a function of the different bias conditions to determine the best operating S/N ratio. Thus, the optimum bias for that particular detector is determined as shown in figure 5-12.

#### SYSTEM SENSITIVITY

The sensitivity of an infrared system including the optics may be obtained from the usual relations involving the figures of merit: Noise Equivalent Power (NEP) and Noise Equivalent Irradiance (NEI). The NEP of a detector is given as

$$NEP = \frac{A_d \Delta f}{D^* \lambda} \quad (5-15)$$

where

$A_d$  is the area of the detector

$\Delta f$  is the electronic bandwidth

and  $D^*$  is the spectral detectivity of the detector.

The radiant power transferred from the optical system aperture to the detector is given by the product of the irradiance at the aperture, the system transmittance, and the optical aperture area. The NEI of the system is related to the NEP by

$$NEI = \frac{NEP}{A_o T R} \quad (5-16)$$

where

$A_o$  is the clear optical aperture area

$T$  is the system transmittance

$R$  is the response of the system

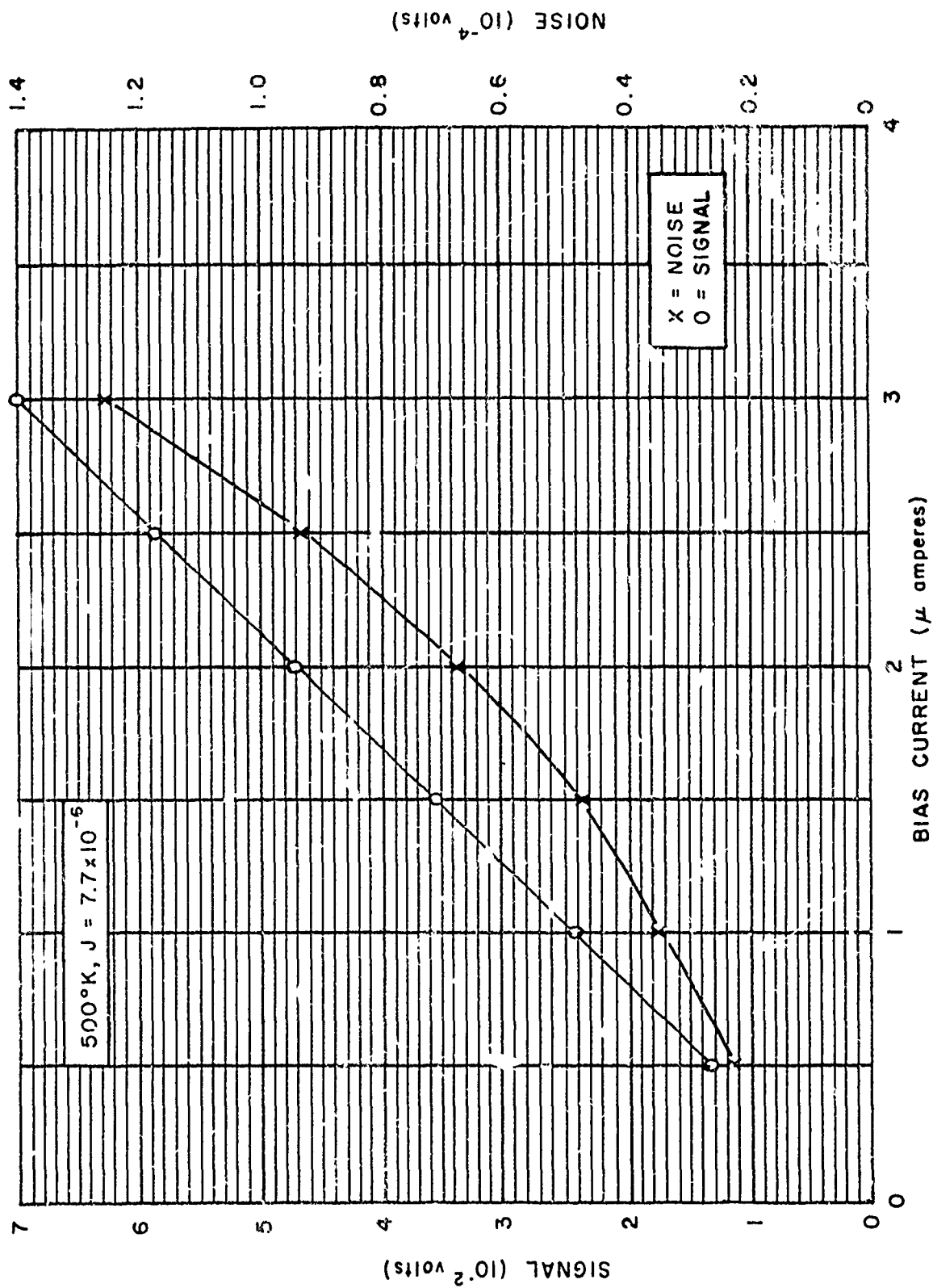


Figure 5-12. Selection of Optimum Bias for Typical Photoconductor Detector.

This gives the equation for calculating the sensitivity of the system:

$$NEI = \frac{A_d \Delta f}{A_o \tau_o R D_o^2} \quad (5-17)$$

This equation may be rearranged into other more suitable forms. The useful area of the detector is related to the solid angle of viewing ( $\Omega$ ), the system effective focal length (F), and the diameter of the collecting optics ( $D_o$ ) by

$$A_d = \Omega_d F^2 = \Omega_d (f/no)^2 D_o^2 \quad (5-18)$$

where

$\Omega_d$  = solid angle of viewing of the detector

F = effective focal length of the system

$D_o$  = diameter of the system collecting optics (clear aperture)

The area of the collecting optics is given by

$$A_o = \frac{\pi D_o^2}{4} \quad (5-19)$$

Inserting these equations yields

$$NEI = 4f, no \frac{\Omega_d \Delta f}{\pi D_o^2 \tau_o R} \quad (5-20)$$

## BORESIGHT CAMERA

A boresight camera is one of the most important tools used to measure moving targets. It provides a direct correlation between the actual measured data and the position of the target along with the time of the event. Thus, selection of a boresight camera is one of the important supporting procedures to be carried out.

The primary parameters to be incorporated into the design of the boresight camera depend upon the target to be photographed. The optical field-of-view should provide maximum tracking ease consistent with a large object image on the film. When photographing a moving target, speed of the target and the possibility of various ranges require a variety of film speeds. The camera should allow rapid change from one exposure to another. Individual frames, 10 frames/second, up to a maximum capability of 50 frames/second, either line or pulsed, should be available. High frame-rates require external magazines of sufficient capacity to allow the continuous filming of an entire event. A projected reticle pattern exposed on the film will aid in determining target location in the exposed frame area.

The type of film used depends upon the purposes of the test and the location where the photographs will be put.

High contrast film is used for targets against a bright sky background.

High speed film is used for targets against a dark background.

handling, user familiarity, and enlargement requirements. The use of film which responds to infrared light should not be overlooked, as it may reveal otherwise unseen features.

The camera itself should provide rapid boresighting, adjustable shutters and apertures, provision for inserting filters, and timing lights or coding posts for the inclusion of auxiliary data on the film. Suitable cameras are readily available from a variety of manufacturers.

#### IMAGING SYSTEMS

An imaging system provides a pictorial thermal map of the target. In the past, these have been used to provide qualitative information to locate hot spots on the target.

An imaging system would be used to determine comparative irradiance contours over and around the target to determine plume contours and spatial extent. Rather than specifying temperatures, the instrument would yield "effective" irradiance at the instrument as the parameter of measurement. The ideal imaging system would be spectral, but the data output would be overwhelming, so a practical system is, in essence, merely a spatially scanning radiometer. That is, the radiometer has a small instantaneous field-of-view to provide good spatial resolution, which is then scanned over a wide area to allow large objects to be completely covered.

A total field-of view of 10 x 10 degrees/frame would be satisfactory. An instantaneous field-of-view of about 1 milliradian/element would cover a frame with 174 x 174 resolution elements, or approximately  $3 \times 10^4$  data

points. This corresponds to a spatial resolution of  $1 \text{ ft}^2$  on a target 1000 feet away from the instrument.

The imaging system should scan a frame in at least 0.1 second if the radiant exitance of the target is to remain constant over the time interval of a scan. This means the use of photon or quantum detectors with time constants in the microsecond region. The use of such detectors coupled with logarithmic amplifiers should yield a useful dynamic range of four orders of magnitude in irradiance.

At present, most imaging systems provide an oscilloscope display utilizing brightness contours as the output format. This video picture then can be photographed or recorded.

The operation of one type of imaging system is detailed below.

#### AGA Thermovision

The infrared thermovision, responsive to radiation in the 2.0- to 5.4-micrometer region, was developed primarily for use in medical research. Figure 5-13 is a schematic of its optical unit. Instrument parameters and characteristics are:

Detector: 1/2 mm dia InSb (PV) with 60 degree cold shield

Total Field-of-View scanned: 5 degrees x 5 degrees

Number of lines per frame: 100 total

Optical Resolution: 100 elements/line

Frame Rate: 16 frames/second

Thermal Discrimination at room temperature:  $0.2^\circ\text{C}$ .

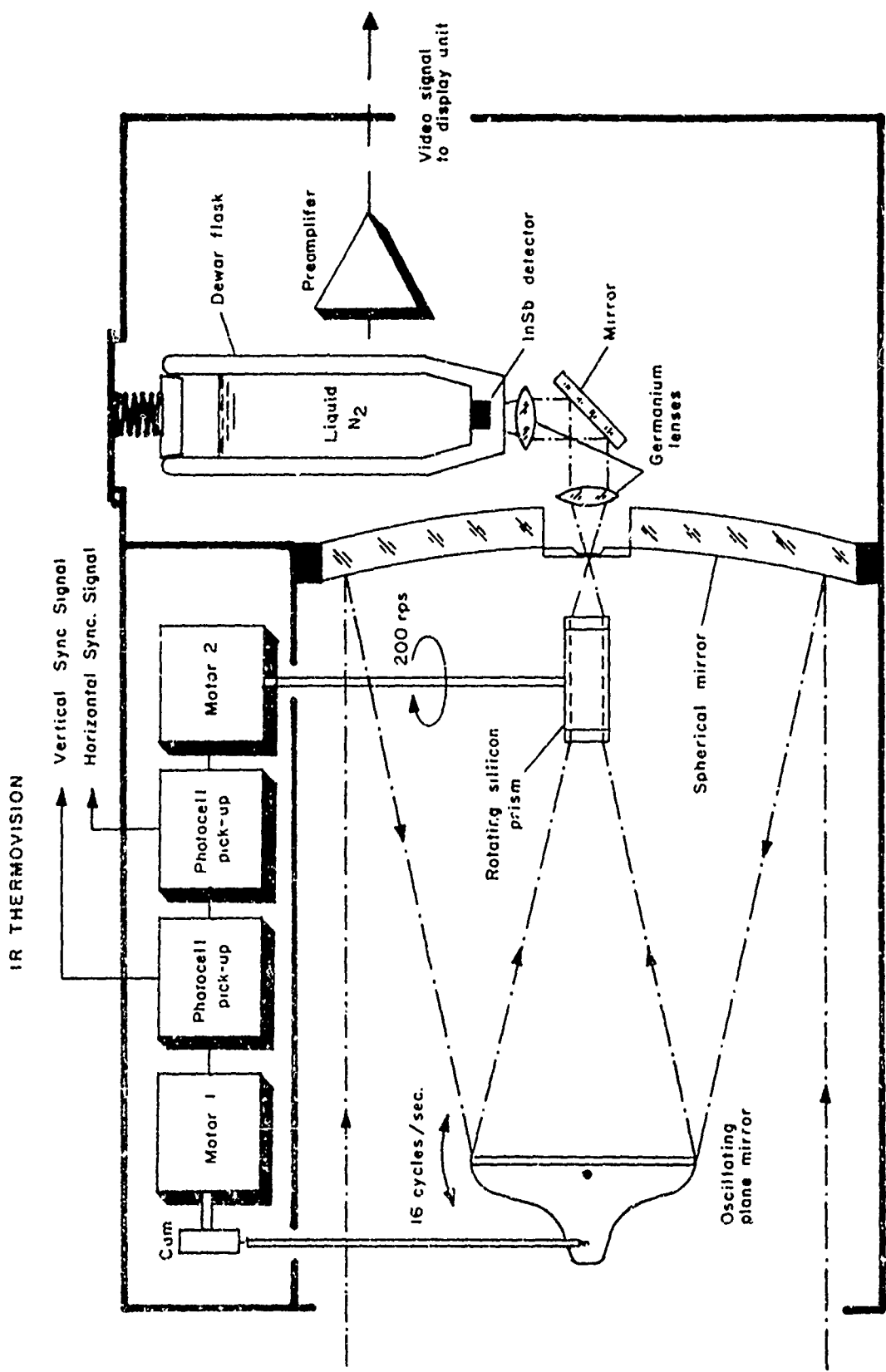


Figure 5 - 13. Schematic of Optical Unit

OPERATION The infrared radiation is focused on the detector through an optical train which consists of the following: a primary spherical mirror, a secondary plane mirror (tilts or oscillates around a horizontal axis at 16 cycles/second, producing 16 frames/second), an octagonal silicon prism (rotating at 200 rps so that eight lines are scanned in each revolution, resulting in 1600 lines per second), small aperture collimating lenses, a vertical direction mirror, condensing lenses, and a detector. The signal from the detector is fed through an amplifying system and displayed on an oscilloscope.

#### METEOROLOGICAL INSTRUMENTS

Various meteorological data is required before we can account for radiation loss due to atmospheric attenuation. The barometric pressure at the site, the relative humidity, and the temperature are required. In some special cases, it also may be necessary to record the relative wind direction and speed. The temperature should be recorded in degrees Centigrade to better than one degree. A psychrometer should be used to determine relative humidity, which should be recorded to within one percent. Similarly, the atmospheric pressure measurements should be recorded to at least tenths of millimeters of mercury. Commercial instruments for these measurements are readily available from many sources.

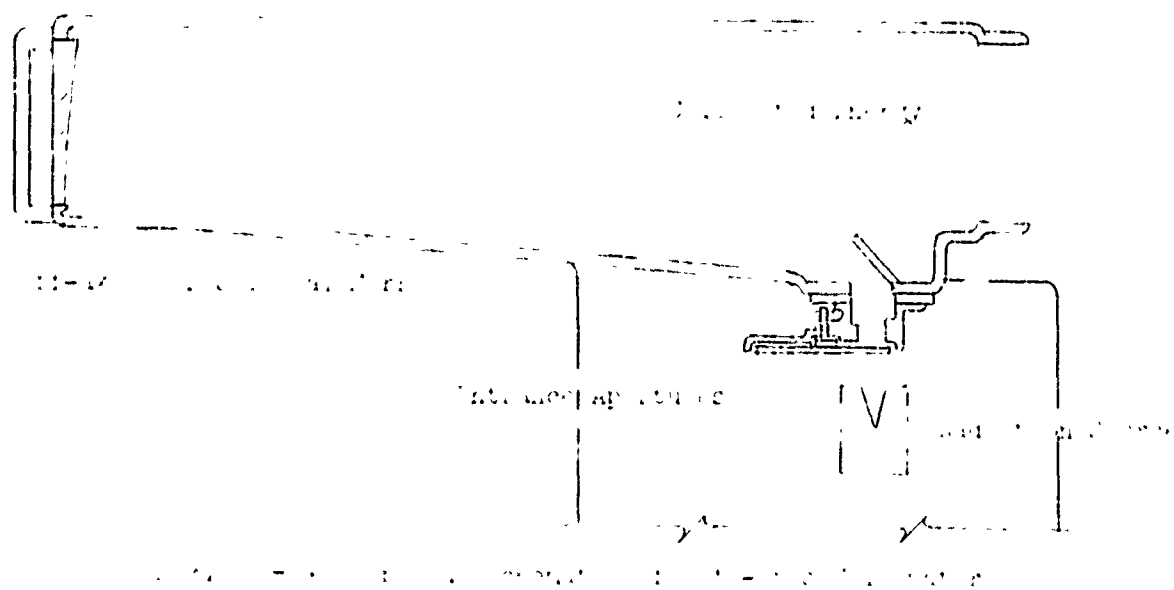
#### COLLIMATOR

An off-axis collimator is an essential part of the equipment used to calibrate, test, and align radiometric and spectrometric equipment. The collimator, when coupled with a standard reference source, provides



a laboratory point source which can simulate the spectral characteristics of infrared targets. It can be used to check the response of missile seekers and other detective elements, and to align and measure the field-of-view of any optical instrument including spectrometers.

An off-axis collimator differs from the normal collimator in that reflecting rather than refracting optics are used. It also provides greater transmission without obscuring the source. The collimator converts divergent radiation from a finite extended source into parallel radiation seeming to come from a point at infinity. The collimator, through the use of an off-axis paraboloidal mirror, produces a uniformly intense beam of parallel radiation. The basic design and layout of an off-axis collimator is shown in figure 5-1.



Radiation from some source (such as a calibrated blackbody) enters the collimator through one of a set of entrance apertures selected for the particular test. The radiation is directed onto a plane mirror which reflects the beam toward the concave mirror where it is collimated and re-directed towards the exit aperture.

The exit aperture of the collimator should be large enough to completely irradiate the optics of any system being tested. The entrance apertures should offer a wide selection of source areas, and the resolution of the instrument should be at least 0.5 milliradian, and preferably better, for best suitability for all applications.

There are many commercial collimators, but the specific type chosen should also be capable of being modified for possible future application. The collimator design should provide for modulating the incoming radiation and interchanging a variety of radiation sources

#### PEDESTAL TRACKING SYSTEM

The proper pedestal tracking system for a specific use is one of the most important and yet one of the most easily neglected items of the instrumentation package used for measurements. In general, so many types of pedestals are available that there is no problem in obtaining the proper type for a particular application. The main problem lies in specifying the particular minimum and maximum requirements for the specific application. Once the system requirements have been clearly defined, an existing pedestal may be modified to meet the specified requirement.

A pedestal that is rugged, reliable, rigid, smooth in operation, and capable of high tracking accuracy is required. An extremely stiff

pedestal system must have a very low resonant frequency, which is a function of moment of inertia and stiffness. Smooth operation at low speeds is a function of static and dynamic friction. Thus, the primary design consideration for static elements is high structural stiffness; for dynamic elements, internal rigidity and low friction.

The important parameters to be specified before acquiring a pedestal include:

Instrumentation Weight

Pedestal Speed Range-Maximum and Minimum

Accuracy and Precision

Velocity Constant

Acceleration Constant

Elevation Tracking Rate

Azimuth Tracking Rate

Mechanical Vibrations of the System

Maximum acceptable error due to tracking velocity and tracking acceleration lag.

The design of the pedestal tracking system must be based on the velocity of the target, the ranges of the expected targets, the flight patterns expected, and the desired tracking accuracies. The pedestal is the usual limiting factor in obtaining the desired tracking accuracy. The method of tracking, whether it be by radar, infrared, or video contrast, is an integral part of the pedestal, but the mechanical system involved in responding to the electrical error signal introduces the gross inaccuracies to the system. The weights of the instrumentation and

field-of-view of the optics influence the pedestal design. For our system, the spectrometer will provide the determining criteria. The following discussion illustrates the above design parameters.

Our target is to be an aircraft--engaged in a fly-by or a hovering mode--and we are to measure the radiant emissions of the aircraft in many different aspects. A sample target will have-

Ranges            0-5-10 km

Altitudes.        0-3000 m

Velocities        0-400 knots (0-200 m/sec)

Assume the worst condition to be an aircraft sweeping horizontally across the field-of-view 1000 meters away from the pedestal at 400 knots. This requires that the pedestal have a maximum speed of 11.7 degrees/second or 205 milliradians/second. The tracking velocity of the pedestal should be continuously variable up to at least 25 degrees/second. To determine the minimum tracking rate, assume an aircraft in the same flight pattern, but at a range of 10 kilometers traveling at 50 knots or 25 m/sec. This requires the positioning pedestal to have a minimum speed of 0.15 degrees/second or about 2.5 mr/sec. The tracking velocity of the pedestal should be continuously variable from 0.05 degree/second to 25 degrees/second. Similarly the tracking acceleration of the pedestal should be continuously variable from 0 to 25 degrees/second/second.

The worst tracking condition is defined by an object at a range of 1000 meters traveling at a speed of 205 m/sec. The spectrometer to be mounted on the pedestal has a field-of-view of 4 mr and the object (tail-pipe opening) to be tracked subtends a 0.5 mr angle. Then the tolerable error (maximum) due to target velocity and acceleration should not exceed

1.75 mr for the target to remain in the field-of-view of the measuring instrument. This, of course, depends upon the size of the target. From the above data, we may calculate the required system velocity and acceleration constants

$$K_v = \omega/e_v = \frac{205 \text{ mr/sec}}{1.75 \text{ mr}} = 117 \text{ sec}^{-1}$$

$$K_a = a/e_a = \frac{10 \text{ mr/sec}^2}{.25 \text{ mr}} = 40 \text{ sec}^{-2}$$

The approximate total error is given by the sum of the velocity and the acceleration error

$$e_T = e_v + e_a = 1.75 + .25 = 2.0 \text{ mr}$$

These errors are caused by the time delay in the servo systems of the pedestal responding to an error signal

Accuracy will be defined as a freedom from error, while precision will be defined as reproducibility. Accuracy is then a measure of total error including all bias (systematic) and noise (jitter) components. Precision will be a measure of noise error only since noise components interfere with the ability of the pedestal to reproduce a position measurement. In either case, the errors should be much less than the velocity and acceleration errors. The minimum smooth tracking rate of the positioning pedestal is limited by static friction and the torque gain that can be achieved with the drive system. At low tracking rates the pedestal executes discrete steps in following the target as the torque delivered by the drive system exceeds and diminishes below the static friction. The tracking smoothness will be influenced by the static friction for target rates that cause servo velocity lag errors less than the ratio of static friction to torque gain. This ratio is

essentially the static positioning accuracy of the pedestal, other noise ignored. A static positioning accuracy of 0.01 mr is easily achieved and allows the low tracking steps to appear to be continuous.

Resonant frequency of the pedestal is a function of moment of inertia and stiffness. The arrangement of the instruments on the pedestal should be chosen to minimize inertia. Resonant frequency calculations should be carried out in order to assure that mechanical vibrations will not interfere with the operation of the instruments. The servo system requires a very stiff pedestal with a maximum resonant frequency of perhaps 15 Hz in azimuth and 30 Hz in elevation.

The design requirements of our system follow:

Maximum tracking speed	205 mr/sec
Minimum tracking speed	2.5 mr/sec
Velocity constant	117 sec <sup>-1</sup>
Acceleration constant	40 sec <sup>-2</sup>
Maximum tolerable error	2 mr
Static positioning accuracy	0.01 mr
Maximum resonant frequency	15 Hz azimuth 30 Hz elevation
Instrumentation weight	1000 pounds

Basically the type of data desired determines the type of instruments and pedestal to be used to collect the data.

## CHAPTER VI

### DATA REDUCTION AND ANALYSIS

The exact technique to be used for data reduction depends upon the type of instrumentation used, the particular calibration procedure for that instrument, the method used for recording data, and the data reduction equipment available. The scope of data analysis is generally limited by instrumentation parameters such as spectral resolution, dynamic range, calibration accuracies, field-of-view, and sensitivity. Included in this chapter will be a general discussion of data reduction and analysis and a specific example of data reduction.

#### ACCUMULATION OF DATA

The reduction of data might be classified into four main headings:

1. Real time data accumulation
2. Data selection by hand
3. Data selection and arrangement by computer
4. Data reduction

During experiment, the real time data which is recorded can consist of many channels of information recorded on magnetic tape, photographic film record, and perhaps other types of permanent record, such as plots and oscillograph records.

After the experiment, the magnetic tape is played back and the boresight film is scanned to reject unsuitable data. The boresight film is scanned to determine the data which corresponds to the aspects needed for the particular experiment. The data is played back and examined for noise, amplitude of signal, band edge, dynamic range, and signal-to-noise ratio to determine usable data.

The selected and edited data is then digitized, formatted, the tapes are blocked, and a listing of the data is produced for further examination. This prepares the tapes for insertion into the computer to be used for the actual data analysis.

The spectral data, along with data on atmospheric attenuation, and range and aspect angles, are fed into a computer for the final data reduction.

The output of the computer is then examined and plots of the data are examined to determine the validity of the data reduction. The spectral radiant intensities and irradiance contours (figure 6-1) are plotted as functions of the aspect angle. The data can then be further analyzed to evaluate the results of the experiment. Lock-on ranges can be calculated, and the contributions of other parameters may be examined.

#### SPECTROMETRIC DATA

The most common quantity measured by spectrometers is spectral irradiance at the entrance aperture, although the quantity of interest is spectral radiant intensity. Spectrometers recommended for use in the measurement of aircraft, or any moving or nonstatic target, scan a relatively wide spectral region at a high rate, thereby producing several sample spectra per second. This large amount of data necessitates the use of digital computer techniques for data reduction. The spectral radiant intensity of the target is determined by applying instrument calibration parameters, distance to the target, and atmospheric transmission data to the instrument output.



The selected and edited data is then digitized, formatted, the tapes are blocked, and a listing of the data is produced for further examination. This prepares the tapes for insertion into the computer to be used for the actual data analysis.

The spectral data, along with data on atmospheric attenuation, and range and aspect angles, are fed into a computer for the final data reduction.

The output of the computer is then examined and plots of the data are examined to determine the validity of the data reduction. The spectral radiant intensities and irradiance contours (figure 6-1) are plotted as functions of the aspect angle. The data can then be further analyzed to evaluate the results of the experiment. Lock-on ranges can be calculated, and the contribution of other parameters may be examined.

#### SPECTROMETRIC DATA

The most common quantity measured by spectrometers is spectral irradiance at the entrance aperture, although the quantity of interest is spectral radiant intensity. Spectrometers recommended for use in the measurement of aircraft, or any moving or nonstatic target, scan a relatively wide spectral region at a high rate, thereby producing several sample spectra per second. This large amount of data necessitates the use of digital computer techniques for data reduction. The spectral radiant intensity of the target is determined by applying instrument calibration parameters, distance to the target, and atmospheric transmission data to the instrument output.

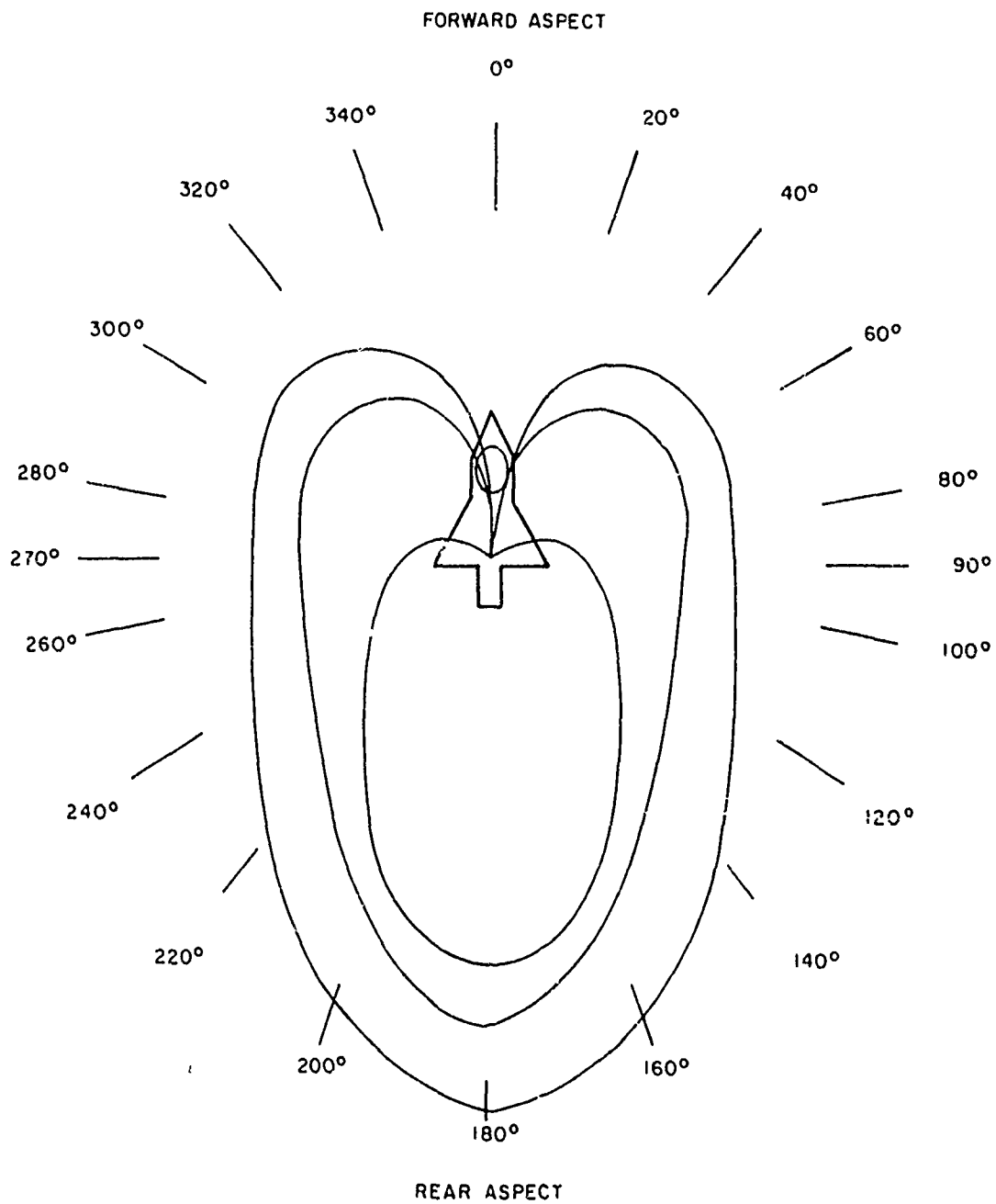


Figure 6-1. Irradiance Contours Emanating from Target as a Function of Azimuth Angle.

From Chapter IV (equation 4-1), the voltage produced by target radiation passing through an attenuating medium and incident upon a detector can be expressed by

$$V(\lambda) = \frac{1}{d^2} \int_{\lambda}^{\lambda+\Delta\lambda} R(\lambda) \tau(\lambda) I(\lambda) d\lambda \quad (6-1)$$

where

$d$  = distance from detector to target

$R(\lambda)$  = Responsivity of the instrument as a function of wavelength

$I(\lambda)$  = Spectral Radiant Intensity of the target

$\tau(\lambda)$  = Atmospheric transmission as a function of wavelength

$\Delta\lambda$  = Resolution of the instrument

In most measurements, values of irradiance  $E(\lambda)$  can be obtained from observation of the target with contributions from the surrounding background, and values of  $E(\lambda)$  from the background alone. The difference of these two values is  $\Delta E(\lambda)$  and is the irradiance at the instrument due to the radiation from the target,  $E_T(\lambda)$ , minus that due to the background radiation obscured by the target,  $E_B(\lambda)$ . Therefore, it is necessary to determine  $E_B(\lambda)$  in order to obtain the target irradiance. In some measurements, this correction may be negligible (Chapter IV) so that

$$\Delta E(\lambda) = E_T(\lambda) \quad (6-2)$$

otherwise (Eq 4-5) we have

$$\Delta E(\lambda) = E_T(\lambda) - E_B(\lambda) \quad (6-3)$$

From Chapter I, equation 1-4, the source spectral radiant intensity traversing through some attenuating medium, at a distance  $d$  from an irradiated detector, is given by

$$I(\lambda) = d^2 E(\lambda) / \tau(\lambda) \quad (6-4)$$

Thus, multiplication of  $\Delta E(\lambda)$  by the target distance squared and by the inverse of the atmospheric transmission coefficient corresponding to wavelength,  $\lambda$ , yields the spectral radiant intensity. This must be determined from the pure output voltage of the spectrometer. The voltage output of the instrument over a small resolution element  $V(\lambda)\Delta\lambda$ , at wavelength,  $\lambda$ , is given by

$$V(\lambda)\Delta\lambda = \int_{\lambda}^{\lambda+\Delta\lambda} R(\lambda) E(\lambda) d\lambda \quad (6-5)$$

If the resolution is small enough so that the responsivity of the instrument can be considered constant, and the irradiance (or instrument voltage) is not changing too rapidly, the integration can be performed

$$V(\lambda) = R(\lambda) E(\lambda) \quad (6-6)$$

so that

$$E(\lambda) = \frac{V(\lambda)}{R(\lambda)} \quad (6-7)$$

Thus, irradiance at the instrument is obtained by using the instrument responsivity and the voltage produced by the target. The spectral radiant intensity of the source is obtained by using equation 6-4 incorporating the distance of the target and the atmospheric transmissivities for the particular conditions prevailing during the experiment.

$$I(\lambda) = \frac{d^2 V(\lambda)}{\tau(\lambda) R(\lambda)} \quad (6-8)$$

The reduction of the raw instrument output to values of spectral irradiance is, in general, the reverse process of the irradiance calibration as described in Chapter III. In the case of the calibration, a known source of radiant energy produces a voltage output so the response, or voltage output versus irradiance input, is determined. For the reduction of target data, the responsivity determined by the calibration is used to reduce the voltage output of the instrument to values of irradiance.

The data reduction process then consists of determining values of spectral irradiance from the instrument and calibration parameters, multiplying by the target distance squared and dividing by the atmospheric transmission coefficients, thereby obtaining the spectral radiant intensities of the source.

#### ATMOSPHERIC TRANSMISSION

The attenuation of infrared radiation by the gases present in the atmosphere is due to molecular absorption in vibration-rotation bands of the individual molecules. The molecules in the atmosphere which have absorption bands in the infrared are water vapor ( $H_2O$ ), carbon dioxide ( $CO_2$ ), Ozone ( $O_3$ ), Nitrous Oxide ( $N_2O$ ), Methane ( $CH_4$ ) and carbon monoxide ( $CO$ ). The existence of other oxides of nitrogen and sulphur in the air is well known to urban dwellers, but these constituents, thankfully, are temporal and local in nature.  $H_2O$ ,  $CO_2$ , and  $O_3$  are the strongest absorbers of infrared radiation because they exist in high concentrations and have strong absorption bands. For measurements close to the earth's surface, however, (where distances between the target and the detector will be less than ten kilometers) absorption by ozone will

be negligible. Similarly, since  $N_2O$ ,  $CH_4$ , and  $CO$  only absorb significantly over long pathlengths, their absorption will not be considered in this discussion. Thus, for ground-to-air infrared measurements of aircraft, we have only to consider the absorption of water vapor and carbon dioxide to determine the transmission of the atmosphere from 1 to 20 micrometers.

In general, it is necessary to specify the meteorological conditions that exist at each point along the path between the source (target) and the detector in order to calculate the absorption. These include the pressure, temperature, and concentration of each absorber. For a given wavelength interval, the location, intensity, and shape of each spectral line must be specified as well as the functional relationships between the parameters and the meteorological conditions. If all this information is available, then the absorption can be calculated.

This calculation using the general transmissivity equation for computing slant-path molecular absorption is quite laborious and various empirical methods and approximations are used by different laboratories engaged in these calculations. The Infrared Information and Analysis (IRIA) Center, a part of the Willow Run Laboratories of the University of Michigan's Institute of Science and Technology, has been engaged in atmospheric transmission studies and has compiled a state-of-the-art report on band model methods for computing atmospheric slant-path molecular absorption (Report No. 7142-21 T)

This report has resulted in a computer program which can be used to compute molecular absorption spectra from 1.0 to 20.0 micrometers for

tion of the gases: H<sub>2</sub>O, CO<sub>2</sub>, H<sub>2</sub>O, and O<sub>3</sub>. In our version of the program only the H<sub>2</sub>O and CO<sub>2</sub> portions are utilized. A memo on the IRIA State-of-the-Art Atmospheric Transmission Program (24 July 1967) includes a summary of the equations and empirical constants used by the program to perform the transmission computations. Sample calculations produced by this program are shown in figures 6-2 and 6-3.

The infrared absorption spectrum of water vapor shows regions of total absorption and regions of very low absorption. These features of the spectrum lead to the use of various approximations and methods for the calculation of the absorption depending upon the wavelength. For the region from 1-2 micrometers and also for 4.3-20.4 micrometers, the Beer-Lambert approximation is used. In the intermediate region from 2-4.3 micrometers, the exact statistical model with an exponential distribution of line strengths (Forscan distribution) is used. This leads to the following equations for transmission:

$$\text{Model 1} \quad T = \text{EXP}(-rW^*) \quad (6-9)$$

$$\text{Model 2} \quad T = \text{EXP} \left\{ \frac{-W_1}{1 + (W/W_1)^2} \right\} \quad (6-10)$$

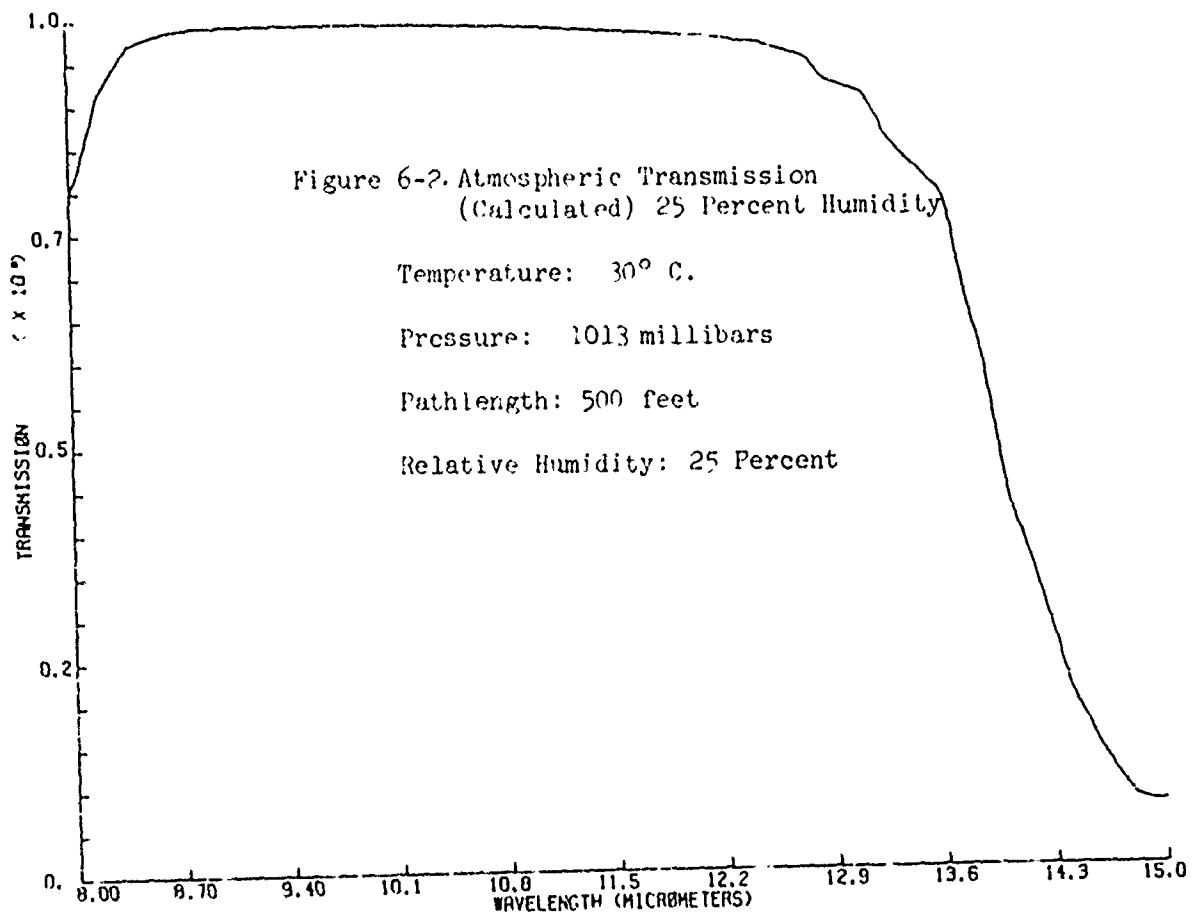
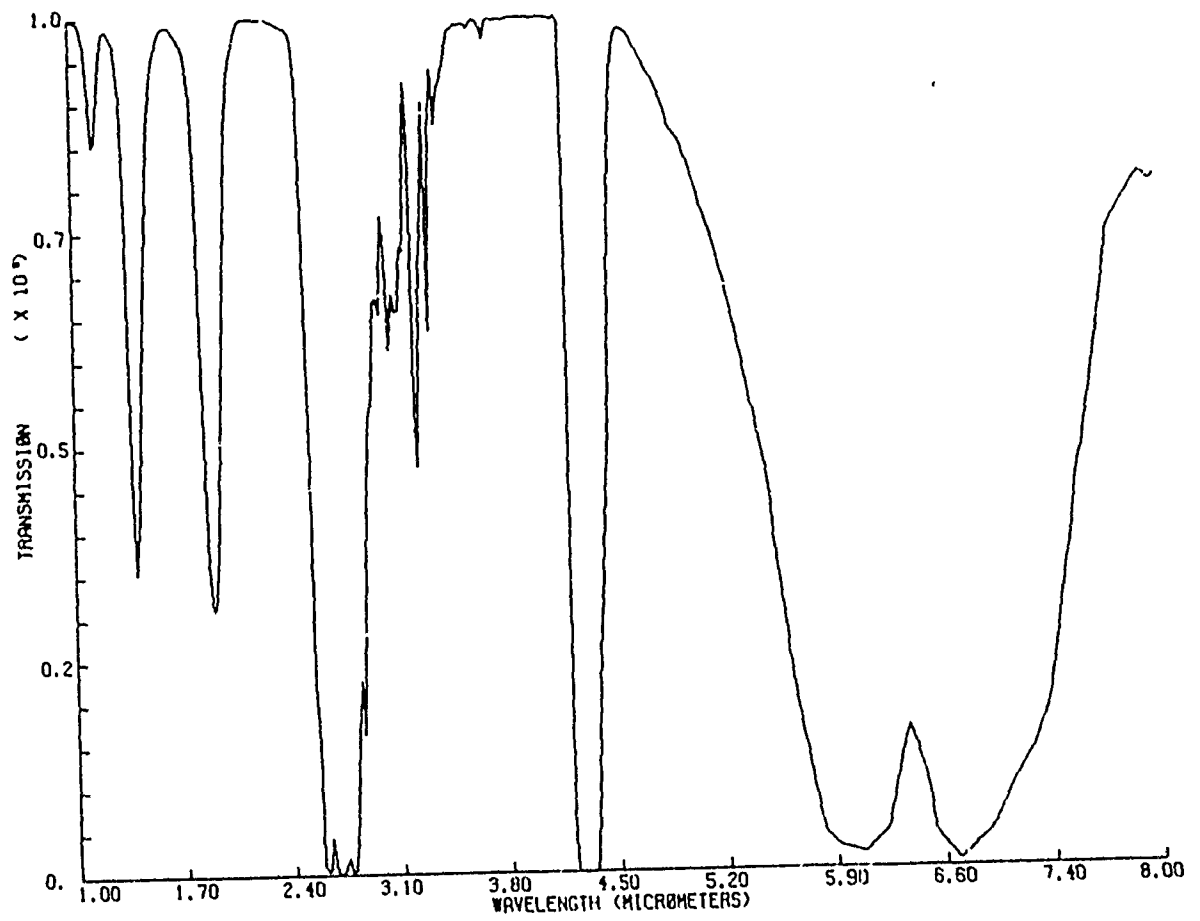
where:

W\* = equivalent air length concentration in percent atmosphere

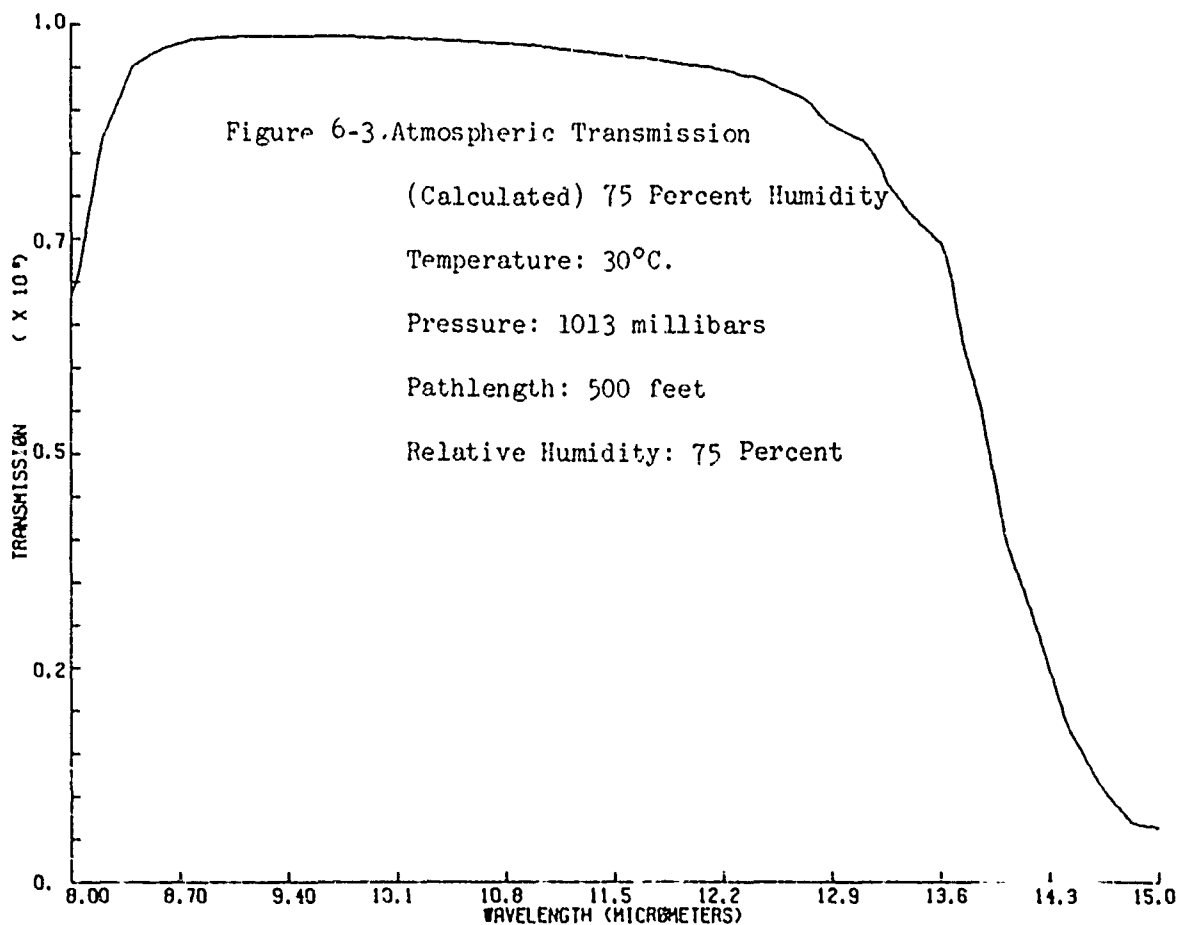
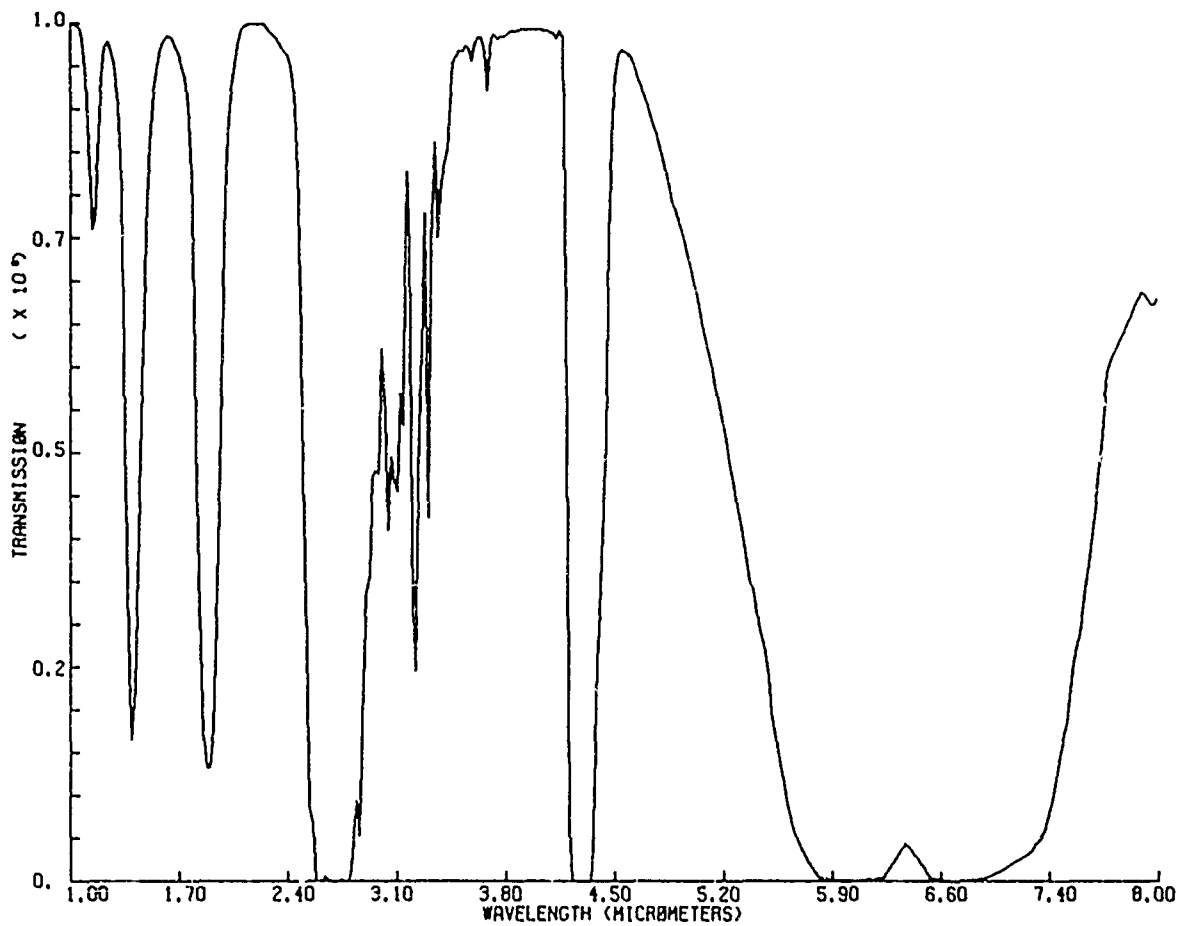
W = equivalent air length in percent atmosphere

W<sub>1</sub> = equivalent air length in percent atmosphere

The empirical constants are given in table 1 for the quantities n, m, and W<sub>1</sub> which are empirical parameters. This requires that the equivalent air path parameter be a function of concentration (W), the







Curtis-Godson equivalent pressure ( $\bar{P}$ ), and the equivalent sea level concentration ( $W^*$ ) be calculated separately. Computer programs and methods for this calculation are detailed in the IRIA Report No. 7142-21-T referred to previously.

Absorption by  $CO_2$  is calculated by the assumption of regularly spaced Lorentz lines (Elsasser Model) and by an empirical model correlating transmission with the generalized absorption coefficient ( $K$ ) and the equivalent sea level concentration in atmospheric centimeters ( $W^*$ ). The empirical relationship is used in the spectral regions 1-2.63 and 4.45-19.0 micrometers while the exact Elsasser equation is used in the intermediate region 2.63-4.45 micrometers. The equations used are:

$$\text{Model 1} \quad T = T(KW^*) \quad (6-11)$$

$$\text{Model 2} \quad T = 1 - \sinh \beta \int_0^Y I_0(Y) \text{EXP}(-Y \cosh \beta) dY \quad (6-12)$$

where

$$Y = \frac{SW/d}{\sinh \beta}$$

$$\beta = \frac{2\pi\alpha'_0 \bar{P}}{d}$$

For certain values of  $\beta$  and  $Y$ , the transmission for model 2 is given in terms of the error function:

$$\text{erf}(x) = \frac{2}{\sqrt{\pi}} \int_0^x e^{-x^2} dx$$

The total transmission of the atmosphere at any wavelength for which the above approximations are valid is then given to a good approximation by

$$T(\text{Total}) = T(H_2O) \times T(CO_2) \quad (6-13)$$

As yet we have no method to account for the attenuation of infrared radiation due to scattering. The atmospheric transmission function as determined above can then be used for data reduction.

### Scattering

The attenuation of infrared radiation caused by particles much larger than individual molecules is due both to scattering and absorption. The extinction coefficient can be written

$$\epsilon_{\text{total}} = \epsilon_{\text{abs-gas}} + \epsilon_{\text{abs-aerosol}} + \epsilon_{\text{scattered}}$$

Pure scattering occurs if there is no absorption of the energy incident, but only a deviation from the path.

Scattering (pure) can be treated in three ways depending upon the relationship between the wavelength of the radiation being scattered and the size of the particles leading to scattering. Rayleigh scattering is applicable when the radiation wavelength is much larger than the particle size. Mie scattering theory applies when the particle size is comparable to the radiation wavelength. Nonselective scattering occurs when the particle size is very much larger than the radiation wavelength. The principal theory used in the infrared is the Mie scattering theory.

The scattering coefficient as given by Mie theory, caused by a distribution of particles with a range of particle sizes from  $a_1$  to  $a_2$ , is given as a function of wavelength by

$$\sigma_{\lambda} = \pi \int_{a_1}^{a_2} N(a) K(a,n) a^2 da \quad (6-14)$$

where

$\sigma_{\lambda}$  = scattering coefficient for wavelength

$N(a)$  = volume concentration of particles

$K(a,n)$  = scattering area coefficient

a = radius of spherical particle

n = index of refraction of particle

Reliable scattering coefficient data in the infrared is difficult to obtain because of the contributions of both scattering and selective absorption to the measured value of the extinction coefficient. Because the scattering properties of the atmosphere can vary appreciably, it is not possible to state a scattering coefficient that will permit accurate predictions over a wide range of conditions. An empirical relationship frequently used is

$$\sigma = c\lambda^{-\gamma} \quad (6-15)$$

where c and  $\gamma$  are constants determined by the concentration and size-distribution values for the aerosol. Junge observed several size distributions for atmospheric aerosol particles at equilibrium and gave the distribution function for particles greater than 0.1 micron as

$$\frac{dN(a)}{d \log a} = c a^{-\nu^*} = C a^{-\beta} \quad (6-16)$$

where

N = volume concentration of particles

a = radius of spherical particle

$\nu^*$  = slope of log-log plot of large to small particles

and  $\beta = \nu^* + 1$

c = a constant representing the total concentration

Thus, if the sizes of the scattering particles can be determined, a knowledge of their size distribution is available, or vice-versa. There are basically two methods to determine size. The simplest but

most tedious is collection and microscopic examination. The other is to use an instrument which measures the light scattered at right angles from an incident beam. This is generally a function of the particle size, shape, and refractive index, but simplifications allow particles with diameters from 0.1 to 100 micrometers to be measured.

Currently an investigation is being conducted to establish a relationship between particle sizes, distributions, and concentration versus the infrared attenuation produced as a function of wavelength. A sample absorption spectrum of microgram quantities of atmospheric dust (in a KBr matrix) is shown in figure 6-4 which shows the general regions over which attenuation by dust particles might be important.

The scattering coefficient is related to the transmission (due to scattering) of a given optical path by the relationship

$$T = \exp (- \sigma x) \quad (6-17)$$

where

$x$  = optical path length (cm)

$\sigma$  = scattering coefficient ( $\text{cm}^{-1}$ )

Since scattering predominates over absorption in the visible portion of the electromagnetic spectrum, it may be necessary to determine scattering in the infrared portion from measurements taken in the visible portion (about 0.5 micrometers) and to compare this with the Mie theory and actual data on extinction coefficients to determine the absorption in the infrared. This problem is being studied at many laboratories.

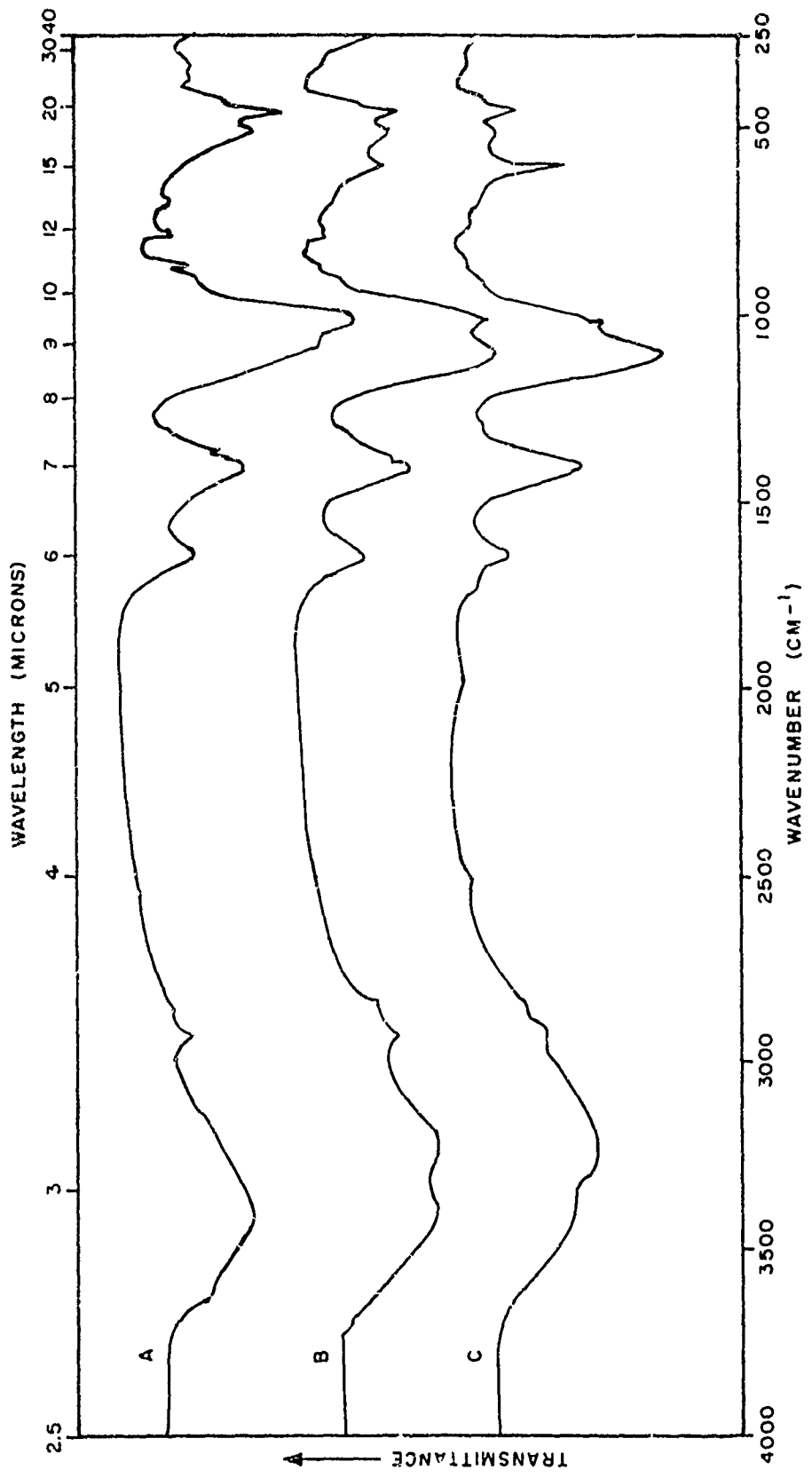


Figure 6-4. Infrared Absorption by Atmospheric Dust.

## DATA ANALYSIS

Data analyses is a broad area, and only that which is performed as a matter of course will be discussed. This is:

1. The calculation of acquisition range as a function of aspect angle and signal-to-noise ratio for various missile seekers
2. Integration of the spectral radiant intensity data to determine the value of total radiant intensity in a given spectral band
3. Determination of the effective blackbody temperatures and gaseous emission lines or bands.

## ACQUISITION RANGE

The infrared signal emitted from a target which reaches the infrared detector of a missile seeker may or may not be strong enough to cause a sufficient voltage change recognizable from the noise level. The maximum range at which a given signal-to-noise ratio is produced by a specific target, which causes the servomechanisms of the missile seeker to "lock-on" to the target is termed the acquisition range. Acquisition ranges are measured for each particular target as a function of aspect angle.

These acquisition ranges are derived from spectral data obtained with a spectrometer. The spectral data is checked for accuracy by measuring acquisition ranges independently with actual missile seekers for a given signal-to-noise ratio. This S/N ratio does not have to correspond to the actual "lock-on" S/N ratio. Because of this, a specially designed radiometer (providing S/N ratios as output) may be used in place of the missile seeker. In either case, the spectral data is checked against the results of an independent measurement in the following manner:

The distance or range at which a seeker or radiometer will detect a target can be expressed by the equation

$$S/N = \frac{1}{NEI (d^2)} \int_{\lambda_1}^{\lambda_2} I(\lambda) R(\lambda) \tau(\lambda) d\lambda \quad (6-18)$$

which merely states that the signal voltage (Eq. 6-1) divided by the value of the noise equivalent irradiance (NEI) is equal to some signal-to-noise ratio. A particular missile seeker will lock-on for a given signal-to-noise ratio. This must be determined for each individual seeker. The above equation then yields for the acquisition range

$$d^2 = \frac{1}{NEI (S/N)} \int_{\lambda_1}^{\lambda_2} I(\lambda) R(\lambda) \tau(\lambda, d) d\lambda \quad (6-19)$$

where

$d$  = distance to the target

NEI = noise equivalent irradiance of the seeker or radiometer

$S/N$  = signal-to-noise ratio corresponding to range  $d$

$I(\lambda)$  = spectral radiant intensity of the target

$R(\lambda)$  = spectral responsivity of the seeker or radiometer

$\tau(\lambda, d)$  = atmospheric transmission as a function of wavelength and

$\lambda_1, \lambda_2$  = wavelength limits of response

The spectral radiant intensity  $I(\lambda)$  is measured by the spectrometer and the response of the seeker  $R(\lambda)$  and NEI are determined by the calibration procedure. The signal-to-noise ratio is measured for the distance  $d$ . With this information, equation (6-19) is solved for range using the measured spectral data and atmospheric transmission, and the calibration parameters of the seeker or radiometers.



The calculated range and actual range for a given S/N ratio can then be compared to give a degree of confidence to the measured spectral data. If this degree of accuracy is shown to be acceptable the spectral radiant intensity can be used for the calculation of range for any missile seeker provided that the NEI and spectral response are known. These calculations can be performed for any desired signal-to-noise ratio or atmospheric condition, or as a function of aspect angle.

This information serves to characterize the response of a particular missile to some target. The characterization is spatial, enclosing a sphere around the target by means of the azimuth and elevation aspect angles, and the range. The target can be characterized by polar plots of the spectral radiant intensity or irradiance contours, whereas the missile seeker's response is characterized by polar plots of the signal-to-noise ratios produced by the target. Similarly, a polar plot of various acquisition ranges will show the effectiveness of a particular missile seeker, radiometer, or detector against a specific target.

#### Total Radiant Intensity

Integration of the spectral radiant intensity data is simply a summation across the spectral band of interest. This yields the total radiant intensity

$$I_{\lambda_1-\lambda_2} = \int_{\lambda_1}^{\lambda_2} I(\lambda) d\lambda \quad (6-7)$$

The value of the total radiant intensity is useful in determining the total emission within a given spectral band. This is used in evaluating the effectiveness of IRCM devices and in determining threshold levels of radiant emissions of selected targets.

### Signal-to-Noise Ratios of Seekers or Radiometers

The voltage output of a seeker or radiometer is not directly suitable for the calculation of acquisition ranges. It must be converted into a signal-to-noise ratio. This signal-to-noise ratio differs from the ratio of signal voltage to NEI by inclusion of sky background noise. This reduction is performed as a function of both the distance (range) to the target and the aspect angle. Signal-to-noise ratios are determined in the following manner.

The radiometer or seeker measurement is performed so that one part of the measurement represents radiation due to the target plus background, and the second part includes only the background. These measurements may be obtained by periodically moving the optical path on and off the target during a measurement. The two voltage outputs are related by the equation

$$V_1(\text{rms})^2 = V_2(\text{rms})^2 + V_s(\text{rms})^2 \quad (6-21)$$

where

$V_1$  = the voltage output of the seeker including target and background radiation

$V_2$  = the voltage output of the seeker due only to background, internal and external to the seeker

$V_s$  = the voltage produced only by the target

This equation can be rearranged to yield

$$V_1(\text{rms})^2 = V_2(\text{rms})^2 \left[ 1 + \frac{V_s}{V_2} \frac{(\text{rms})^2}{(\text{rms})^2} \right] \quad (6-22)$$

Therefore, the signal-to-noise ratio can be defined as

$$S/N = \left( \frac{V_1(\text{rms})^2}{V_2(\text{rms})^2} - 1 \right)^{1/2} \quad (6-23)$$

The values of the voltages  $V_1$  and  $V_2$  are determined as follows:

The a-c outputs of the seeker or radiometer are digitized and the rms values determined by the usual relation

$$X_{\text{rms}} = \left( \frac{1}{N} \sum_{j=1}^{j=N} X_j^2 \right)^{1/2} \quad (6-24)$$

where

$X$  = the digitized amplitude of the voltage

$N$  = the number of samples

#### EMISSION SPECTROSCOPY

A determination of the components within the exhaust gases which produce emission is essential for a characterization of the target. A knowledge of the gaseous products and their absorption and emission bands should serve to characterize the exhaust emission spectrum. Determining the lines or bands depends upon the spectral resolution and the dynamic range of the instrument. Each laboratory engaged in the collection of infrared signatures of aircraft should attempt the storage of a data bank, or library, of signatures of various infrared emitting objects. The use of such a data bank would be quite beneficial for those engaged in comparative evaluation of both IRCM devices and missile seekers

Radiation emitted by matter carries information concerning the physical and chemical properties of the radiating bodies; spectral analysis of this information yields what is called the emission spectrum of the source of the radiation

Spectral analysis of radiation determines how much radiation of each wavelength is present. A plot of the intensity versus the wavelength or wavenumber of the radiation is referred to as a spectrum

## CHAPTER VII

### TYPES OF AIRCRAFT

The following catalog of Army aircraft, both helicopters and fixed wing, is intended to give a general idea of the nature of the craft to be tested. Detailed information on specific aircraft can be obtained from the Army Technical Manuals -10 and -20. General information, which includes schematics of each aircraft, covers size, shape, utility, and engine types used in the aircraft shown in figure 7-1. Utility, armed observation, cargo, and reconnaissance craft are described.

#### HELICOPTERS

##### UH-1


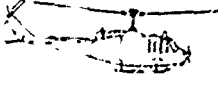

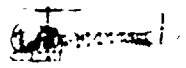
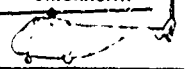
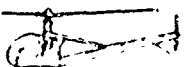
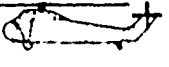
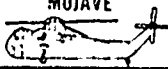
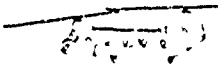
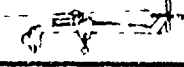

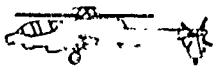
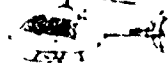
Manufacturer: Bell Helicopter Co.

Description: Military type aircraft of a compact design, featuring a low silhouette and low vulnerability in order to meet combat requirements. Wide cargo-passenger compartment allows a variety of services. The engine is located aft of the cabin and mounted above the fuselage in a platform to provide maximum accessibility. Figures 7-2 and 7-3 show the general construction of the UH-1.

Weights: Operating weight: 6000 pounds

Maximum gross weight: 9500 pounds

Height: 17'

HELICOPTER SERIES		
DESIGNATION	ENGINE	POPULAR NAME
AH-1G	T53-L-13/A/B	COBRA 
TH-1G	T53-L-13/A/B	
UH-1A	T53-L-1A	IROQUOIS 
UH-1B	T53-L-9A,11/B/C	
UH-1C	T53-L-11/B/C/D	
UH-1D	T53-L-9A,11/B/C/D	
UH-1H	T53-L-13 A/B	
UH-1M	T53-L-13 A/B	
OH-6A	T63-A-5A	CAYUSE 
OH-13E	0-335-5D	SIOUX 
OH-13G	0-335-5D	
OH-13H	0-435-23C	
OH-13K	6V5-335A	
OH-13S	0-435-25A	
TH-13T	0-435-25A	
UH-19C	R-1340-57	CHICKASAW 
UH-19D	R-1300-3D	
OH-23B	0-335-5D	RAVEN 
OH-23C	0-335-5D	
OH-23D	0-435-23C	
OH-23F	0-540-9A	
OH-23G	0-540-9A	
CH-34C	R-1820-84C	CHOCTAW 
VH-34C	R-1820-84D	
CH-37B	R-2800-54	MOJAVE 
CH-47A	T-55-L-5,7	CHINOOK 
CH-47B	T55-L-7, B, C	
CH-47C	T55-L 7C, 11	
CH-54A	T73-P-1	TARHE 
CH-54B	T73-P-700	
TH-55A	H10-360B1A	OSAGE 
AH-56A	T64 GE-16	CHEYENNE 
OH-38A	T63-A-709	KIOWA 


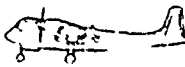

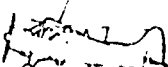
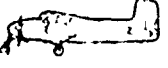
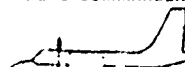


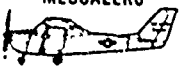
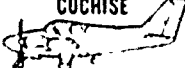
OBSERVATION SERIES		
DESIGNATION	ENGINE	POPULAR NAME
O-1A	O-470-11B	BIRD DOG 
O-1D	O-470-15	
O-1E	O-470-11B	
O-1G	O-470-11B	
TO-1A	O-470-11B	
TO-1E	O-470-11B	
YO-3A	10-360-D	
VTOL AND STOL SERIES		
OV-1A	T53-L-7,7A	MOHAWK 
OV-1B	T53-L-7,7A	
OV-1C	T53-L 7,7A,15	
OV-1D	T53-L-701	
UTILITY SERIES		
U-1A	R-1340-61	OTTER 
RU-1A	R-1340-61	
U-6A	R-985-AN-39/A	BEAVER 
RU-6A	R-985-AN-39/A	
U-8D	0-480-1A,1B	SEMINOLE 
RU-8D	0-480-1A,1B	
U-8F	0-480-3,3A	
U-8G	0-480-1A,1B	
U-9B	G0-480-G1B6	AERO COMMANDER 
U-9C	G50-480-B1A6	
RU-9D	G50-480-B1A6	
YU-9	G0-435-C2B1	COURIER 
U-10A	G0-480-G1D6	
U-21A	T74-CP-700	UTE 
RU-21A	T74-CP-700	
RU-21B	T74-CP-702	
RU-21C	T74-CP-702	
RU-21D	T74-CP-700	
RU-21E	T74-CP-700	
TRAINER SERIES		
T-41B	10-360-D	MESCALERO 
T-42A	10-470-L	COCHISE 

Figure 1-1. Designation of Army Aircraft

1

2

APPROXIMATELY 10:00 AM - 10:15 AM

... ..

... ..

---

---

---

---

---

APPROXIMATELY

...

...

APPROXIMATELY

... ..

...

APPROXIMATELY

...

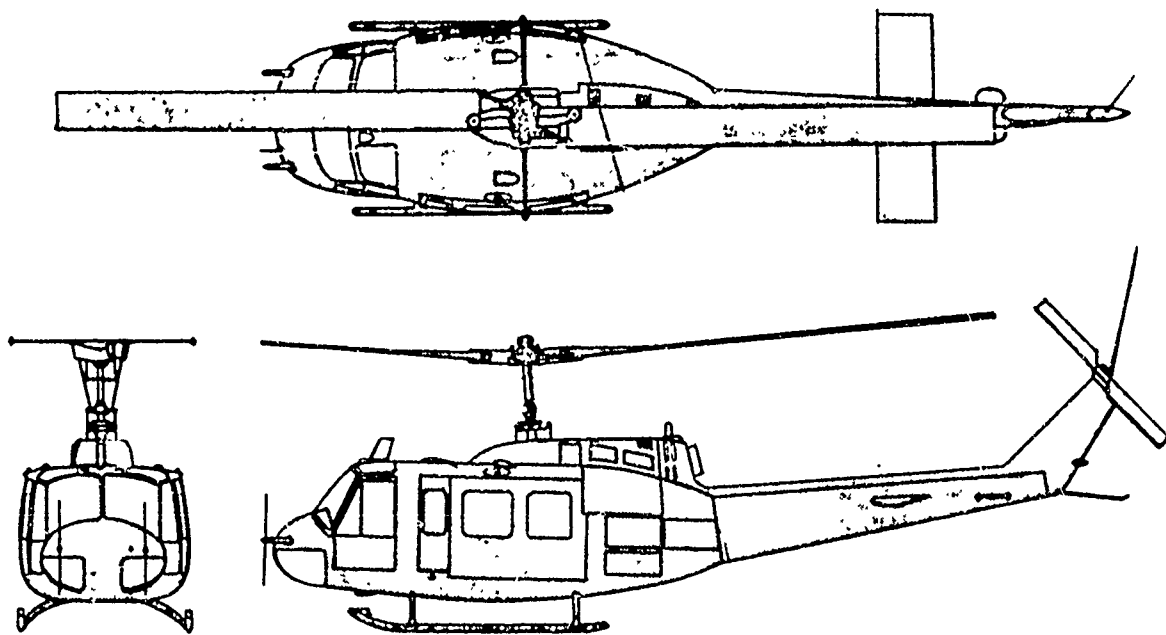
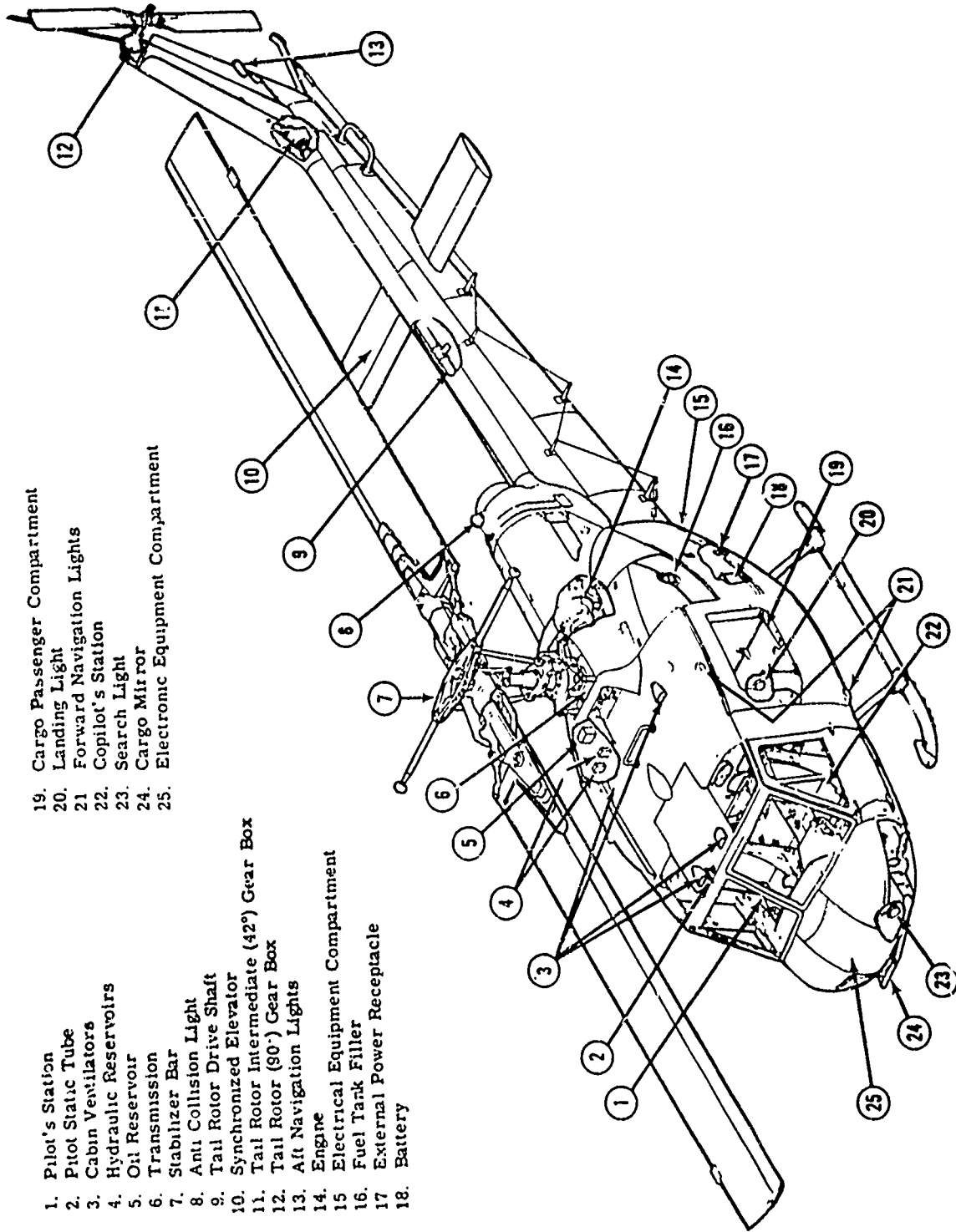


Figure 7-2. YUH-1D and UH-1D/H Helicopter





- 19. Cargo Passenger Compartment
- 20. Landing Light
- 21. Forward Navigation Lights
- 22. Copilot's Station
- 23. Search Light
- 24. Cargo Mirror
- 25. Electronic Equipment Compartment

- 1. Pilot's Station
- 2. Pitot Static Tube
- 3. Cabin Ventilators
- 4. Hydraulic Reservoirs
- 5. Oil Reservoir
- 6. Transmission
- 7. Stabilizer Bar
- 8. Anti Collision Light
- 9. Tail Rotor Drive Shaft
- 10. Synchronized Elevator
- 11. Tail Rotor Intermediate (42°) Gear Box
- 12. Tail Rotor (90°) Gear Box
- 13. Aft Navigation Lights
- 14. Engine
- 15. Electrical Equipment Compartment
- 16. Fuel Tank Filler
- 17. External Power Receptacle
- 18. Battery

Figure 7-3. General Arrangement -- Typical UH-1D

AH-1G

Manufacturer: Bell Helicopter Co.

Description: A tandem, two-place, high-speed, conventional helicopter designed specifically for the combat role. The tactical helicopter is an aggressive high-speed combat helicopter designed and built around the fighting mission. Distinctive features are the very narrow sleek fuselage, small, tapered swept midwings, aerodynamic dynamic cleanliness, and integral turret. Maximum fuselage width is thirty-six inches. The mission profiles completely cover the air-to-ground environment with suppressive fire at an area. The helicopter is fast, light, highly maneuverable, and capable of self-protection in hostile air and ground battle situations.

Weight: Basic aircraft with crew: 6000 pounds

Maximum gross weight. 9000 pounds.

Height: 11' 7"

Length: 44' 6"

Width: 3'

Engines: The turbine engine and its accessories are located aft of the transmission and mounted on a platform deck to provide maximum accessibility. The engine is a free turbine type designed for low fuel consumption, of a minimum size and weight for maximum performance. The T53-L-13 engine is torque-limited to 1100 hp for normal power.

Exhaust Gas Temperature.

400 - 625°C Continuous

760°C Maximum

Airspeed: 70-190 Knots

Infrared Suppression: There are no louvers or screens in the side of the cowling to allow a direct view of the engine. The tailpipe is surrounded by an ejector shroud that extends several inches past the end of the tailpipe. This ejector mixes cool air with the exhaust gases to reduce IR radiation. The open end of the tailpipe is directly above the tailboom and directed slightly upward so that a view of the hot end of the turbine is possible only from a position that is above and behind the helicopter. Figure 7-4 gives the principal dimensions of the AH-1G; figure 7-5 shows the engine and transmission compartment cooling.

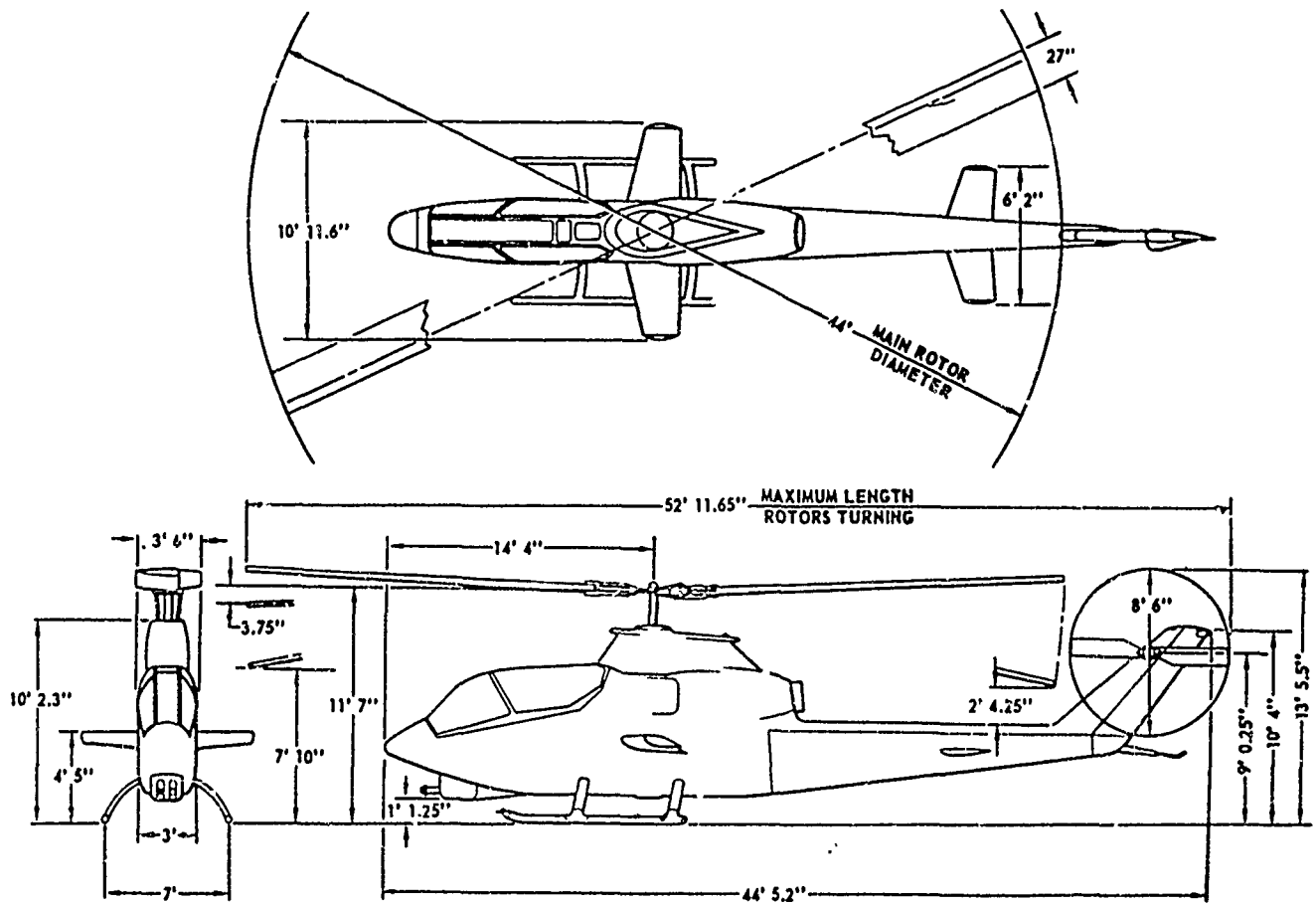


Figure 7-4. Principal Dimensions -- AH-1G

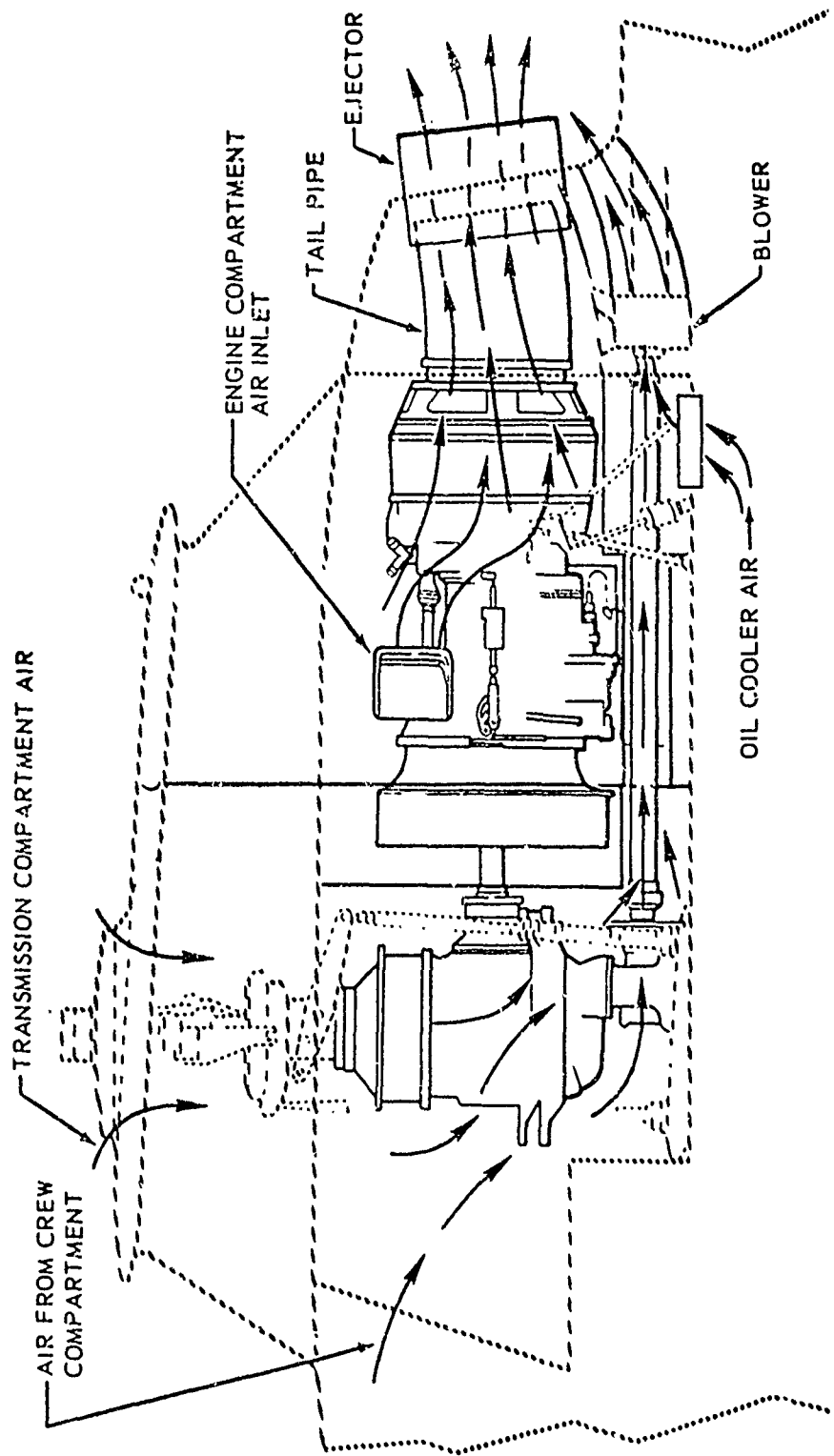


Figure 7-5. Engine and Transmission Compartment Cooling -- AH-1G

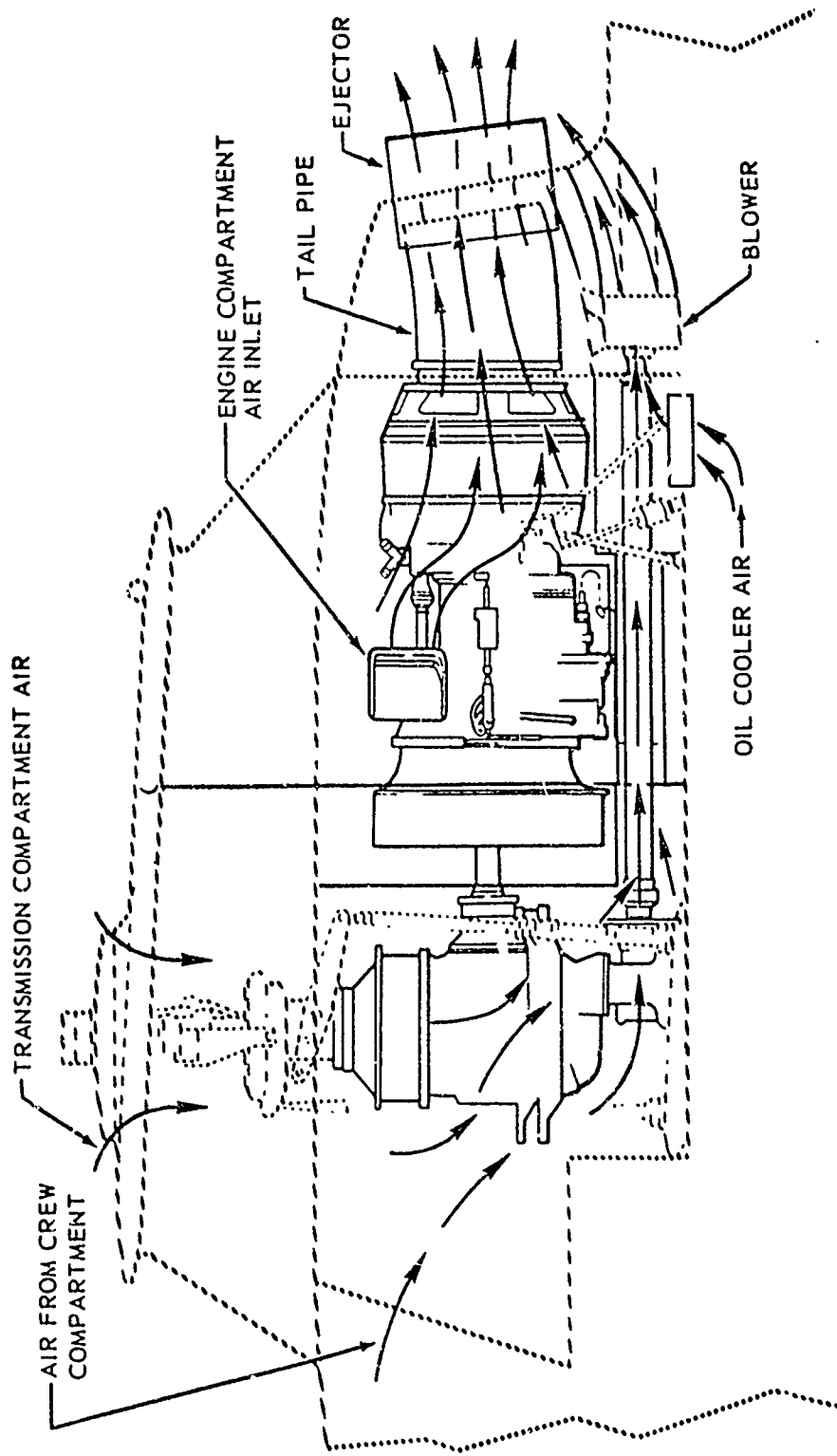


Figure 7-5. Engine and Transmission Compartment Cooling -- AH-1G

OH-6A

Manufacturer: Hughes Aircraft Company

Description: The OH-6A aircraft basically is an all metal, single engine, rotary wing aircraft. It is powered by an Allison T63-A-5A turbine engine driving a four-bladed main rotor and a tail-mounted anti-torque rotor. Primarily an observation aircraft, it is capable of carrying passengers, cargo, or armament subsystem. The aircraft can be equipped with armor for combat operations, and also can be used for target acquisition, reconnaissance, and command and control.

Weight: Mission gross weight: 2163 pounds

Height: 8' 6"

Length: 30' 3 3/4"

Width: 4' 7"

Engine: The Allison T63-A-5A is a free turbine turboshaft engine rated at 252 SHP in the OH-6A. The engine cooling system consists of air scoops, mounted on top of the aircraft and necessary ducting to direct air through the air cooler and into the engine compartment. There is also a blower mounted on the main transmission input shaft. The air exhausts through an annular opening around the exhaust pipe between the pipe and engine cowling doors.

Exhaust Gas Temperature (turbine outlet temperature)

Normal-385 - 693°C

Maximum-749°C

Airspeed: 40-121 Knots operating speed

Figure 1-1 is a side view of the OH-6A and figure 1-2 shows the general construction.

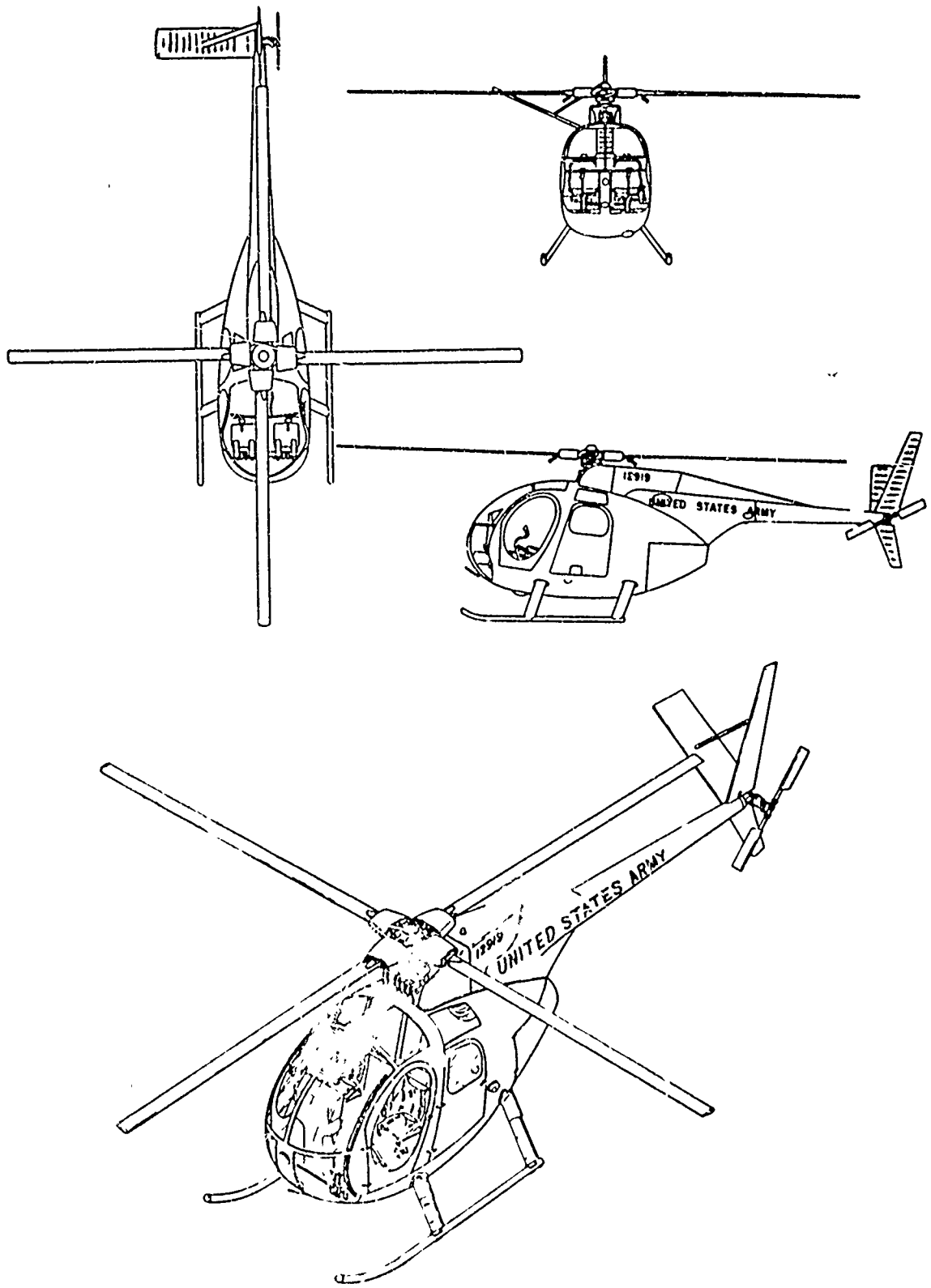
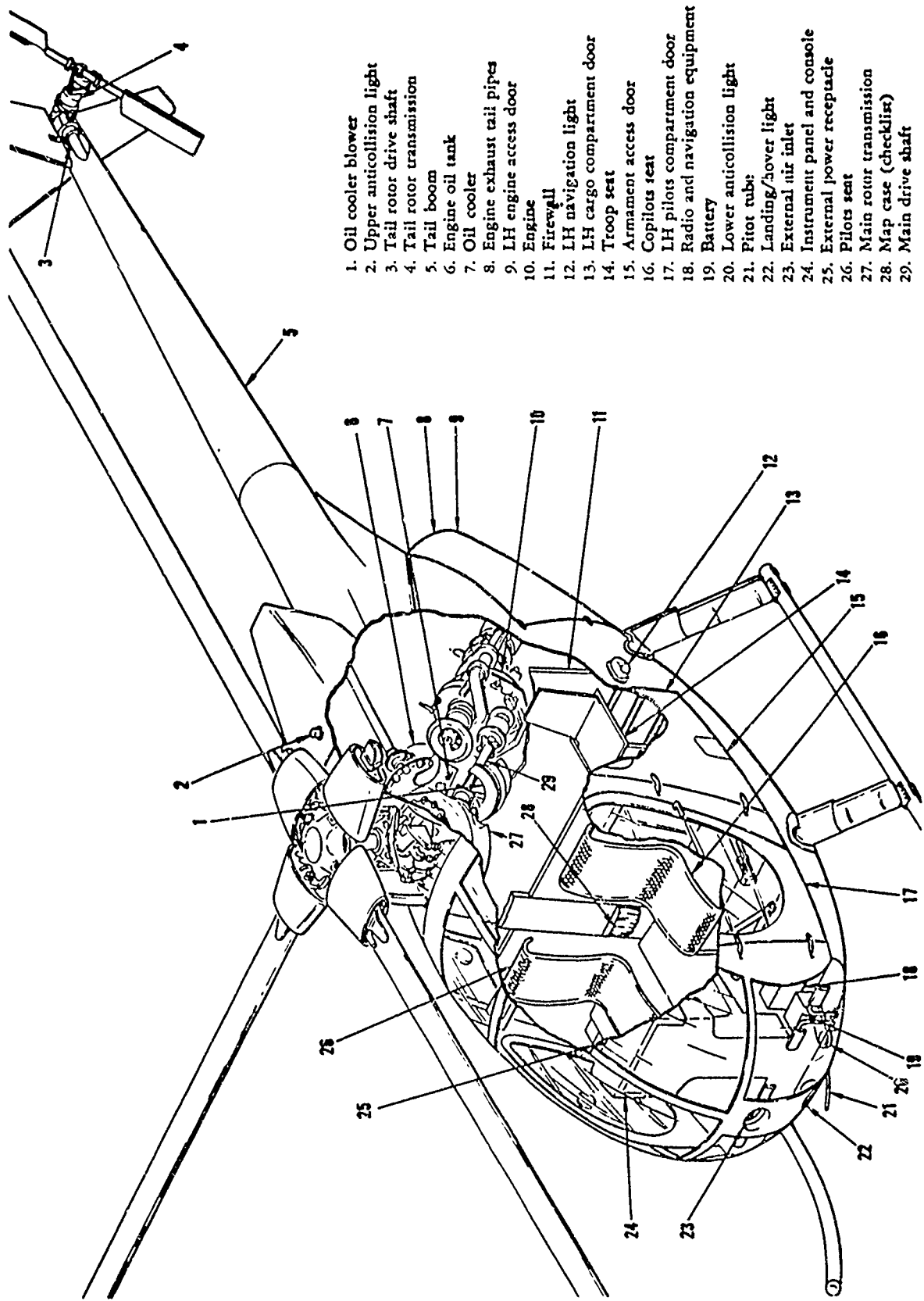


Figure 1-6. OH-6A Helicopter





1. Oil cooler blower
2. Upper anticollision light
3. Tail rotor drive shaft
4. Tail rotor transmission
5. Tail boom
6. Engine oil tank
7. Oil cooler
8. Engine exhaust tail pipes
9. LH engine access door
10. Engine
11. Firewall
12. LH navigation light
13. LH cargo compartment door
14. Troop seat
15. Armament access door
16. Copilots seat
17. LH pilots compartment door
18. Radio and navigation equipment
19. Battery
20. Lower anticollision light
21. Pitot tube
22. Landing/hoover light
23. External air inlet
24. Instrument panel and console
25. External power receptacle
26. Pilots seat
27. Main rotor transmission
28. Map case (checklist)
29. Main drive shaft

Figure 7-7. General Arrangement Diagram --- OH-6A

OH-58A

Description: The OH-58A is a single-engine, observation helicopter designed to land and take off from prepared or unprepared surfaces. The fuselage consists of the forward section which encloses the cabin and fuel cell and provides pylon support. The intermediate, or transition section, supports the engine and includes the equipment and electronics section. The tailboom section supports the horizontal stabilizer, vertical stabilizer, and tail rotor.

Missions: Visual observation, target acquisition, armed reconnaissance, and command and control. In its armed configuration, the helicopter provides ground forces at the lowest practicable echelon with a capability for armed reconnaissance, observation and screening observations where high mobility is required.

Weight: Operating weight, including crew, 2000 pounds

Maximum gross weight: 3000 pounds

Height: 10'

Length: 40'

Width: 6' 6"

Engine: The OH-58A is equipped with a T63-A-700 gas turbine engine. The engine is light weight and is designed for low fuel consumption, minimum size, maximum reliability, and ease of maintenance. It is installed aft of the mast and passenger compartment to simplify the drive system, improve the inlet-exhaust arrangement, reduce cabin noise level and provide better structural integrity. The engine cowl aft of the engine air inlet screen is removable. Louvered openings

are provided on both sides of the engine for cooling. The aft fairing covers the engine oil cooler, provides an area for oil cooler exit air, and the center cowl section houses the engine air inlet. The engine is rated at 300 hp.

Exhaust Gas Temperature: (turbine outlet temperature)

Continuous: 330-700°C

Maximum: 750°C

Airspeed: 120 Knots maximum.

Figure 7-8 is a side view of the OH-58A helicopter. Figure 7-9 shows its general construction.

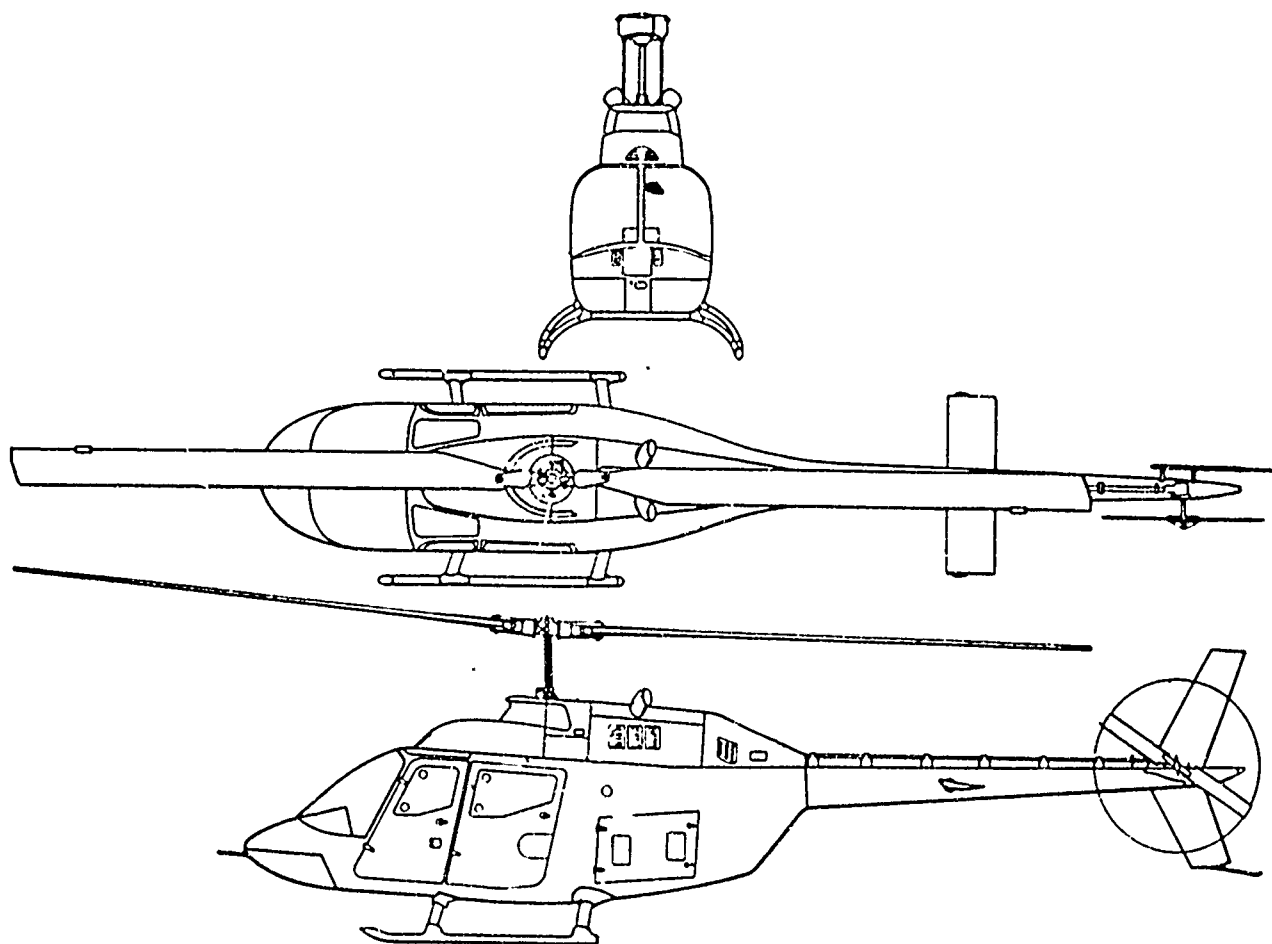
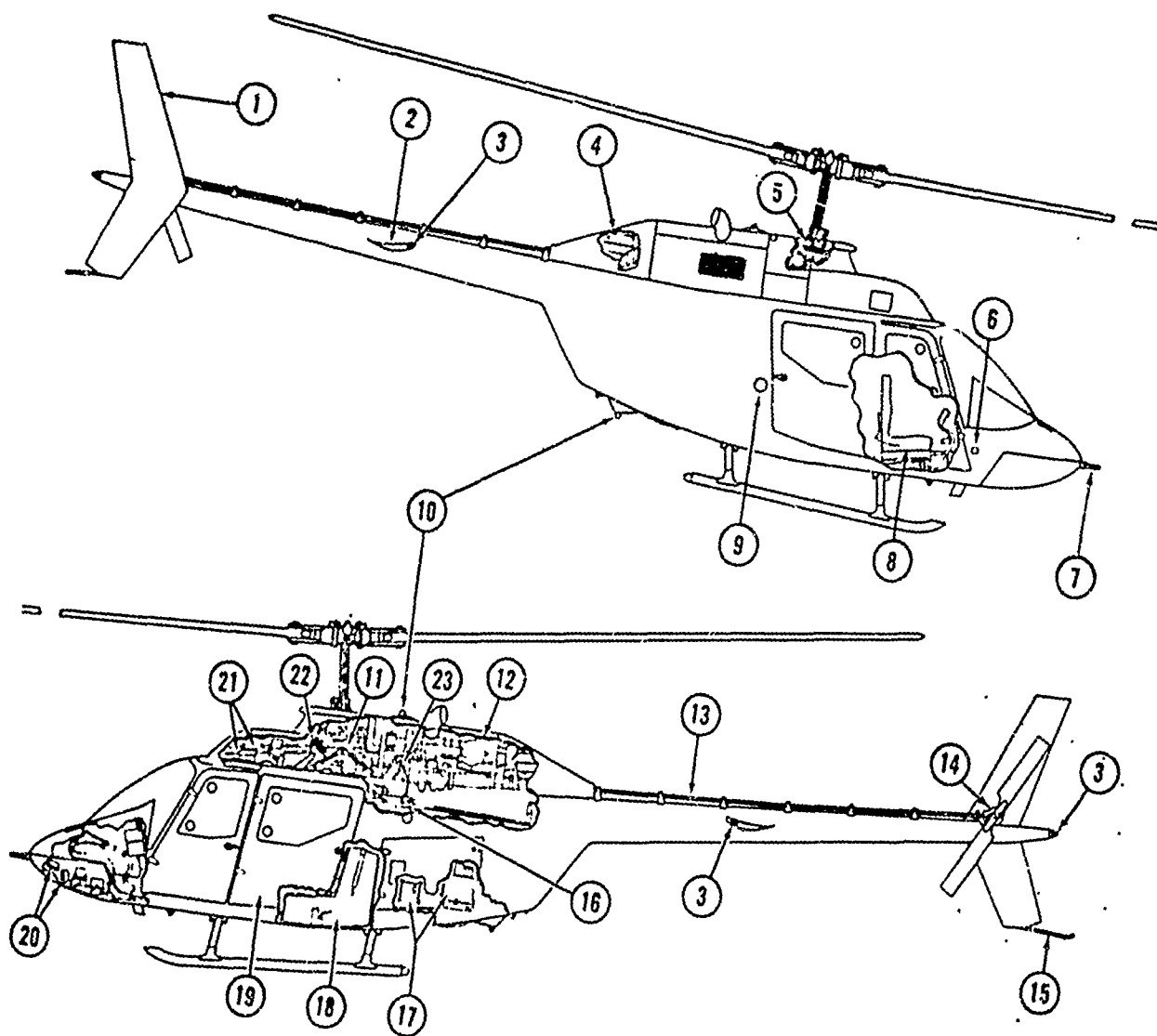


Figure 7-8. Three Views of the OH-58A Helicopter



- |                           |   |
|---------------------------|---|
| 1. Vertical Fin           | 13. Tail Rotor Drive Shaft                |
| 2. Horizontal Stabilizer  | 14. Tail Rotor Gearbox                    |
| 3. Navigation Lights      | 15. Tail Skid                             |
| 4. Oil Tank Filler        | 16. Bleed Air Heater                      |
| 5. Swashplate             | 17. Battery and Avionics                  |
| 6. Static Port            | 18. Fuel Cell                             |
| 7. Pitot Tube             | 19. Passenger Station                     |
| 8. Pilot's Station        | 20. Landing Lights                        |
| 9. Fuel Tank Filler       | 21. Cyclic and Collective Servo Actuators |
| 10. Anti-Collision Lights | 22. Hydraulic Pump and Reservoir          |
| 11. Transmission Assembly | 23. Freewheeling Unit                     |
| 12. Engine                |   |

Figure 7-9. General Arrangement -- OH-58A

CH-47

Manufacturer: Boeing Company, Vertol Division.

Description: The CH-47B and CH-47C are twin turbine engines tandem-rotor aircraft designed for transportation of cargo, troops, and weapons. Each helicopter is powered by two Lycoming T55 series shaft-turbine engines mounted on the aft fuselage. The engines simultaneously drive two tandem 3-blade rotors.

Weights: Operating weight: 24,000 pounds.

Maximum gross weight: 40,000 pounds.

46,000 for CH-47C (T55-L-11 engine)

Height: 18'

Length: 50'

Width: 12'

Engines: The two engines are housed in separate nacelles mounted externally on each side of the aft fuselage.

CH-47B Lycoming T-55-L-7, L-7B 2200 SHP normal

CH-47C Lycoming T-55-L-7C 2400 SHP normal

T-55-L-11 3000 SHP normal

Exhaust Gas Temperature.

L-7 Engines.

230-650°C Normal

650-700°C Military

L-11 Engines:

230-770°C Normal

770-810°C Military

Engine Oil Temperature:

Maximum: 138°C -- Oil coolers located on the aft pylon section.

Fuel JP-4

Airspeed. 60-160 knots

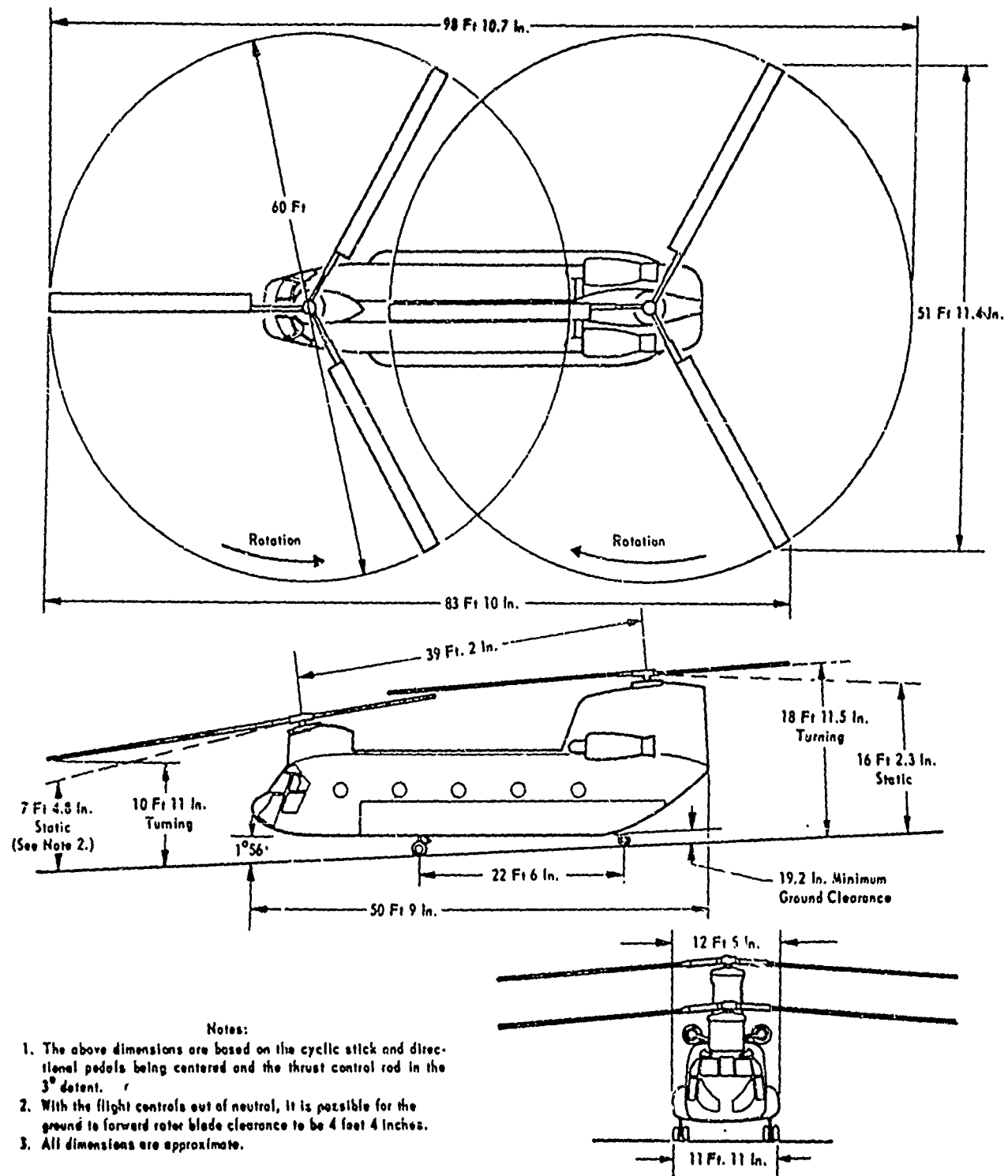


Figure 7-10. Overall Dimensions -- CH-47

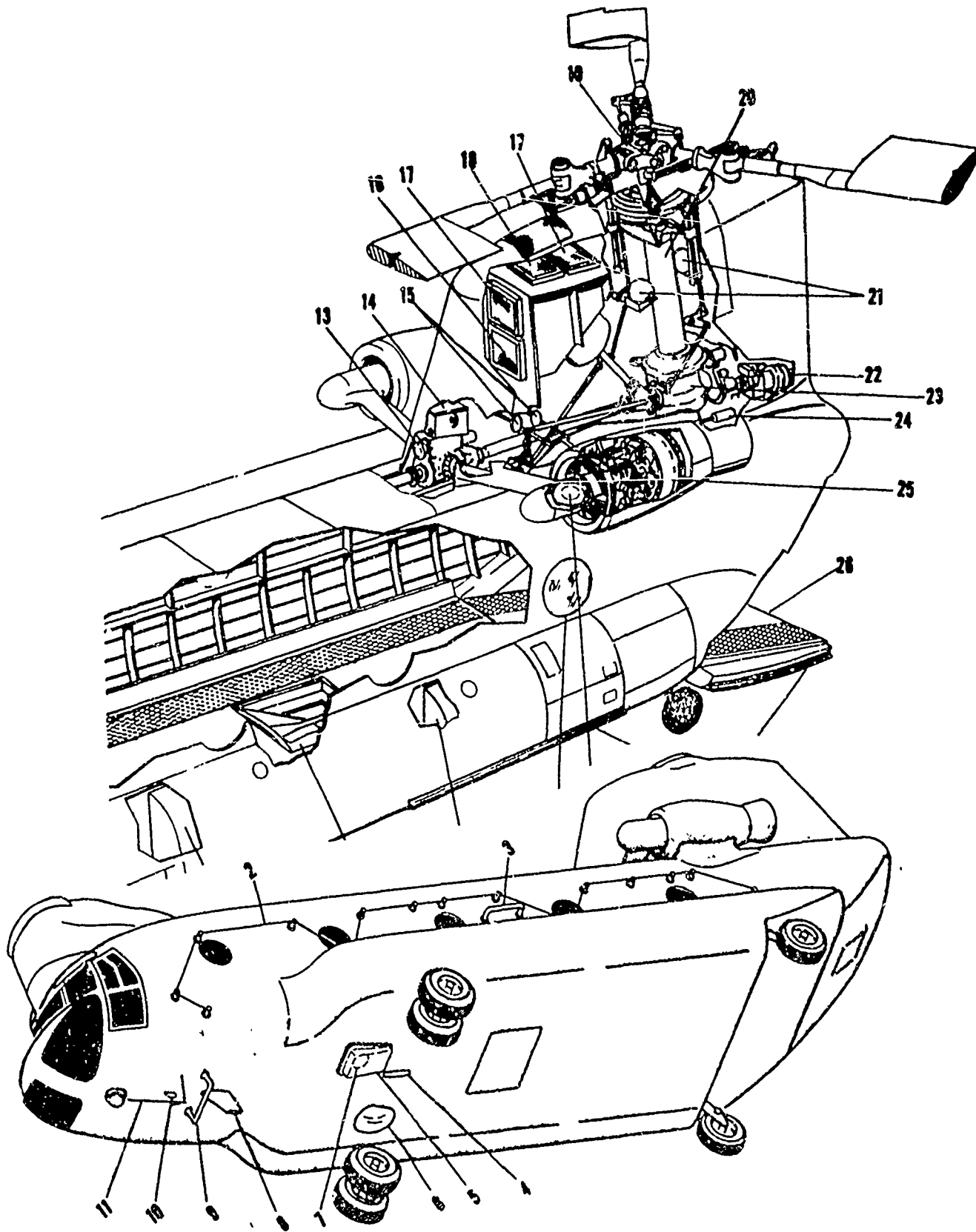


Figure 7-11. Rear and Lower Views of Engine Section -- CH-47



CH-54A

Manufacturer: Sikorsky Aircraft

Description: A twin-turbine, all-metal, flying crane. It has a design gross weight of 38,000 pounds and a maximum alternate gross weight of 42,000 pounds. The helicopter is designed to carry detachable pods for transporting personnel and cargo, and to carry externally attached loads.

Weight: 19,695 pounds.

Length: 52' 5"

Width: 7' 1"

Height: 25' 5"

Engines: The helicopter is powered by two axial-flow gas turbine engines mounted side-by-side on top of the fuselage above and aft of the pilot's compartment.

Pratt & Whitney JFT D124-1: 4050 SHP

T73-P-1: 4500 SHP

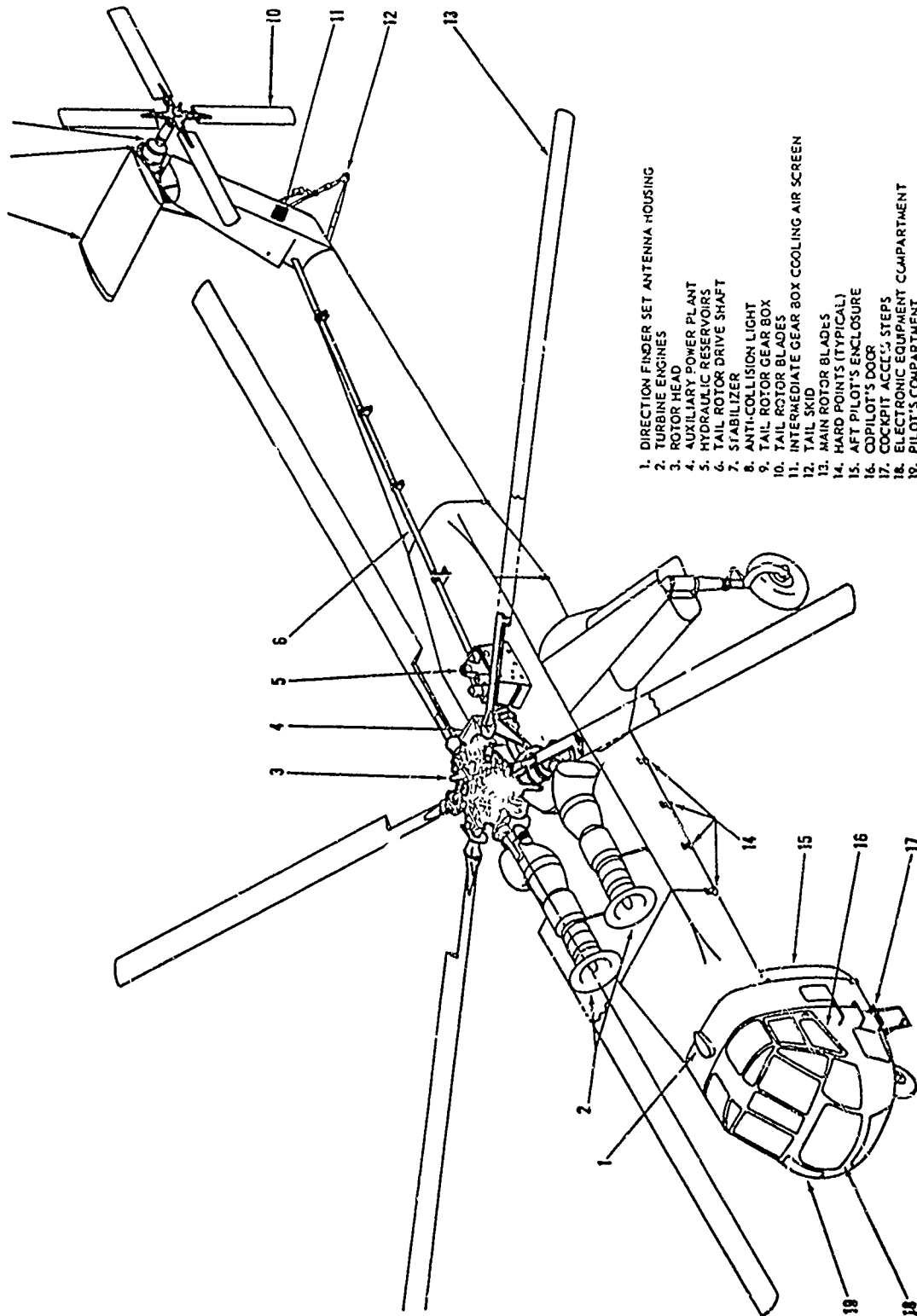
Power Turbine Inlet Temperature:

JFT Engine 515-565°C Normal

T-73 Engine: 515-655°C Normal

Airspeed: 115 Knots.

Figure 1-1 shows the general construction of the CH-54A, and figure 1-2 is a diagram of the engine intake



- 1. DIRECTION FINDER SET ANTENNA HOUSING
- 2. TURBINE ENGINES
- 3. ROTOR HEAD
- 4. AUXILIARY POWER PLANT
- 5. HYDRAULIC RESERVOIRS
- 6. TAIL ROTOR DRIVE SHAFT
- 7. STABILIZER
- 8. ANTI-COLLISION LIGHT
- 9. TAIL ROTOR GEAR BOX
- 10. TAIL ROTOR BLADES
- 11. INTERMEDIATE GEAR BOX COOLING AIR SCREEN
- 12. TAIL SKID
- 13. MAIN ROTOR BLADES
- 14. HARD POINTS (TYPICAL)
- 15. AFT PILOT'S ENCLOSURE
- 16. COPILOT'S DOOR
- 17. COCKPIT ACCESS STEPS
- 18. ELECTRONIC EQUIPMENT COMPARTMENT
- 19. PILOT'S COMPARTMENT

Figure 7-12. General Arrangement - Exterior CH-54A

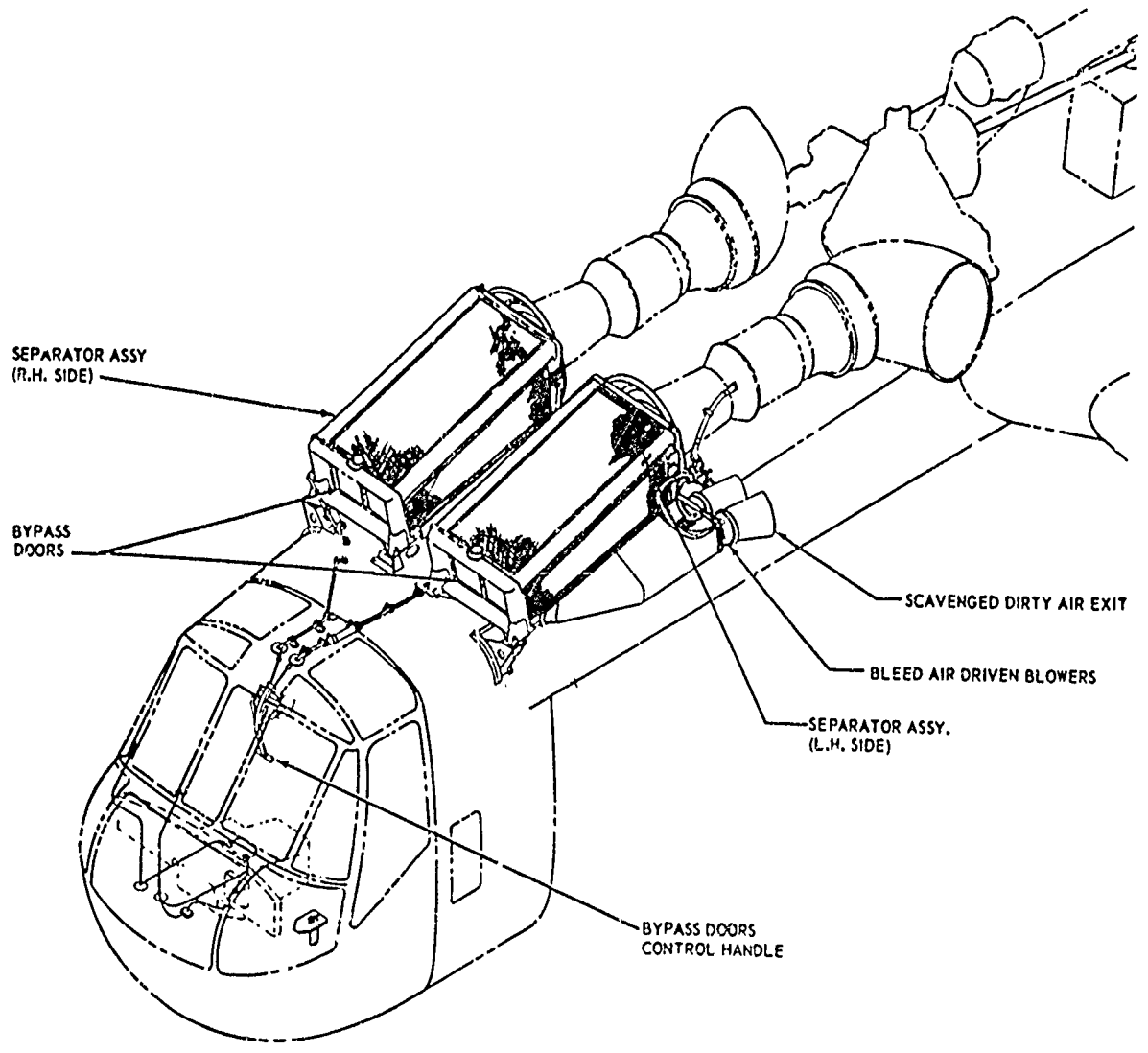


Figure 7-13. Diagram of Engine Intake -- CH 54-A

OH-13H

Manufacturer: Bell Helicopter Company.

Description: The helicopters are designed for observation, reconnaissance, rescue, and general utility missions. Power is supplied by a vertically-mounted, six-cylinder, opposed-type air-cooled, nonsupercharged engine.

Height: 8' 10"

Weight: Operating weight: 2000 pounds maximum.

Length: 41' 5"

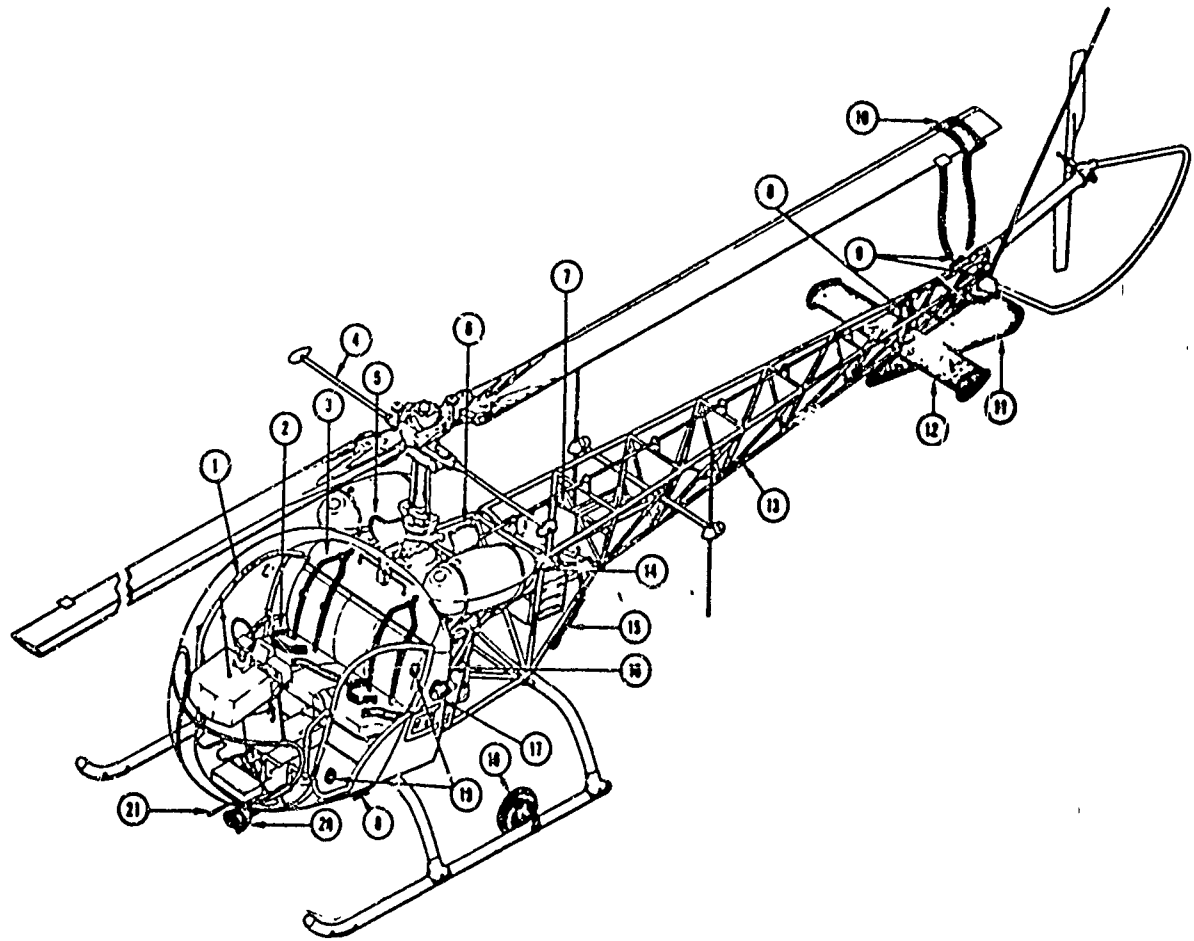
Width: 7' 6"

Engine: The OH-13H helicopter utilizes a 250 BHP O-435 engine. The engines are six-cylinder, horizontally-opposed, forced-air, fan-cooled aircraft units. The engine is located aft of the cabin and is mounted in the center section.

Hovering Limitations: Hovering between 10 and 400 feet shall be avoided since a power failure under these conditions is likely to result in an extremely hard landing.

Airspeed: 91 Knots maximum.

Figure 7-14 is a diagram of the general construction of the OH-13H helicopter.



- |                                   |                               |
|-----------------------------------|-------------------------------|
| 1. Entrance door                  | 12. Synchronized elevator     |
| 2. Seat belts                     | 13. Tail boom                 |
| 3. Shoulder harness               | 14. Fuel tank                 |
| 4. Stabilizer bar                 | 15. Engine hand crank         |
| 5. Carburetor air intake          | 16. External power receptacle |
| 6. Oil tank                       | 17. Forward navigation light  |
| 7. Battery                        | 18. Ground handling wheels    |
| 8. Rotating beacon (fore and aft) | 19. Cabin ventilator          |
| 9. Aft navigation light           | 20. Landing light             |
| 10. Blade mooring block           | 21. Pitot tube                |
| 11. Ventral fin                   |                               |

Figure 7-14. General Arrangement Diagram -- OH-13H Aircraft

OH-23G

Manufacturer: Fairchild Hiller Corp.

Description: Multipurpose helicopters designed for reconnaissance, observation, training, and medical evacuation. Power is supplied by a Lycoming six-cylinder, opposed-type, air-cooled engine. The basic body section and tailboom are all metal, stressed-skin construction.

Length: 40' 8"

Height: 10' 2"

Width: 7' 6"

Maximum Gross Weight: 2750 pounds

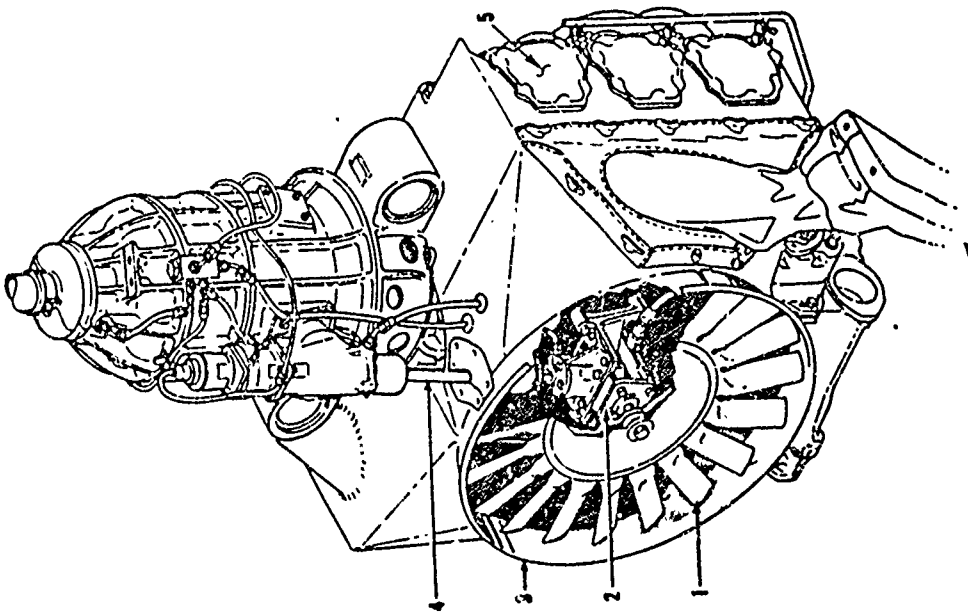
Basic Operating Weight: 2100 pounds

Engine: These aircraft are powered by Lycoming direct-drive, six-cylinder, opposed-type, air-cooled engines, mounted vertically. The engine is located directly below the center of the main rotor drive shaft. Cooling air from the fan mounted on the fan gear box is forced over the engine cylinder fins.

Power: 305 BHP

Airspeed: 83 Knots maximum.

Figure 7-15 shows three views of the aircraft and the engine-cooling fan.



1. Cooling fan
2. Fan gear box
3. Fan shroud
4. Fan drive coupling
5. Engine

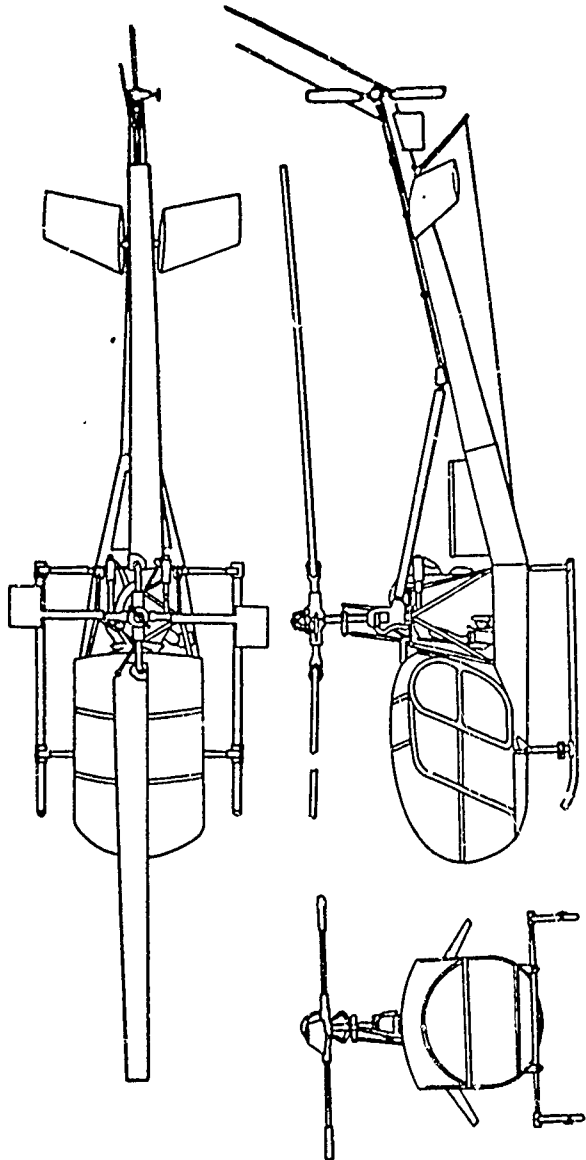


Figure 7-15. Diagram Showing Three Views of OH-23F Aircraft and Cooling System

CH-34A, C

Manufacturer: Sikorsky Aircraft

Description: Designed for transportation of cargo and personnel. Configuration is single-engine, four-bladed, main-lifting rotor. The fuselage is of all-metal construction.

Length: 37'

Height: 14' 10"

Width: 13'

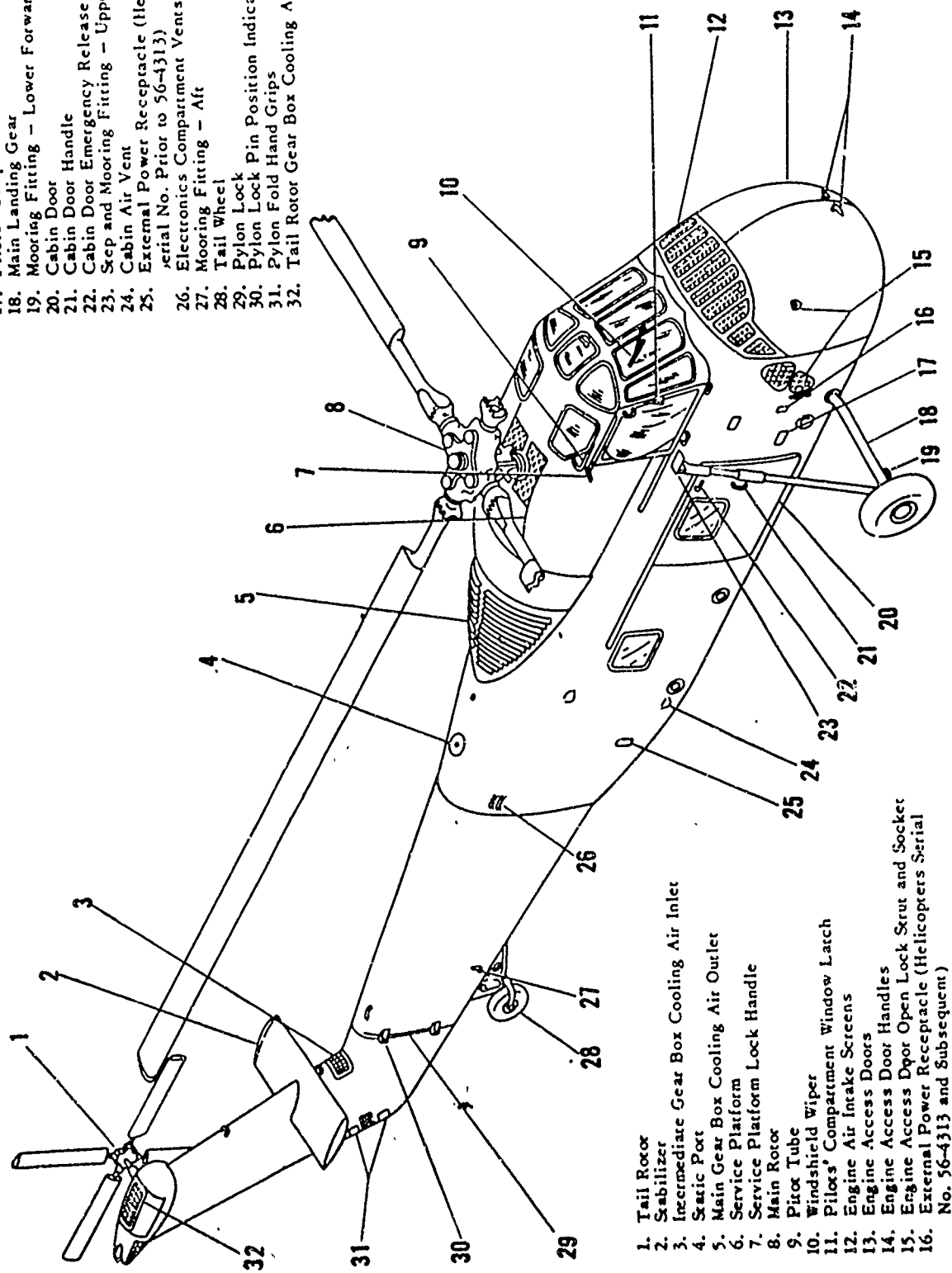
Gross Weight: 12,060 pounds

Engine: The CH-34 helicopter is powered by a Wright R-1c20-84A, -84C air-cooled, nine-cylinder, single-row, radial engine with special provisions for installation with the drive shaft inclined upwards.

Figure 1-11 shows the general construction of the CH-34A, C helicopter.



- 17. Pilots' Compartment Access Foot Wells
- 18. Main Landing Gear
- 19. Mooring Fitting - Lower Forward
- 20. Cabin Door
- 21. Cabin Door Handle
- 22. Cabin Door Emergency Release Handle
- 23. Step and Mooring Fitting - Upper Forward
- 24. Cabin Air Vent
- 25. External Power Receptacle (Helicopters serial No. Prior to 56-4313)
- 26. Electronics Compartment Vents
- 27. Mooring Fitting - Aft
- 28. Tail Wheel
- 29. Pylon Lock
- 30. Pylon Lock Pin Position Indicator
- 31. Pylon Fold Hand Grips
- 32. Tail Rotor Gear Box Cooling Air Inlet



- 1. Tail Rotor
- 2. Stabilizer
- 3. Intermediate Gear Box Cooling Air Inlet
- 4. Scaric Port
- 5. Main Gear Box Cooling Air Outlet
- 6. Service Platform
- 7. Service Platform Lock Handle
- 8. Main Rotor
- 9. Pitot Tube
- 10. Windshield Wiper
- 11. Pilots' Compartment Window Latch
- 12. Engine Air Intake Screens
- 13. Engine Access Doors
- 14. Engine Access Door Handles
- 15. Engine Access Door Open Lock Strut and Socket
- 16. External Power Receptacle (Helicopters Serial No. 56-4313 and Subsequent)

Figure 7-16. General Arrangement -- Right-hand Side (Typical) of the CH-34A Helicopter

UH-19D

Manufacturer: Sikorsky Aircraft

Description: Primarily designed for rescue operation, but because of its versatility is used for observation, cargo transport, and assault operations.

Gross Weight: 7500 pounds

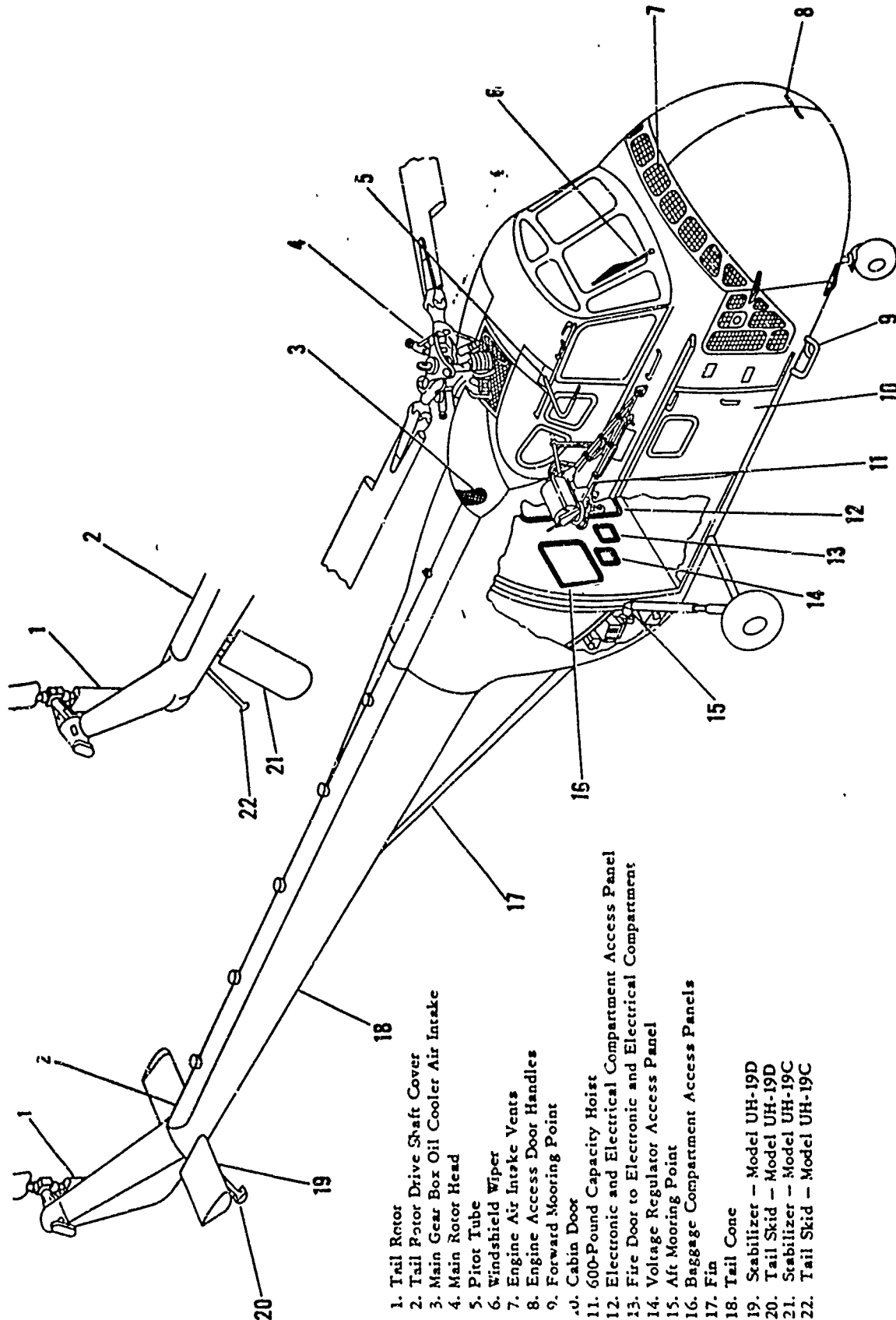
Length: 14' 3"

Height: 13' 4"

Width: 11' 6"

Engine: A Wright R-1300-3 seven-cylinder engine.

Figure 7-17 shows its general construction.



- 1. Tail Rotor Drive Shaft Cover
- 2. Tail Rotor Drive Shaft Cover
- 3. Main Gear Box Oil Cooler Air Intake
- 4. Main Rotor Head
- 5. Pitot Tube
- 6. Windshield Wiper
- 7. Engine Air Intake Vents
- 8. Engine Access Door Handles
- 9. Forward Mooring Point
- 10. Cabin Door
- 11. 600-Pound Capacity Hoist
- 12. Electronic and Electrical Compartment Access Panel
- 13. Fire Door to Electronic and Electrical Compartment
- 14. Voltage Regulator Access Panel
- 15. Aft Mooring Point
- 16. Baggage Compartment Access Panels
- 17. Fin
- 18. Tail Cone
- 19. Stabilizer - Model UH-19D
- 20. Tail Skid - Model UH-19D
- 21. Stabilizer - Model UH-19C
- 22. Tail Skid - Model UH-19C

Figure 7-17. General Arrangement of the CH-19D Helicopter

FIXED WING AIRCRAFT

OV-1

Manufacturer: Grumman

Description: The OV-1 aircraft (Mohawk) is a two-place twin turboprop aircraft capable of operating from small fields and unimproved runways. The aircraft is capable of performing missions of observation, surveillance, artillery gun-fire spotting, air-control, emergency supply and radiological monitoring. The armed version of the aircraft is capable of carrying a wide variety of tactical weapons at low-speed and low-altitude.

Weight: Normal takeoff: 13,800 pounds

Length: 41'

Height: 13'

Width: 48'

Engines: The aircraft is powered by two Lycoming gas turbine engines turning three-blade Hamilton standard hydromatic propellers. Additional power plants used by the aircraft: T53-L-3, T53-L-3A, T53-L-7, which are single-stage, and the T53 L-15, which is two-stage.

Exhaust Gas Temperature:

T53-L-3: 300-590°C

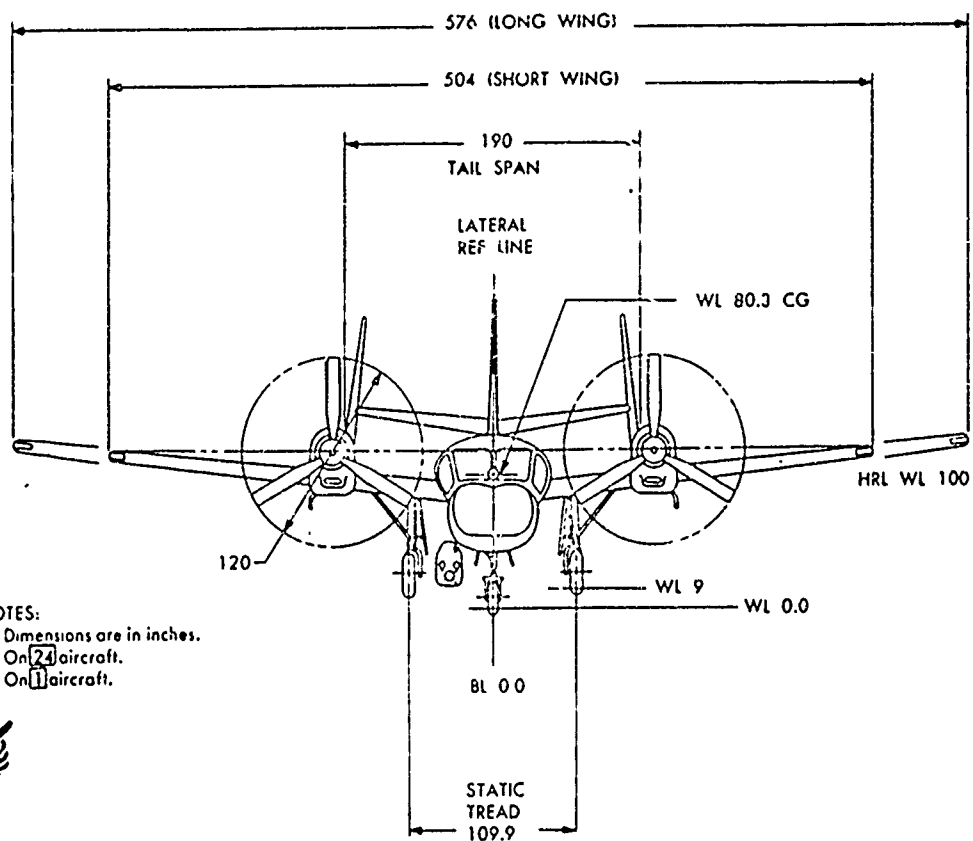
T53-L-3A: 300-590°C

T53-L-7: 300-605°C

T53-L-15: 300-625°C

Airspeed. Maximum, 385 Knots

Figure - shows the general construction and dimensions of the OV-1



- NOTES:
1. Dimensions are in inches.
  2. On 24 aircraft.
  3. On 11 aircraft.

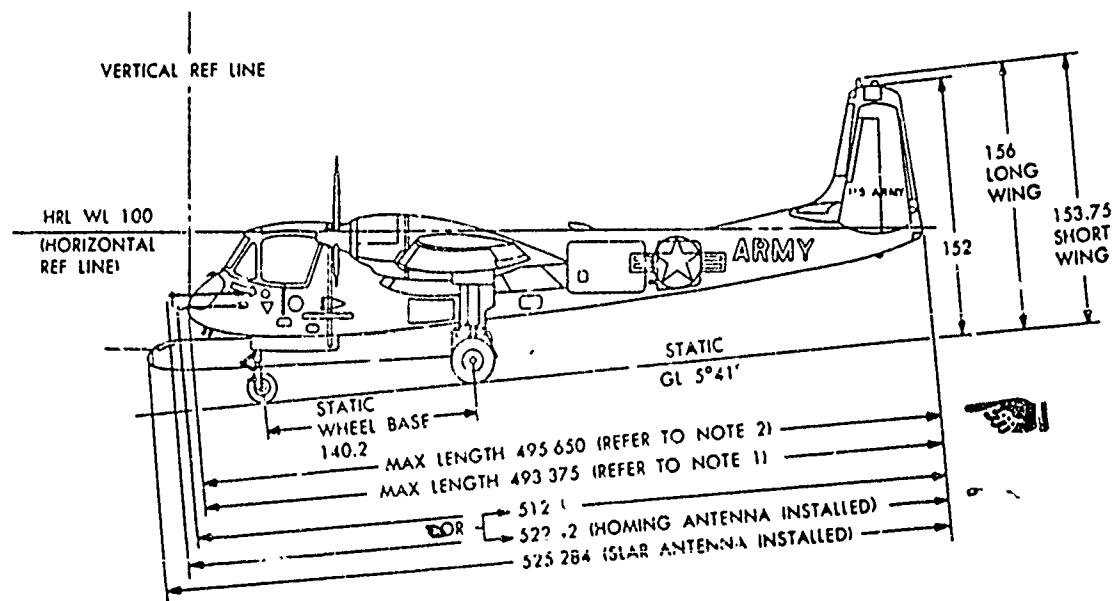


Figure 7-18. Diagram Showing Overall Dimensions of the Mohawk Aircraft

Manufacturer Beechcraft

Description A six-place, all-metal, low-wing monoplane powered by two supercharged engines (Beech) with fuel injection. Mission is personnel transport and light cargo.

Gross Weight Maximum gross takeoff weight for the U-8F is 7700 pounds. Normal operating weight is 5550 pounds.

Length 33.3'

Height 14.2'

Width 45.9' wing span

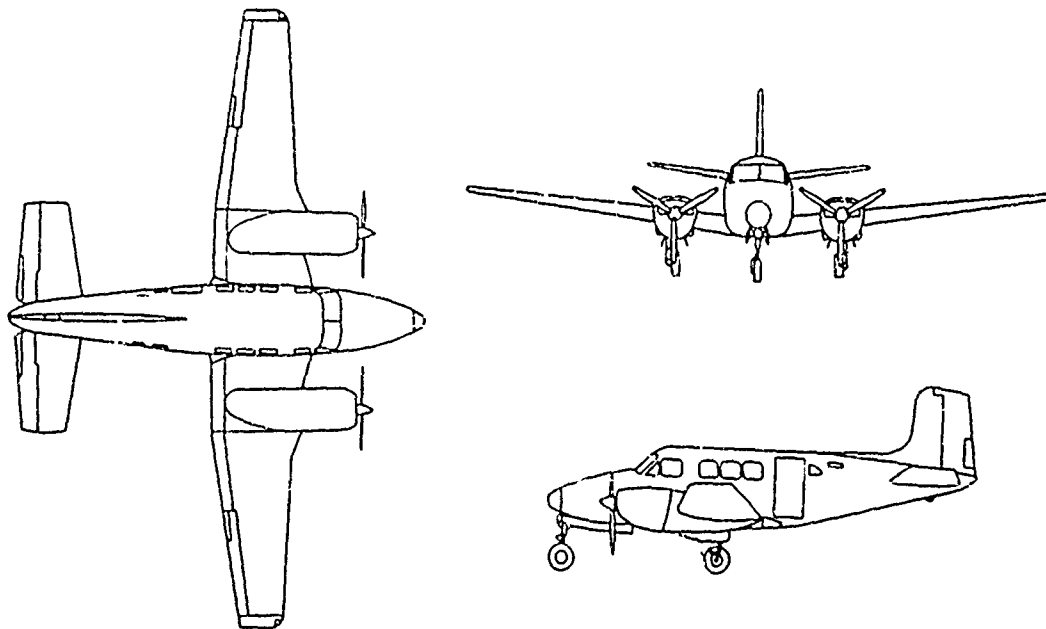
Engines Two Lycoming Model O-480-3 fuel injection engines are used for aircraft power. The engines are six-cylinder horizontally opposed, and supercharged. Added thrust is derived from the two-stage augmentor tube exhaust system which provides adequate cooling under all conditions and eliminates the need for cowl flaps.

BHP 150-200

Airspeed 130-234 knots operating range The aircraft will operate efficiently at takeoff gross weight during single-engine flight.

Engine Cooling The augmentor-type exhaust system employs the velocity and pumping action of the exhaust gases being ejected into the augmentor tube throat, from each bank of cylinders, to induce airflow through the engine nacelles and to vary the flow of cooling air around the engine.

Figure -11 shows various views of the aircraft



U-8F

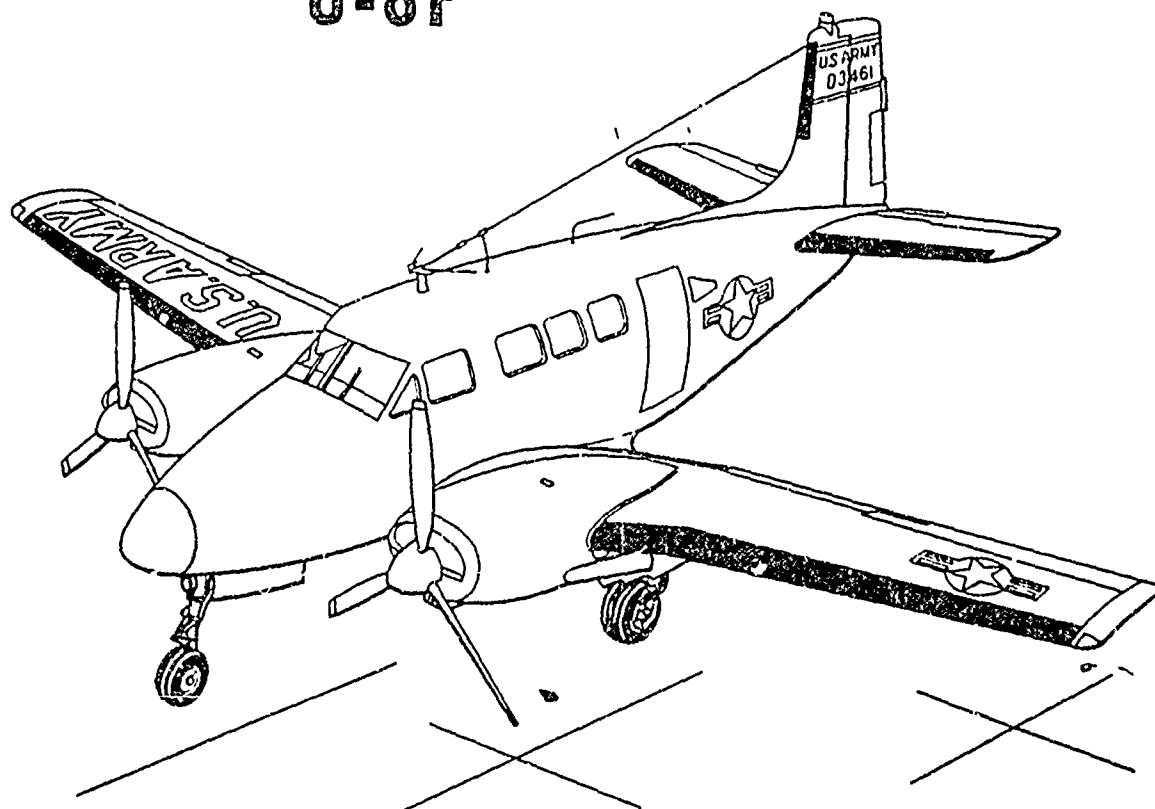


Figure 7-19. Four Views of the U-8F Aircraft (Seminole)

U-21

Manufacturer. Beechcraft

Description The U 21 series are unpressurized low-wing, all-metal, utility aircraft of versatile design with an all-weather capability. The basic mission is to provide a diversified utility service in the combat zone.

Weight Maximum takeoff gross weight is 9650 pounds

Maximum landing weight is 9168 pounds

Length 31' 6"

Height 14' 3"

Width 45' 11" wing span

Engines The aircraft is powered by two T74-CP-700 turboprop engines rated at 550 H.P. This engine is a reverse-flow, free-turbine type.

Interstage Turbine Temperature 750°C maximum

Airspeed 92-208 knots normal

Figure shows three external views of the aircraft



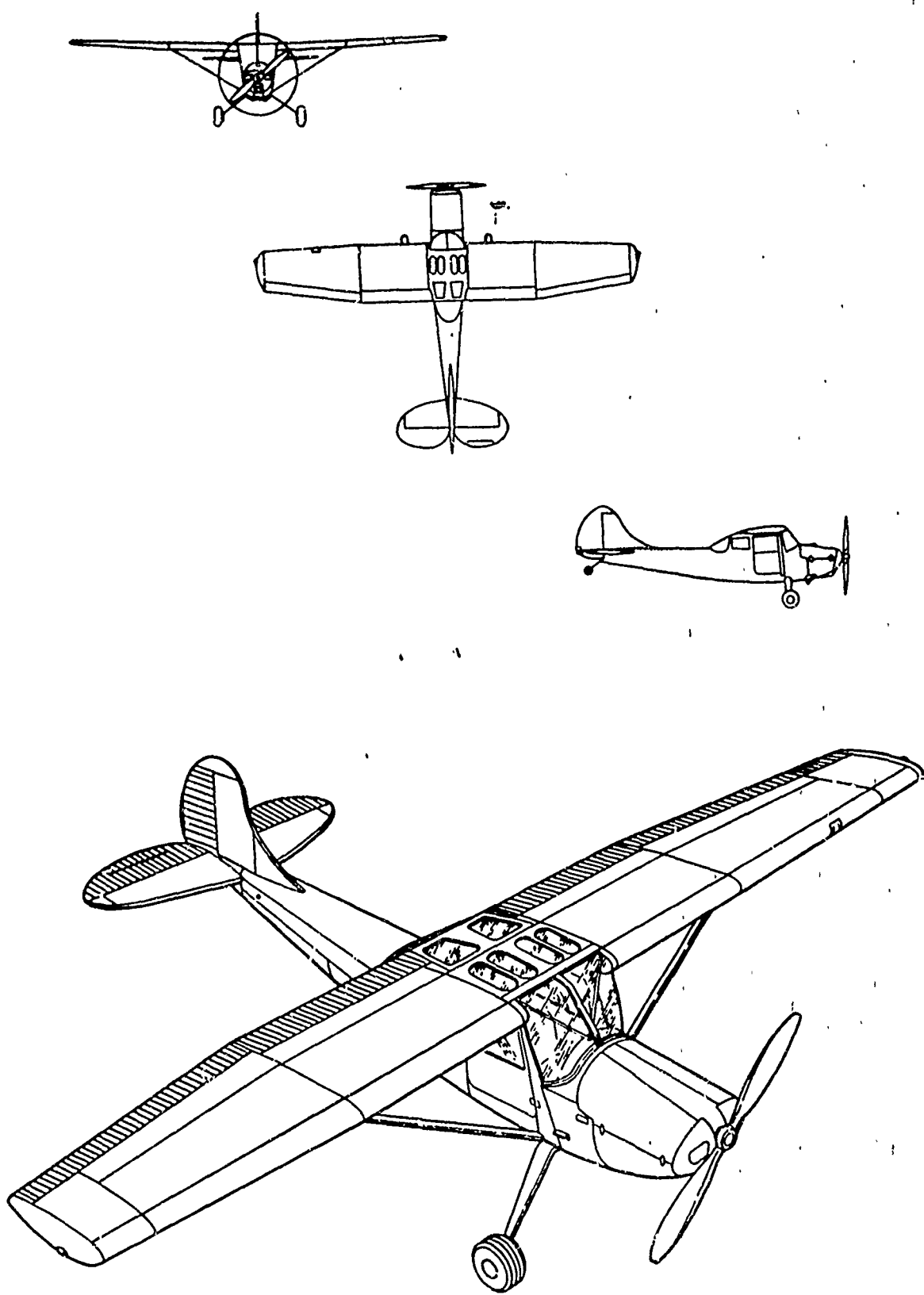


Figure 7-21. Four Views of the O-1 Aircraft

U-1A

Manufacturer: DeHavilland Aircraft of Canada

Descriptions: The U-1A aircraft is an all-metal, high-wing monoplane powered by a single Pratt and Whitney Wasp engine driving a Hamilton standard constant-speed propeller. The aircraft is designed to carry up to ten passengers.

Gross Weight: 8000 pounds

Length: 41' 10"

Height: 12' 5"

Wing Span: 58'

Engine: The aircraft is powered by a Pratt and Whitney 1340-59, or 1340-61, radial, single-row, nine-cylinder, air-cooled, supercharged engine rated at 600 BHP.

Figure 7-22 shows various external views of the aircraft.

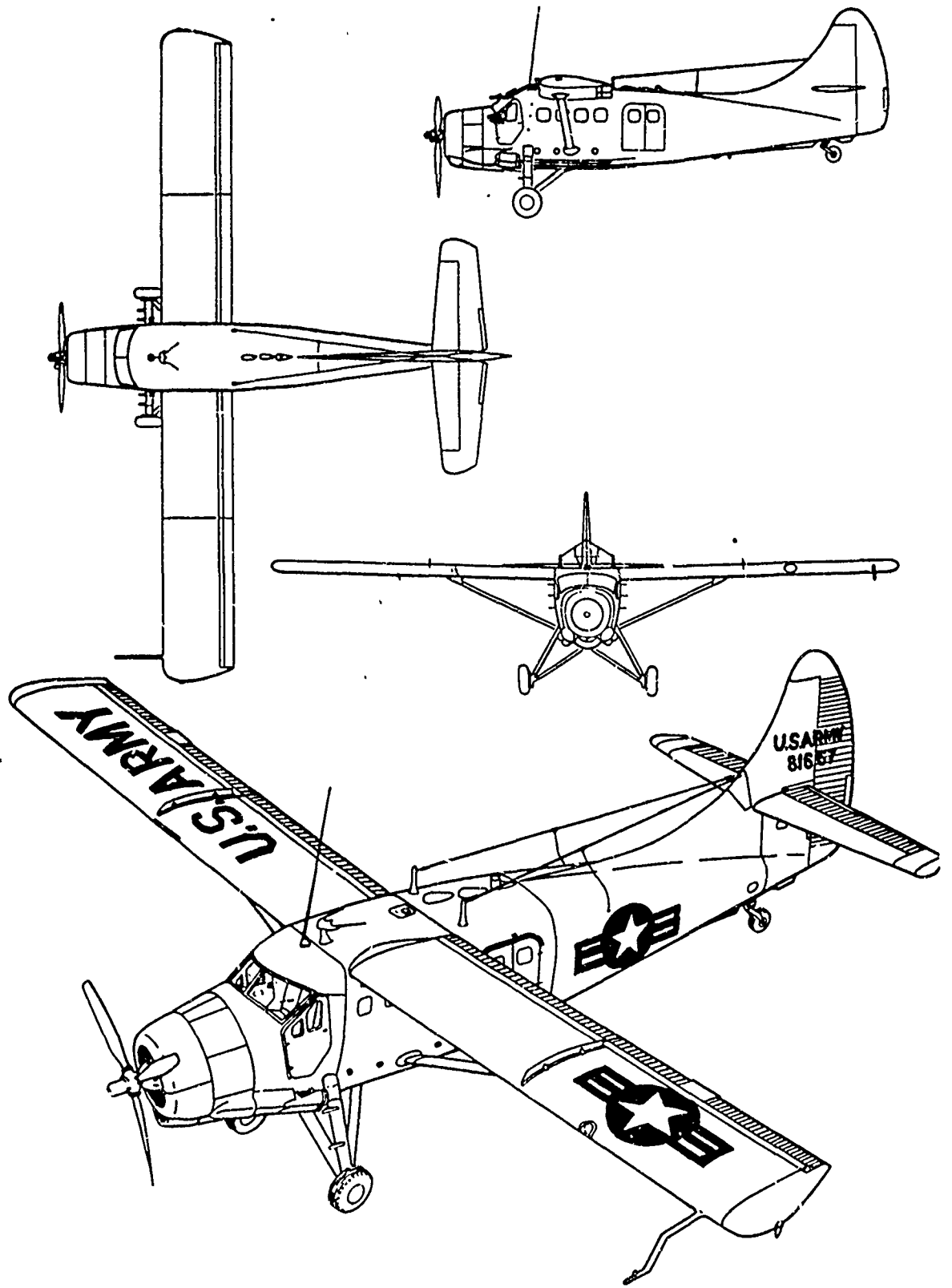


Figure 7-22. Various Views of the U-1A Aircraft (Otter)

U-6A

Manufacturer: DeHavilland Aircraft of Canada

Description: The U-6A aircraft is an all-metal, high-wing monoplane powered by a single Pratt and Whitney Wasp junior engine driving a Hamilton standard constant-speed propeller. It is designed to carry five passengers.

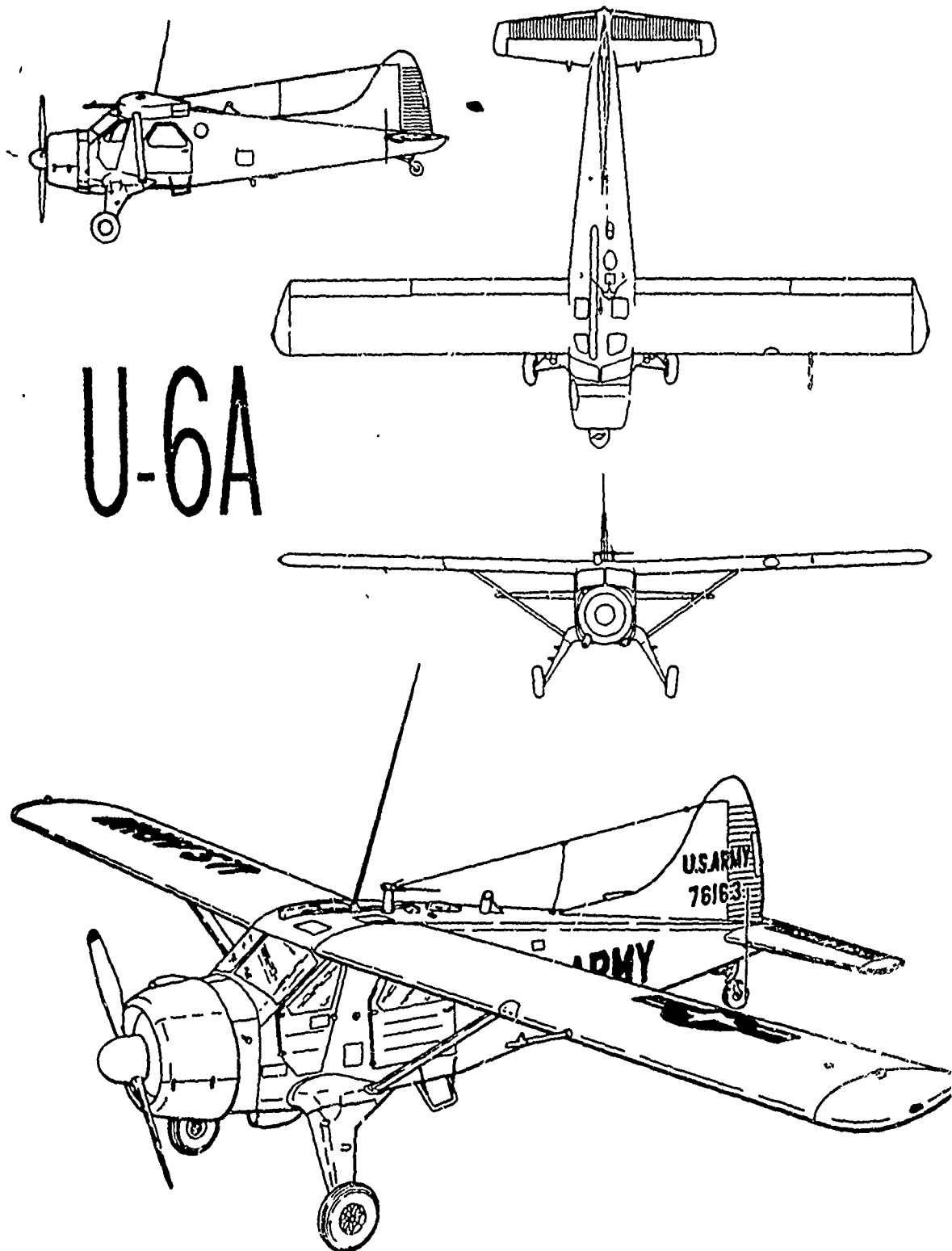
Gross Weight: 5100 pounds

Length: 30' 5"

Height: 10' 5"

Engine: The engine is a Pratt and Whitney Wasp Junior (Model R-985-AN-39A) nine-cylinder, air-cooled radial-type.

Figure 7-23 shows various external views of the aircraft.



U-6A

Figure 7-23. Various Views of the Beaver Aircraft

## BIBLIOGRAPHY

- Wolfe, William L., Handbook of Military Infrared Technology, Office of Naval Research, Department of the Navy, Washington, D.C., 1965.
- Holter, M.R., Nudelman, S., Suits, G.H., Wolfe, W.L., and Zissis, G.J., Fundamentals of Infrared Technology, The Macmillan Company, New York, 1962.
- Bramson, M.A., Infrared Radiation. A Handbook for Applications, Plenum Press, New York, 1968.
- Smith, R.A., Jones, F.E., and Chasmar, R.P., The Detection and Measurement of Infra-red Radiation, Oxford Press, London, Second Edition, 1968.
- Conn, G.K.T., and Avery, D.G., Infrared Methods, Principles and Applications, Academic Press, New York, Vol 7, 1960.
- Gaydon, A.G., The Spectroscopy of Flames, Wiley and Sons, Inc., New York, 1957.
- Hadni, A., Essentials of Modern Physics Applied to the Study of the Infrared, Pergamon Press, Oxford, 1967.
- Penner, S.S., Quantitative Molecular Spectroscopy and Gas Emissivities, Addison-Wesley, Reading, Massachusetts, 1959.
- Sears, F.W., Optics, Addison-Wesley, Cambridge, Massachusetts, 1949.
- Anon., Infrared Technology, U.S. Army Missile Command, Redstone Arsenal, Alabama, 1966.
- Steel, W.H., Interferometry, Cambridge University Press, Cambridge, 1967.
- Lipson, S.G., and Lipson, H., Optical Physics, Cambridge University Press, Cambridge, 1969.
- Hudson, R.D., Infrared System Engineering, Wiley and Sons, New York, 1969.

BIBLIOGRAPHY (Cont)

- Simmons, F.S. and Yamada, H.Y., "Spectral Radiances of Hot Gases Viewed Through Cool Intervening Atmospheres," University of Michigan, Infrared Lab., 1969.
- Arnold, C.B. and Simmons, F.S., "Some Measurements of Sky Emission in the 5-25 Micrometer Region," UM WRL Report 8418-1-12, 1968.
- Weinberg, J.M., "Jet Aircraft Spectroscopic Analysis," Block Engineering Inc., Cambridge, Massachusetts, 1968.
- Nicodemus, F.E. and Zissis, G.J., "Methods of Radiometric Calibration," Report of Bamirac 4613-20-R, October 1962.
- Holden, L.H., "A Method for Determining Spectral Responsivity of Spectrally Selective Radiometric Instruments," ECOM-5103, January 1967.
- Downie, A.R., Crawford, B., et al., "The Calibration of Infrared Prism Spectrometers," J. Optical Soc. Am., Vol 43, p 941, 1953.
- IUPAC, "Tables of Wavenumbers for the Calibration of Infrared Spectrometers," Butterworths, Washington, 1961.
- Illuminating Engineering Society, "USA Standard Nomenclature and Definitions for Illuminating Engineering," USA Z7.1-1967 Revision of Z7.1-1942.
- Anding, David, "Band-Model Methods for Computing Atmospheric Slant-Path Molecular Absorption," IRIA Rpt 7142-21-T, University of Michigan, Ann Arbor, Michigan, February 1967.
- Anding, David and Rose, Harvey, "IRIA State-of-the-Art Atmospheric Transmission Program," IRIA Memo, University of Michigan, Ann Arbor, Michigan, 24 July 1967.
- Blanco, A.J. and Hoidale, G.B., "Infrared Absorption Spectra of Atmospheric Dust," ECOM-5193, Atmospheric Sciences Lab, White Sands Missile Range, New Mexico, 1968.
- Hoidale, G.B., et al., "Variations in the Absorption Spectra of Atmospheric Dust," ECOM-5274, Atmospheric Sciences Office, White Sands Missile Range, New Mexico, 1969.

BIBLIOGRAPHY (Cont)

- Hoidale, G.B., et al., "A Study of Atmospheric Dust," ECOM-5067, Atmospheric Sciences Office, White Sands Missile Range, New Mexico, 1967.
- Anon., "The UH-1D Helicopter IR Suppression Device-Radiation Characteristics and Effectiveness Against IR Seeking Missiles" (U), SECRET, Report ECOM 5251, 5252, MEWTA, White Sands Missile Range, New Mexico, May 1969.
- Ashley, G.W., et al., "Test Results Infrared Evaluation of a Radiation Suppressor Kit for the UH-1D Helicopter" (U), SECRET, TM-6-349-279, General Dynamics, Pomona Division, April 1969.
- Anon., "The UH-1D Helicopter IR Suppression Device-Radiation Characteristics and Effectiveness Against IR Seeking Missiles" (U), SECRET Report ECOM-5254, Naval Weapons Center, China Lake, California, May 1969.
- Thompson, J.F., et al., "Design, Fabrication, Test, and Evaluation of an Infrared Suppression System for the OH-6A Helicopter" (U), SECRET, USAAVLABS Tech Rpt 68-43, Hayes Int. Corp., Birmingham, Alabama, November 1968
- Reed, J.L., "Infrared Measurements of the XV-5A Aircraft (Hover Flight Mode)" (U), SECRET NOTS TP 4222, U S Naval Ordnance Test Station, China Lake, California, June 1967.
- Reed, J.L. and Terral, L.G., "An Infrared Evaluation of the AH-1G Helicopter" (U), SECRET NWC TP 4545, Naval Weapons Center, China Lake, California, August 1968.
- Jones, T.K., "Results of Helicopter IR Signature Tests by NWC" (U), SECRET TN 4056-4, Naval Weapons Center, China Lake, California, January 1969
- Hacker, G.R., "Optical Attitude Reduction on Irregular Shaped Objects Flying Erratic Paths," Physical Science Laboratory Report, New Mexico State University, Las Cruces, New Mexico, 1969
- Holden, L.H., "80-watt Compact Xenon Lamp-Spectral Radiance," (U) CONFIDENTIAL, ECOM-5310, White Sands Missile Range, New Mexico, 1969.

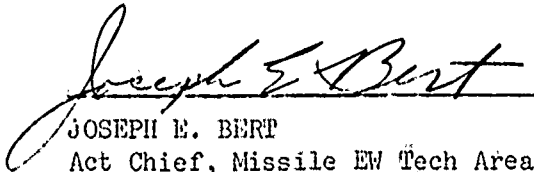


BIBLIOGRAPHY (Cont)

- Holden, L. H., "CH-47 Helicopter Infrared Suppression Device - Radiation Characteristics and Effectiveness Against Infrared Seeking Missiles" (U), SECRET, ECOM-5342, White Sands Missile Range, New Mexico, November 1970.
- Holden, L. H., "UH-1 Helicopter - Infrared Suppression Device - Radiation Characteristics and Effectiveness Against Infrared Seeking Missiles" (U), SECRET, ECOM-5360, White Sands Missile Range, New Mexico, January 1971.
- Holden, L. H., "UH-1 Infrared Spectral Radiant Intensity - Ablative Tailpipe IR Suppressor" (U), SECRET, ECOM-5371, White Sands Missile Range, New Mexico, April 1971.
- Holden, L. H., "AH-1G Helicopter - Infrared Spectral Signature" (U), SECRET, ECOM-5375, White Sands Missile Range, New Mexico, April 1971.
- Holden, L. H., "Addendum to ECOM-5251 - The UH-1D Helicopter IR Suppression Device - Radiation Characteristics and Effectiveness Against IR Seeking Missiles" (U), SECRET, ECOM-5309, White Sands Missile Range, New Mexico, July 1970.
- Holden, L. H., "OH-58 Helicopter Infrared Radiation Spectral Characteristics" (U), SECRET, ECOM-5382, White Sands Missile Range, New Mexico, May 1971.
- Holden, L. H., "Addendum to ECOM-5342 - CH-47 Helicopter Infrared Suppression Device - Radiation Characteristics and Effectiveness Against IR Seeking Missiles" (U), SECRET, ECOM-5361, White Sands Missile Range, New Mexico, February 1971.
- Yamada, H. Y., "A High-Temperature Blackbody Radiation Source," Infrared Physics Laboratory, Willow Run Laboratories, The Institute of Science and Technology, The University of Michigan, Ann Arbor, Michigan, August 1966.
- Meredith, R. E. and Kent, N. F., "A New Method for Direct Measurement of Spectral Line Strengths and Widths," Infrared Physics Laboratory, Willow Run Laboratories, Institute of Science and Technology, The University of Michigan, Ann Arbor, Michigan, April 1969.
- Hall, E. C., et al, "Measurement of the Time-Varying Component of Radiation from Infrared Sources," Infrared Physics Laboratory, Willow Run Laboratories, Institute of Science and Technology, The University of Michigan, Ann Arbor, Michigan, April 1969.

MISSILE ELECTRONIC WARFARE TECHNICAL AREA  
ELECTRONIC WARFARE LABORATORY, USA ELECTRONICS COMMAND  
WHITE SANDS MISSILE RANGE  
NEW MEXICO

Approval: Technical Report ECOM-5386 has been reviewed and approved for publication.

  
JOSEPH E. BERT  
Act Chief, Missile EW Tech Area  
Electronic Warfare Laboratory

---

GEORGE K. ROBERTS  
Act Technical Manager  
Missile EW Tech Area  
Electronic Warfare Laboratory